



Contents.

>	Introduction	4
>	News and events	8
>	Accelerator operation and construction	18
>	Highlights · New technology · Developments	30
>	References	66

The year 2016 at DESY.

Chairman's foreword

The year 2016 has – again – seen tremendous progress and extremely intense work in all the divisions and departments at DESY – in accelerator development, photon science, and particle and astroparticle physics.

With the construction of the European XFEL X-ray free-electron laser drawing to a close, it is already a remarkable success story: Within only six years, the world's most advanced electron linear accelerator was assembled in a tunnel from DESY to Schenefeld with no major delays, no major budget adjustments and no major accidents. I congratulate all the European XFEL and DESY teams for this impressive achievement. On 6 October, the commissioning phase was launched in a celebration with around 350 guests. We are all looking forward to the start of European XFEL operation for users in 2017. As the most powerful facility of its kind in the world, it will offer unique opportunities for fascinating science.

During the past years, DESY has developed into a powerhouse that attracts the best scientists from all over the world. This great success was achieved thanks to the focused development of a world-leading research infrastructure and

the consistent build-up of an ambitious research profile. The additional research opportunities offered by the modern beamlines in the second experimental hall at the FLASH soft X-ray free-electron laser and in the two extension halls at the PETRA III synchrotron radiation source are instrumental in strengthening DESY's role in advanced materials design and biological research.

What challenges will DESY face in the coming years?

Photon science at DESY critically hinges on the successful operation of PETRA III and FLASH for users. Ensuring the two facilities' long-term competitiveness also entails their advancement in order to maintain their world-leading position. For both facilities, DESY has set up project teams to devise the next generation of storage-ring-based X-ray sources and linear-accelerator-based X-ray lasers, respectively.

An upgrade of PETRA III – the diffraction-limited light source PETRA IV – will be exploiting novel technologies based on so-called multiband achromats, which enable unprecedented



Figure 1

Katharina Fegebank, Senator for Science, Research and Equality for the Free and Hanseatic City of Hamburg, and Piotr Dardziński, Under-Secretary of State of the Polish Ministry of Science and Higher Education, bolt in a section of beamline in the European XFEL tunnel together with European XFEL Director Massimo Altarelli and DESY Director Helmut Dosch, signifying the start of commissioning of the facility.



Figure 2
 Pushing the buttons uncovered the names “Ada Yonath” and “Paul P. Ewald” of the new PETRA III experimental halls: (from left) Harsh Vardhan, India’s Minister of Research, Edelgard Bulmahn, Vice-President of Germany’s Bundestag, Olaf Scholz, First Mayor of Hamburg, Ada Yonath, Israeli Nobel laureate who conducted important research at DESY, Georg Schütte, State Secretary at the German Federal Ministry of Education and Research (BMBF), John-Paul Davidson, grandson of Paul P. Ewald, Mikhail Rychev from the Russian Kurchatov Institute, Ulf Karlsson, head of the Swedish delegation of the Röntgen Angström Cluster and DESY Director Helmut Dosch.

beam qualities and in turn innovative ways of exploring the structure and function of matter, materials and biomatter. The new light source will be accommodated into the existing PETRA tunnel, aiming for the most advanced facility worldwide at moderate construction costs. The FLASH upgrade plans – denoted FLASH2020 – encompass new tuneable undulators as well as options for seeding and continuous-wave operation.

Both facility developments must take into account the needs of the users coming from Europe and from all over the world. The novel analytical technologies offered by PETRA IV and FLASH2020 therefore need to be integrated into a European framework. To this end, in 2015 already, DESY launched the League of European Accelerator-based Photon Sources (LEAPS) initiative, which aims at a European roadmap and a better integration of all European synchrotron radiation and X-ray laser facilities. The goal is to deliver a strategy document in the second half of 2017 and to influence the upcoming European Framework Programme FP9.

Future accelerators are not only one of the topics of the LEAPS initiative, they are also a building block of the future strategy of DESY’s Accelerator Division. Increasing efforts and resources are being devoted to this field of research, which will hopefully one day give rise to novel particle accelerators that are much smaller and more powerful than the ones in operation around the world today.

DESY’s facilities invite scientists from all over the world and from all scientific disciplines to carry out their research at highly specialised experimental stations. The challenge of the future is to unlock the innovation potential of these advanced and at the same time mature technologies. In 2016, DESY therefore initiated important steps to foster further partnerships and cooperation with industry. In particular, a new DESY Innovation and Technology Transfer unit was established under the direction of Arik Willner, DESY’s newly appointed first Chief Technology Officer (CTO). The successful technology transfer effected within the European XFEL project will serve as a key example for future activities at DESY.

All in all, the DESY Accelerator Division is well prepared to tackle the future challenges. My thanks go to its dedicated scientists, engineers and technicians and all the research and development groups and their staff who have been contributing to this wonderful success.

Helmut Dosch
 Chairman of the DESY Board of Directors

Accelerators at DESY.

Introduction

In 2016, DESY's accelerator activities culminated in the completion of the construction of the linear accelerator for the European XFEL X-ray laser. After the installation work in the 2.1 km long accelerator tunnel was essentially finished in November, the tunnel was closed and the cool-down procedure for the 96 superconducting, 12 m long accelerator modules began. By the end of the year, all helium tanks of the almost 800 installed cavities were filled with liquid helium at a temperature of 4 K, ready for the final step to 2 K foreseen for the beginning of 2017. No serious vacuum breakdown occurred during the procedure, proving that thousands of welding seams had stayed tight and not developed any "cold leaks".

This eminently important milestone marked the transition of the construction phase of the European XFEL accelerator complex to the beam commissioning phase, which will eventually lead to the operation phase and the start of scientific use of the facility by autumn 2017. The achievement was made possible thanks to the extremely intense and dedicated efforts by many DESY groups, colleagues from collaborating institutes in the European XFEL Accelerator Consortium and co-workers from external companies, who joined forces in a complex choreography of installation work for various components and subsystems taking place simultaneously in various sections of the machine. Some technical work will still have to be performed in 2017 on the last sections of the linear accelerator, but the gradient performance that the accelerator modules showed on the test stands in the Accelerator Module Test Facility (AMTF) is beyond specification and sufficient to reach decisive beam energy goals without the need to have every single one of the 24 installed radio frequency (RF) stations in operation. Achievements at the European XFEL were many and remarkable, too many to be listed here, but an outstanding one is certainly the fact that during years of accelerator construction and installation work, there was no serious accident detrimental to the health of any of the many people involved in this work.

Beam commissioning of the European XFEL injector, which was put into operation for the first time just before Christmas 2015, continued very successfully until July 2016. All essential objectives of this first phase of beam tests were reached, including commissioning of beam diagnostics and of the third-harmonic RF system, verification of the design goals for the beam emittance and demonstration of acceleration of long bunch trains up to the injector design energy of 150 MeV. This, together with the main linear accelerator being "cold" at the end of the year, provided excellent perspectives for a rapid and exciting progress in commissioning the entire machine in 2017.

The FLASH soft X-ray free-electron laser (FEL), the "little brother" of the European XFEL, from the experience of which the latter profited enormously, had a very successful year of user operation. In 2016, FLASH played a pioneering role again as the worldwide first FEL facility with simultaneous user operation at two separate undulator beamlines, FLASH1 and FLASH2. This parallel operation mode, where the bunch train is split between the two beamlines, worked very well and demonstrated the possibility to run with quite different beam parameters (such as bunch charge) in the same RF pulse by dynamically adjusting the low-level RF control on a microsecond scale. The variable-gap undulators in FLASH2 not only permitted independent wavelength tuning for FLASH2 users, but also gave the FEL experts a chance to explore advanced concepts such as tapering, higher-harmonic lasing etc., which they had conceived years ago and were now, with the eagerly awaited new undulators, able to put into practice. Among the remarkable achievements obtained during these studies are new records in photon pulse energy and wavelength. In parallel to user operation, plans for possible upgrades at FLASH have taken more concrete shape. Besides continuing important studies at sFLASH that among other results demonstrated a new wavelength record for the "seeded" FEL radiation, the seeding team worked out a proposal for the implementation of seeding for user operation at FLASH2. And, with a larger scope and on a longer time scale, considerations for converting the FLASH linear accelerator from pulsed to continuous-wave mode of operation are becoming more concrete and will be followed up in the future.

The PETRA III synchrotron radiation source had a good start in 2016 with very good availability figures in the first approximately two months of the user run, reproducing the reduced RF breakdown rate already achieved in 2015. However, later the reliability was compromised by more frequent failures in different areas of the machine's subsystems, so that by the end of the run in autumn 2016, the average availability did not significantly exceed the typical figure of 95% obtained in previous years. While consistent with the original goal for PETRA III, this performance is not fully satisfactory in comparison with availabilities obtained elsewhere. The PETRA team organised a workshop with experts from other accelerator laboratories to review availability/reliability issues and define measures to improve the figures for PETRA III in the future.

The studies for a major upgrade of PETRA towards an ultralow-emittance "diffraction-limited" storage ring continued. The goal for such a PETRA IV ring is an emittance of <20 pm rad at 6 GeV beam energy, an improvement of the present horizontal



Figure 1
Reinhard Brinkmann

emittance by a factor of more than 50, which would yield an unprecedented research potential for a facility of this kind. The design work concentrated mainly on the challenges for the magnet lattice and the beam optics/dynamics. Essentially two approaches have been studied, one based on the design for the upgrade of the ESRF synchrotron radiation source in France, the other on a more unconventional approach employing an exchange of horizontal and vertical phase spaces. The studies need to be continued and conclusions are premature, but preliminary results give reason for optimism that a design can be found with sufficient dynamic acceptance to be able to still use the DESY II synchrotron as an injector, although likely in a configuration with improved emittance performance. The goal is to settle the most important design questions by autumn 2017 so that a PETRA IV conceptual design report can be presented by spring 2018.

In the area of advanced accelerator concepts, laser plasma wakefield acceleration (LWFA) was achieved for the first time on the DESY site. The LAOLA/LUX experiment led by the University of Hamburg used pulses from the 200 TW ANGUS laser to produce electron bunches in a few-centimetre-long gas cell with a beam energy up to 400 MeV and an energy spread down to 1%. After these encouraging first results, the challenge for the future will be to make the beam more stable and reproducible. Progress at the electron-beam-driven plasma wakefield experiment FLASHForward included installation work in the FLASH2 tunnel, commissioning of the 25 TW laser that will be used to ionise the plasma, and successful tests of a plasma cell focusing a beam from the MAMI accelerator at the University of Mainz. A collaborative effort of

the FLASHForward, FLASH and SINBAD teams at DESY together with CERN and PSI in Switzerland was launched to design and build an X-band deflecting structure system for femtosecond-resolution bunch profile diagnostics. At the PITZ photoinjector test facility at DESY in Zeuthen, self-modulation of a bunch at the plasma frequency was demonstrated for the first time while sending a 20 MeV beam through a low-density lithium vapour cell. The EU-funded multi-GeV LWFA design study EuPRAXIA, coordinated at DESY, held its kickoff meeting in summer 2016 and rapidly gathered momentum. Preparations and necessary refurbishments for building up the ARES linear accelerator in the SINBAD accelerator R&D infrastructure in the former DORIS building at DESY continued, including necessary refurbishments of the building. The same infrastructure will also house the AXISIS experiment for THz-driven, ultrashort electron and photon beam generation, and preparation work for installing the AXISIS accelerator systems and beamline started. In cooperation with MIT in the USA, the generation of a beam from a miniature electron gun by means of a laser-generated THz field was demonstrated.

Enjoy reading more about our exciting accelerator activities on the following pages!

A handwritten signature in blue ink that reads "R. Brinkmann".

Reinhard Brinkmann
Director of the Accelerator Division



News and events.

News and events.

A busy year 2016

March

First undulator installed in European XFEL

The installation of the 35 segments of the first European XFEL undulator was completed in February 2016. The 3.4 km long X-ray free-electron laser will comprise three such undulators, each up to 210 m long, that will produce X-ray laser light exceeding the intensity of conventional X-ray sources by a billion times – making the facility the world's brightest X-ray source when completed. The X-ray pulses will allow scientists to study the nanocosmos using revolutionary experimental techniques, with applications in many fields including biochemistry, astrophysics and materials science. DESY is the main shareholder of the European XFEL, which is one of Europe's largest research projects. It is due to open to users for research in early autumn 2017.



An undulator segment is lowered down a shaft into the underground tunnels of the European XFEL.

This first completed undulator will generate short-wavelength, hard X-rays that will be used for experiments with a focus on structural biology and ultrafast chemistry. Each of the 35 undulator segments is 5 m long, weighs 7.5 t and is composed of two girders facing one another, each holding a line of alternating strong permanent magnets. When accelerated electrons pass through the field of alternating polarity generated by the magnets, ultrashort flashes of X-ray laser

light are produced. Components between adjacent segments help ensure a consistent magnetic field between them. Control systems allow components within the undulator to be mechanically moved, enabling the generation of a broad spectrum of photon wavelengths.

The undulator systems were devised in a joint collaboration of European XFEL and DESY, whose resources and experience were essential for the development. The same technology is now also used in a number of projects at DESY, including the FLASH soft X-ray free-electron laser and the PETRA III storage ring radiation source.

The undulator systems were built in a multinational collaboration. The challenging production involved DESY and Russian, German, Swiss, Italian, Slovenian, Swedish and Chinese institutes and companies. It included a number of in-kind contributions, such as electromagnets for the electron beamline designed and manufactured at several institutes in Russia and tested in Sweden; temperature monitoring units from the Manne Siegbahn Laboratory in Sweden; and movers, phase shifters and control systems designed and manufactured by CIEMAT in Spain.



The first undulator of the European XFEL consists of 35 segments, each 5 m long and weighing 7.5 t.

April

First user operation at FLASH2

On 8 April, DESY's FLASH soft X-ray free-electron laser (FEL) was operated for the first time in parallel for user experiments at two different FEL lines, one in the experimental hall "Albert Einstein" (FLASH1) and one in the new hall "Kai Siegbahn" (FLASH2). A first record for this parallel user operation was set one day later, with FLASH1 delivering 4000 X-ray pulses per second with an energy of up to 140 μJ per pulse and FLASH2 generating in parallel 110 pulses per second with about 100 μJ each.



FLASH is the first X-ray laser worldwide that can serve experiments at two beamlines simultaneously.

The second FEL line, FLASH2, was realised from 2011 to 2015. Soon after FLASH2 successfully generated intense radiation for the first time in August 2014, parallel operation of FLASH1 and FLASH2 was established. With the first user beamline in the new hall "Kai Siegbahn" operational, it was then possible to run two experiments simultaneously at FLASH1 and FLASH2, both delivering intense, ultrashort laser pulses with user-specific parameters.



View into the experimental hall "Kai Siegbahn" at FLASH in spring 2016: Beamline FL24 (right) just took up user operation, while Beamline FL26 (left) was still in the final equipment phase.

Reinhard Brinkmann elected EPS fellow



Reinhard Brinkmann

Reinhard Brinkmann, DESY Director in charge of the Accelerator Division, was appointed fellow of the European Physical Society (EPS). The EPS elected him in recognition of his outstanding leadership and achievements in accelerator physics and technology, including ground-breaking solutions for modern free-electron lasers and linear colliders based on superconducting accelerator technology and the success of longitudinally polarised electron beams in the HERA collider.

Reinhard Brinkmann started working at DESY in 1984. As the machine coordinator of the HERA electron ring accelerator from the late 1980s to the mid-1990s, he contributed decisively to the successful and swift commissioning of this highly complex facility. In 1995, he was appointed leading scientist for accelerator physics at DESY. He was instrumental in designing the TESLA superconducting linear accelerator and in drawing up the technical design report for the project, which was published in 2001. In 2003, he became the project leader for the preparation of the European XFEL project at DESY. In 2007, he took over as Director of the Accelerator Division.

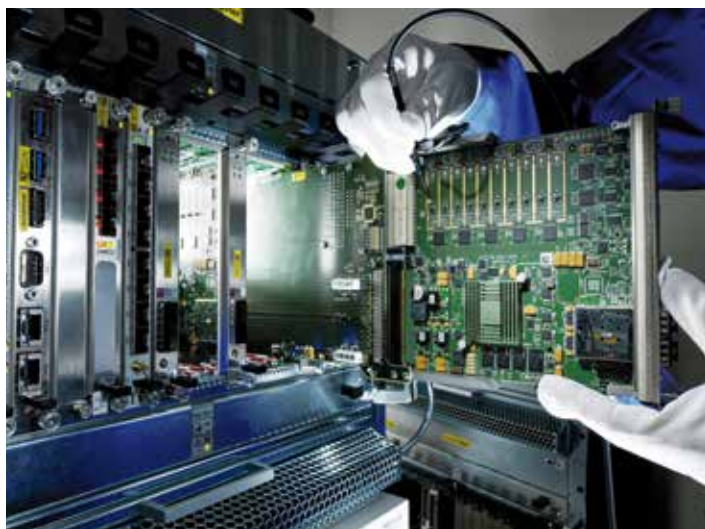
May

Green light for industrial alliance MicroTCA.4 Tech Lab

Together with private enterprises, DESY set up the MicroTCA.4 Technology Lab, a cooperative venture aiming to further develop the MicroTCA.4 electronics standard and establish it for a large market. Over the next three years, the project will be funded as a Helmholtz Innovation Lab – strategically designed, long-term technology alliances between Helmholtz centres and industrial enterprises – with the Helmholtz Association providing almost 2.5 million euros. Together with the funds contributed by DESY and private-sector companies, the budget of the innovation lab will amount to 5.07 million euros.

The Micro Telecommunications Computing Architecture (MicroTCA.4) electronics standard combines ultrafast digital electronics with the option to integrate analogue components within extremely small spaces. Its outstanding stability and scalability make it ideal for controlling particle accelerators and detectors, but also for a range of potential industrial uses, including in telecommunications, online inspection, aviation, medical engineering and high-precision measurements. MicroTCA.4 was developed by a consortium of research institutions and industrial enterprises led by DESY, up to the point where it was ready for use in the superconducting linear accelerator of the European XFEL X-ray free-electron laser.

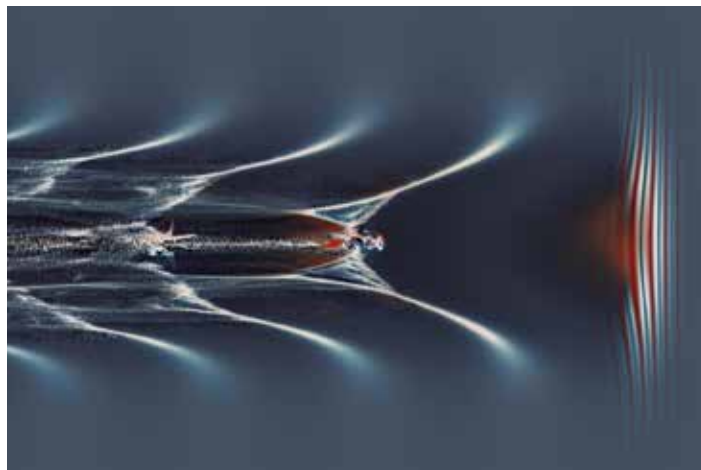
The new MicroTCA.4 Tech Lab aims to open up novel areas of application for this universally deployable technology. By continuously refining hardware, software and support services, its use is to be simplified. To this end, new laboratory and testing facilities are being created, which will allow new configuration and integration possibilities to be tested and verified. Direct customer support and an individualisation of possible applications right up to turn-key systems are also planned.



MicroTCA.4 printed circuit boards

June

Plasma wakefield accelerator project produces first particle beam



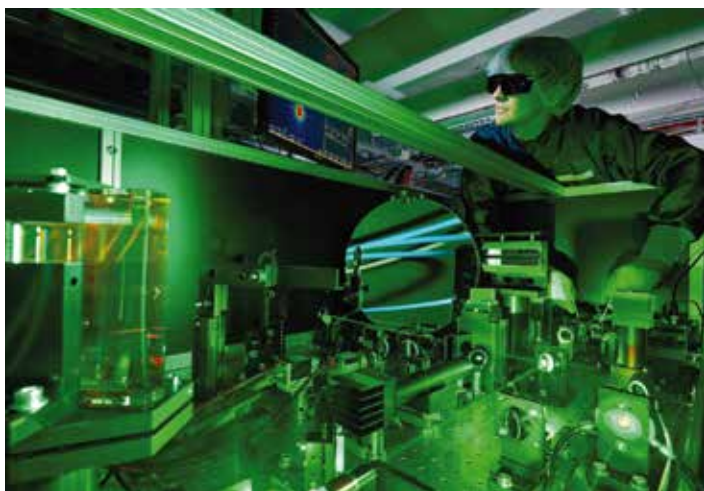
Simulation of plasma waves in the LUX capillary

An innovative accelerator project at DESY has produced its first electron beam. The experimental facility goes by the name of LUX and is being operated in collaboration with the University of Hamburg. It is based on the promising technology of plasma wakefield acceleration, which will hopefully one day give rise to smaller and more powerful particle accelerators. During a first test run, LUX accelerated electrons to about 400 MeV, using a plasma cell just a few millimetres long. This corresponds very nearly to the energy produced by DESY's 70 m long linear pre-accelerator LINAC II. The result is a first important milestone on the path to developing compact laser-driven plasma accelerators in Hamburg. However, the new technology still has to overcome a number of hurdles before it can be used in accelerators.

In plasma wakefield acceleration, a wave is produced in an electrically charged gas, known as a plasma, inside a narrow capillary tube. There are several different ways of doing this, which are being tried out in various projects on the DESY campus in Hamburg. LUX uses a special laser at the ANGUS laboratory, with a power of 200 TW, which fires ultrashort pulses of laser light into hydrogen gas at a particularly high frequency of up to five pulses per second. Each pulse lasts a mere 30 fs and ploughs its way through the gas in the shape of a narrow disk, 0.01 mm long and 0.035 mm high. The pulses strip the hydrogen molecules of their electrons, sweeping them aside. The electrons collect in the wake of the light pulse and are accelerated by the positively charged plasma wave in front of them – much like a wakeboarder riding the stern wave of a boat.

The physicists are hoping to use this technology to accelerate particles to up to 1000 MeV. The technology is still in the very early stages of development, but as it is able to produce up to 1000 times the acceleration of conventional facilities, it will allow far more compact accelerators to be built for future applications in fundamental research and in medicine. Over the coming months, the physicists will examine and further optimise the as yet “untidy” electron beam produced by LUX. To this end, additional beam diagnostics will be added. A short undulator will also be installed in order to test whether the fast electrons from the plasma accelerator can be used to produce X-rays.

The experimental LUX accelerator was developed and built by a junior research group at the Center for Free-Electron Laser Science (CFEL), a cooperative venture of DESY, the University of Hamburg and the Max Planck Society. The junior research group is part of the accelerator physics group at the University of Hamburg. LUX is operated as part of the LAOLA cooperation between the University of Hamburg and DESY, in which various groups from the two institutions work closely together to study pioneering new accelerator designs. Another important partner is the ELI Beamlines project in Prague, Czech Republic.



The joint ANGUS laser laboratory of DESY and the University of Hamburg features a 200 TW laser for research and development of laser-driven plasma acceleration.

DESY mourns Helen Edwards

On 21 June, Helen T. Edwards passed away at the age of 80 at her home in Illinois, USA. Helen Edwards was the chief scientist in charge of building and operating the Tevatron proton–antiproton collider at Fermilab, and from the early 1990s on she played a key role in developing the TESLA superconducting accelerator technology. She maintained close ties with DESY for over three decades, and together with her husband Don, she was an essential driving force behind years of fruitful collaboration of Fermilab and DESY.



Helen Edwards

During the early stages of the HERA electron–proton collider project, DESY profited enormously from her experience at the Tevatron, and in the course of numerous visits to DESY, she contributed to getting the HERA proton ring accelerator up and running. Within the TESLA collaboration, she organised crucial contributions of Fermilab towards the design of the linear collider as well as the design and construction of the TESLA test facility, which was later converted into the FLASH free-electron laser. Numerous colleagues at DESY remember and value Helen Edwards from many years of collaboration, and were extremely fond of her.

With her own brand of curiosity and her desire to get to the bottom of things, she worked with accelerator physicists at DESY until shortly before her death to analyse beam effects at FLASH. She will be remembered at DESY as a competent, dedicated and open-minded scientist who was always open for discussions, and her fond memory will always be cherished. Our thoughts go out to her husband and family.

EuPRAXIA kick-off meeting in Pisa



Participants of the EuPRAXIA workshop in Pisa

The EU project EuPRAXIA (European Plasma Research Accelerator with eXcellence in Applications) is gathering pace. At a workshop in Pisa, Italy, particle accelerator experts from all over the world met with experts working in the field of novel laser accelerators to discuss the design of a new, innovative European plasma accelerator, which is to be built in the context of EuPRAXIA and the EuroNNAc project. The EuPRAXIA consortium brings together the necessary expertise from Europe, Japan, China and the USA to build such a facility in Europe and demonstrate its benefits.

Through EuPRAXIA, which is funded as part of the EU programme Horizon 2020, accelerator physicists from 32 institutions, 24 of them European, are aiming to study the design and potential applications of new types of plasma-based accelerators. The researchers are seeking to develop an ultracompact 5 GeV plasma accelerator that could be used both in research and in industry or medicine.

The scientific workshop with over 120 participants took place from 29 June to 1 July at a venue steeped in history, especially for accelerator physicists: In 1589, the Italian scientist Galileo Galilei performed his seminal experiments on acceleration in Pisa. Using the very limited means at his disposal, such as his own pulse for measuring time, he discovered that the distance travelled by balls rolling down an incline was proportional to the square of time. Galileo's groundbreaking experiments on acceleration revolutionised classical physics at the time. With EuPRAXIA, accelerator physicists are now setting out to realise revolutionary particle accelerators.

DESY welcomes 104 summer students from 33 countries



DESY summer students in Hamburg ...

For seven weeks, 104 young scientists from 33 countries were given the opportunity to gain practical insight into research at DESY in Hamburg and Zeuthen as part of the DESY summer student programme, which is one of the largest and most international summer schools in Germany. The DESY summer student programme is extremely popular among students, both because of the practical experience it provides in genuine research projects and because of its internationality.

The 86 students from 28 countries at the Hamburg site and 18 students from 14 countries at the Zeuthen site were integrated into various DESY groups in the fields of particle and astroparticle physics, accelerator physics and photon science, where they experienced everyday life in science at first hand. A series of lectures providing the necessary theoretical background complemented the practical experience.



... and Zeuthen

European XFEL electron injector exceeds expectations

In July 2016, DESY successfully concluded tests of the first section of the linear accelerator for the European XFEL X-ray free-electron laser. The 40 m long electron injector performed distinctly better than expected, completing a whole week under operating conditions. The successful start-up of the injector was a huge success for the accelerator team and its international partners.

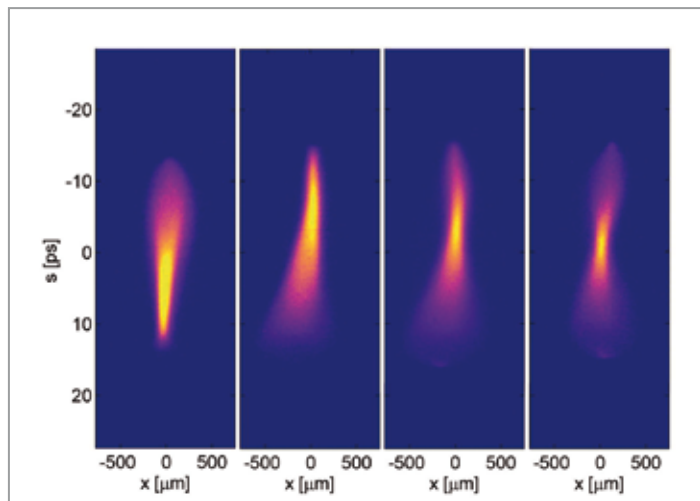
As the world's best X-ray laser, the European XFEL will produce extremely bright and ultrashort X-ray pulses, enabling a multitude of experiments to be carried out in the nanocosm – from determining the precise atomic structure of pathogens to making ultraslow-motion films of chemical reactions. The brilliant X-ray flashes will be produced by bunches of high-energy electrons brought to speed in a linear accelerator and then sent down a zigzag magnetic path in three undulator systems. At each bend in the path, the electron bunches emit X-rays that add up to a laser-like pulse in a self-amplifying manner.



The 30 m long injector of the European XFEL

As the main shareholder of European XFEL, DESY is responsible, among other things, for building and operating the 2.1 km long electron accelerator. The injector, which is located at the very beginning of the facility, supplies tailor-made bunches of electrons to the main accelerator. The quality of these electron bunches is crucial to the quality of the X-ray laser pulses at the experimental stations, about 3.5 km away. One important quality criterion is the emittance of the beam, a measure of how narrowly the electron bunches can be focused. As the injector tests showed, the emittance is some 40% better than specified.

Ten times every second, the injector produces a train of up to 2700 short bunches of electrons. To test the quality of the



The diagnostic system produces elongated images of individual electron bunches, allowing them to be analysed in slices.

beam, a special diagnostic system picks out individual bunches. Only about four bunches per train are needed to analyse the beam. These bunches are tilted by a cavity before striking the diagnostic screen. The elongated image they leave behind as a result can be used to study the longitudinal structure of each bunch in detail. The analysis revealed the outstanding quality of the bunches.

In the seven months since the injector produced its first electron beam in December 2015, it gave the accelerator team an opportunity to get to know all major subsystems of the entire accelerator facility: as the injector includes all the subsystems used in the main accelerator, the operators were able to test and familiarise themselves with them. All in all, no major obstacles were encountered throughout the several months of test operation. The injector went offline on 25 July so that it could be connected to the main accelerator.



The European XFEL section of the DESY accelerator control centre

September

Polish contribution to European XFEL successfully completed

To mark the successful conclusion of the Polish contribution to the construction of the European XFEL X-ray laser, a delegation including Maciej Chorowski, Director of the Polish National Centre for Research and Development (NCBiR), visited DESY and European XFEL. On this occasion, DESY renewed its cooperation agreement with the National Centre for Nuclear Research (NCBJ), which coordinated the Polish contributions to the European XFEL.



At the signing ceremony (left to right): NCBJ Deputy Director Ewa Rondio, NCBiR Director Maciej Chorowski, NCBJ Director Krzysztof Kurek, DESY Director Helmut Dosch, NCBJ Deputy Director Zbigniew Golebiewski and European XFEL Director Massimo Altarelli

The Polish in-kind contributions to the European XFEL were among the most important in the construction of the superconducting linear accelerator. In the past several years, in addition to assembly of components, around 50 Polish scientists performed intensive tests, first of individual components and later of the complete accelerator modules, prior to their installation in the European XFEL tunnel. In total, the Polish in-kind contributions are valued at around 19 million euros (in 2005 prices). The total Polish contribution adds up to 26.5 million euros.

On the occasion of the visit, DESY and NCBJ extended their long-time collaboration through another cooperation agreement. Both institutions intend to continue and intensify their collaboration not only in accelerator technologies, but also in photon science as well as in the development and application of free-electron lasers. Common experiments and data analyses are also foreseen in particle and astroparticle physics.

Superconducting part of European XFEL accelerator ready

Another important milestone in the construction of the European XFEL X-ray laser was reached in September with the completion of the installation of the 1.7 km long superconducting accelerator in the tunnel. The linear accelerator will bring bunches of electrons to an energy of 17.5 GeV in superconducting niobium cavities cooled to -271°C . In three undulator systems in the next part of the facility, the electron bunches will generate intense flashes of X-ray light, which will allow scientists new insights into the nanocosmos. The European XFEL accelerator will be the largest and most powerful linear accelerator of its type in the world.



Connecting two accelerator modules in the European XFEL tunnel

The accelerator was built by an international consortium of 17 research institutes led by DESY, the largest shareholder of European XFEL. The central section consists of 96 accelerator modules, each 12 m long, which contain almost 800 cavities made from ultrapure niobium surrounded by liquid helium. The modules, which were industrially produced in cooperation with several partners, perform on average about 16% better than specified, so the original goal of 100 modules in the accelerator could be reduced to 96.

The French project partner CEA in Saclay assembled the modules, which were then comprehensively tested at DESY before installation in the tunnel by staff of the Polish partner institute IFJ-PAN in Kraków. Magnets for focusing and steering the electron beam inside the modules came from CIEMAT in Madrid, Spain. The niobium resonators were manufactured by companies in Germany and Italy, supervised by DESY and INFN/LASA in Milano. Russian project partners, such as the Efremov Institute in St. Petersburg and the Budker Institute in Novosibirsk, delivered various parts for vacuum components for the accelerator as well as magnets to steer and focus the electron beam in the non-superconducting, room-temperature sections of the facility. Many other components were manufactured by DESY and its partners, including diagnostics and electron beam stabilisation systems.

European XFEL commissioning begins



Hamburg's Senator for Science Katharina Fegebank (centre), Beatrix Vierkorn-Rudolph from the German Federal Ministry of Education and Research (right), European XFEL Director Massimo Altarelli (left) and DESY Director Helmut Dosch (far left) tightened the final screws on a beamline of the European XFEL X-ray laser.

Commissioning of the 3.4 km long European XFEL X-ray laser started on 6 October, with around 350 guests from politics, administration, the diplomatic corps, scientists from around the world and employees of European XFEL and DESY celebrating the milestone on the new European XFEL campus in Schenefeld. In the underground tunnel near the facility's experiment hall, representatives of the partner countries mounted an approximately 2 m long beamline tube, as a symbolic act of installing one of the final still-missing pieces of the X-ray laser. As the main shareholder of the European XFEL, DESY led the consortium that built the linear accelerator.

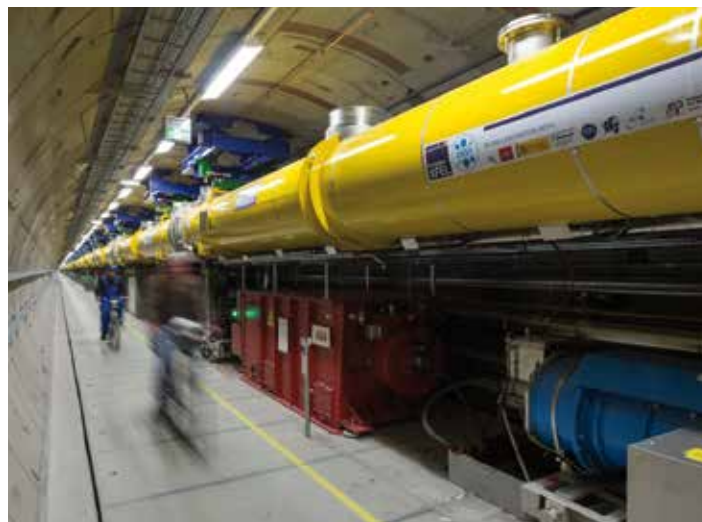
DESY Director Helmut Dosch said on the occasion: "I congratulate the European XFEL Accelerator Consortium for this outstanding achievement. This big success was made possible through the enormous team spirit of the Accelerator Consortium, which collaborated very closely to reach this high aim. I have the highest appreciation that this was accomplished on a tight budget."

European XFEL Director Massimo Altarelli said: "Thanks to the very intense and highly competent work of the European XFEL staff, of the staff of the DESY Accelerator Division and of the partner laboratories, we are now ready to gradually switch on the whole facility, with the goal to start operation of the facility in the early part of 2017. I would like to thank all the people involved who are turning this long-standing dream of the science community into reality."

The accelerator will be commissioned in several steps. As soon as the access control system is installed, the interior of the modules will be slowly cooled to the operating temperature of 2 K – colder than outer space. Then the first electrons will be sent through the accelerator. At first, they will be stopped in an electron dump at the end of the accelerator, until all the beam properties are optimised. Only then will the beam be sent on towards the undulators, where the electron bunches will be forced onto a tight, zigzagging slalom course for a 210 m stretch, thereby generating extremely short and bright X-ray flashes with laser-like properties in a self-amplifying process.

Reaching the conditions needed for this process is a massive technical challenge. Among other things, the electron bunches from the accelerator must meet precisely defined specifications. But the scientists involved have reason for optimism. All basic principles and techniques have been proven at DESY's FLASH free-electron laser, the prototype for the European XFEL. And at the European XFEL itself, the commissioning of the 40 m long injector, which was successfully concluded in July, bodes well for the commissioning of the complete facility.

Starting in fall 2017, scientists from around the world are expected to be able to use two out of the six scientific instruments planned for the medium term, enabling new views of the structure and fast processes of the nanocosmos. Applications range from structural biology, chemistry, physics and materials science to environmental and energy research or explorations of conditions like those found inside of planets.



The European XFEL accelerator tunnel

Robert Feidenhans'l new European XFEL Director

In October, Robert K. Feidenhans'l was appointed as the new chairman of the European XFEL Management Board as of 1 January 2017. The X-ray physicist was previously head of the Niels Bohr Institute at the University of Copenhagen, Denmark, and a member of the European XFEL Council, for which he served as chairman from 2010 to 2014. His predecessor Massimo Altarelli, who was at the head of the European XFEL GmbH since the non-profit company was founded in 2009, retired at the age of 68 at the end of 2016.



Robert K. Feidenhans'l

Robert Feidenhans'l studied at Aarhus University and holds a PhD in surface physics, a field that has since evolved into nanophysics. Starting in 1983, he worked at the Risø National Laboratory in different scientific and leading positions, until joining the Niels Bohr Institute in 2005. As a researcher, he is an expert in new ground-breaking X-ray technologies and research at large-scale X-ray synchrotron research facilities, such as ESRF in France, PSI in Switzerland and DESY.

Feidenhans'l said he is looking forward to his new tasks, which include ensuring a smooth transition of the facility from construction to user operation, which is scheduled to start in fall 2017.

Anton Piwinski receives Robert R. Wilson Prize

Anton Piwinski, a scientist in the DESY accelerator physics group from 1966 until his retirement in 1999, was awarded the 2017 Robert R. Wilson Prize of the American Physical Society (APS). He received the prize jointly with the US scientists Sekazi Mtingwa and James Bjorken, in recognition of his outstanding contribution to accelerator physics, in particular for the development of a detailed theory of intrabeam scattering, which is of fundamental significance for the beam quality that can be achieved by proton and electron storage rings. The prize was presented at the APS Meeting in January 2017.

Piwinski first proposed a largely complete theory of intrabeam scattering in 1974, which was later refined and elaborated by him and in parallel by Mtingwa and Bjorken. The scattering of particles inside the beam leads to an increase in the beam emittance and thereby to a broadening of the beam, which limits the performance of both colliders and synchrotron radiation sources. The effect has been observed in numerous accelerator facilities, including the proton ring of the former HERA collider at DESY, and can be precisely calculated using computer programs based on the theories of Piwinski, Mtingwa and Bjorken.

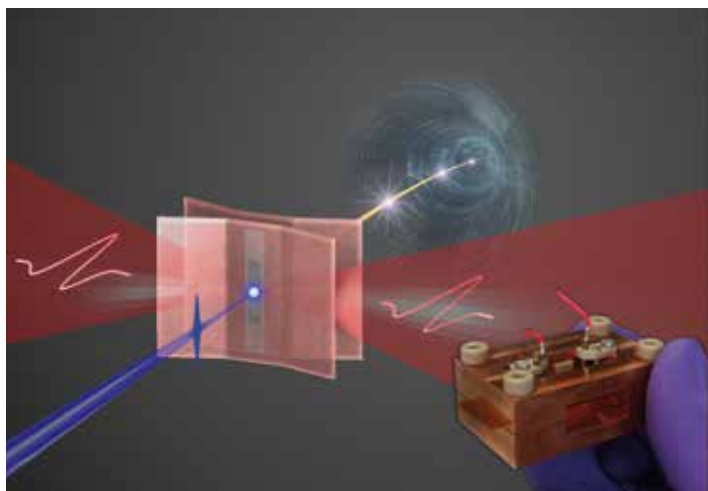
For more than three decades, Piwinski was instrumental in shaping the development of accelerator physics at DESY. In addition to developing his theory of intrabeam scattering, he carried out pioneering research on beam-beam interactions, as well as on transverse-longitudinal coupling and satellite resonances, which was met with international acclaim. In 2005, he was awarded the US Particle Accelerator School (USPAS) prize for his fundamental contributions to the understanding of charged particle beams in circular accelerators.



Anton Piwinsky

Scientists shrink electron gun to matchbox size

In a multinational effort, an interdisciplinary team of researchers from DESY and the Massachusetts Institute of Technology (MIT), USA, has built a new kind of electron source (gun) that is just about the size of a matchbox. The device uses laser-generated THz radiation instead of the usual radio frequency (RF) fields to accelerate electrons from rest. As the wavelengths of THz radiation are much shorter than those of RF radiation, the new electron gun can be made much smaller than conventional ones. While state-of-the-art electron guns can have the size of a car, the new device measures just 34 by 24.5 by 16.8 mm.



Miniature electron gun driven by THz radiation: An ultraviolet pulse (blue) back-illuminates the gun's photocathode, producing a high-density electron bunch inside the gun. The bunch is immediately accelerated by ultra-intense single-cycle THz pulses to energies approaching 1 keV.

Electron guns driven by THz radiation are miniature and efficient, and the materials used to guide the radiation are susceptible to much higher fields at THz wavelengths compared to RF wavelengths, allowing the THz radiation to give a much stronger “kick” to the electrons. This has the effect of making the electron beams much brighter and shorter. Such ultrashort electron beams with narrow energy spread, high charge and low jitter could be used for ultrafast electron diffraction experiments to resolve phase transitions in metals, semiconductors and molecular crystals, for example.

The new gun includes a nanometre-thin film of copper which, when illuminated with ultraviolet light from the back, produces short bursts of electrons. Laser radiation with THz frequency is fed into the device, which has a microstructure specifically tailored to channel the radiation in order to maximise its impact on the electrons. This way, the device reached an

accelerating gradient of 35 MV/m, almost twice that of current state-of-the-art guns. It accelerated a dense packet of 250 000 electrons from rest to 0.5 keV with minimal energy spread, allowing electron beams from the gun to already be used for low-energy electron diffraction experiments.

In the new gun, the ultraviolet flash used to eject the electrons from the copper film is generated from the same laser as the accelerating THz radiation. This ensures absolute timing synchronisation, substantially reducing jitter. The gun worked stably over at least one billion shots, easing every-day operation.

Electron guns are used ubiquitously for making atomic-resolution movies of chemical reactions using ultrafast electron diffraction. With smaller and better electron guns, biologists can gain better insight into the intricate workings of macromolecular machines, including those responsible for photosynthesis, and physicists can better understand the fundamental interaction processes in complex materials.

Furthermore, electron guns are an important component of X-ray laser facilities. Next-generation THz electron guns producing ultrashort and ultrabright electron bunches up to relativistic energies and of only 10 fs duration are currently in development at Center for Free-Electron Laser Science (CFEL) in Hamburg, a cooperation of DESY, the University of Hamburg and the Max Planck Society. These devices will be used as photoinjectors for attosecond table-top X-ray lasers. At DESY, such electron guns and X-ray lasers are being developed within the AXSIS (Frontiers in Attosecond X-ray Science: Imaging and Spectroscopy) programme.



Accelerator operation and construction •

➤	PETRA III	22
➤	FLASH	24
➤	PITZ	26
➤	European XFEL	28

In March 2016, DESY's PETRA III synchrotron radiation source took up operation again after a shutdown period that had started in November 2015 and that was mainly used to install further components for the beamlines in the extension hall East. After a short commissioning period of only four weeks, user operation resumed on 7 April. In 2016, a total of 5256 h of synchrotron radiation beam time was delivered to users at 16 beamlines, including the two new beamlines in the extension section North. During the next winter shutdown, further undulators will be installed, which should become operational in 2017.

User operation

During the four-month-long winter shutdown 2015–2016, which ended in March 2016, further components were installed for the beamlines mainly in the extension section East. User operation restarted on 7 April after a commissioning period of only four weeks and continued until 23 December. The necessary maintenance was done in five dedicated service weeks distributed over the year. The last service week in November 2016 was already used to prepare the next winter shutdown. In addition, a two-week period in August 2016 was used for test runs and extended machine developments. On Wednesdays, user operation was interrupted by weekly regular maintenance, machine development activities and test runs for about 24 h. The distribution of the different machine states in 2016 is shown in Fig. 1. In total, 4421 h were scheduled for the user run 2016 and, in addition, 1118 h of test run time were made available to users.

During user runs, the storage ring was operated in two distinct modes, characterised by their bunch spacing. In the “continuous mode”, 100 mA were filled in 480 or 960 evenly distributed bunches corresponding to 16 ns or 8 ns bunch spacing, respectively. The “timing mode” allows users to perform time-resolved experiments and is thus characterised by a considerably larger bunch spacing of 128 ns or 192 ns, corresponding to 60 or 40 evenly distributed bunches. In the timing mode, 100 mA were filled in 60 bunches and 90–100 mA in 40 bunches. Due to a high demand for time-resolved measurements, PETRA III was operated to a large extent in the timing mode. The detailed distribution of the operation modes in 2016 is shown in Fig. 2. For beam operation in the timing mode, very good bunch purity is required. Unwanted satellite bunches were routinely cleared by making use of the multibunch feedback system.

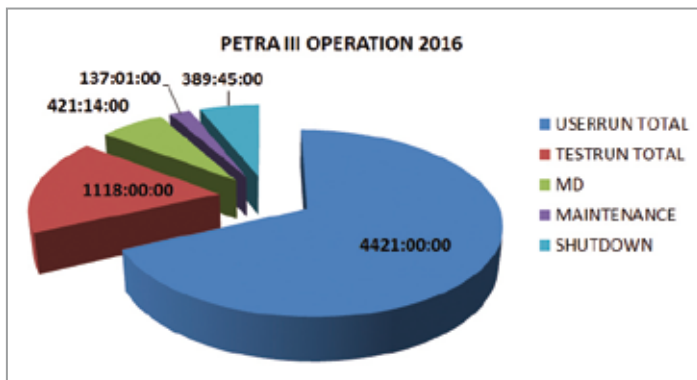


Figure 1
Distribution of the different machine states during the run period 2016

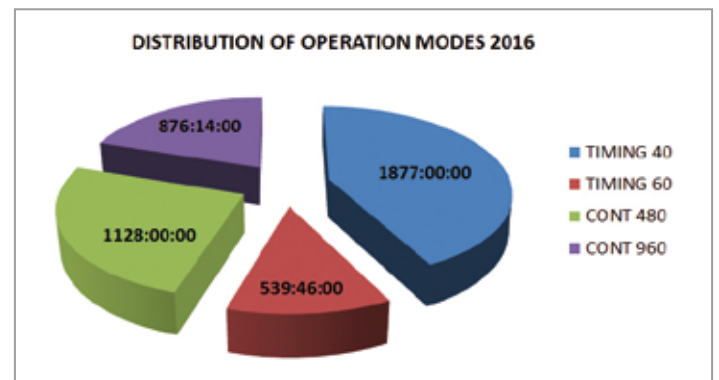


Figure 2
Distribution of the different operation modes in 2016

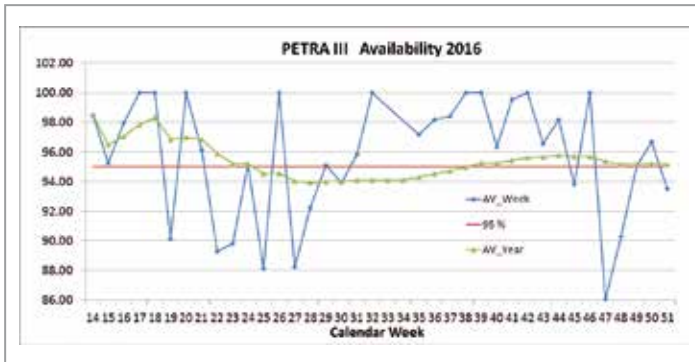


Figure 3

Availability in 2016. The blue curve shows the weekly average, the green curve the yearly average. The red line indicates an availability of 95%.

High reliability is one of the key requirements for a synchrotron radiation facility. The key performance indicators are availability and mean time between failures (MTBF). In 2016, the weekly availability even reached 100% for several weeks of the year, as can be seen in Fig. 3 (blue line). At the end of the user run, however, the average availability only turned out to be 95.2%, which is essentially equal to the availability in the previous year. The development of the average availability over the year is also shown in Fig. 3 (green line).

The average MTBF at the end of 2016 was 37 h, which is slightly better than in the previous year. Nevertheless, the availability and MTBF of PETRA III are not in line with that of other world-leading facilities. In May 2016, an availability review meeting was organised to gain a better understanding of the effectivity of efforts to improve the availability of PETRA III. The organisation, allocation and prioritisation of resources were reviewed by an international review committee with respect to manpower and potential investments, resulting in a review report with eight recommendations and several suggestions.

Several recommendations were already addressed in 2016. During a service week in August 2016, the tuning plungers at one radio frequency (RF) cavity were successfully replaced, and an RF power test stand was completed in December 2016. A working group was formed to improve the fault tracking of critical technical systems, e.g. the fast orbit feedback system. These actions were beneficial for several subsystems. The overall availability nevertheless suffered from a multitude of minor randomly occurring faults, which seemed to be uncorrelated to just a few technical causes.



Figure 4

Dipole magnet with new coil configuration. The magnetic fields are being measured in the magnet laboratory at DESY.

Challenges ahead

In 2015, test operation started at the two new beamlines P64 and P65 in the Paul Peter Ewald experimental hall (extension hall North). However, it turned out that the fringe field of the deflecting dipole between the two undulators had to be improved using a new coil configuration. In December 2016, the first new coils arrived at DESY and measurements of the magnetic field started (Fig. 4). After further improvements, the dipole magnets will be installed at four locations in the Paul Peter Ewald experimental hall and in the Ada Yonath experimental hall (extension hall East).

In 2017, PETRA III will restart with several new undulators: at the beamline P01 in the Max von Laue experimental hall and at the beamlines P22, P23 and P24 in the Ada Yonath experimental hall. In addition, the accelerator components in the Ada Yonath experimental hall will be realigned to correct movements of the components due to the progressive settlement of the new hall. All new undulators should become operational in 2017, an achievement that will only be possible thanks to essential efforts of all the technical groups involved.

Contact: Rainer Wanzenberg, rainer.wanzenberg@desy.de
 Michael Bieler, michael.bieler@desy.de

Consolidating tandem operation with two beamlines

On Friday, 8 April 2016 at 12:14, user operation officially started at FLASH2, the new beamline of DESY's FLASH free-electron laser (FEL) facility. For the first time, two user experiments received beam simultaneously: one in the Albert Einstein experimental hall (FLASH1), the other in the new Kai Siegbahn hall (FLASH2). A unique feature of the FLASH facility is that, besides both beamlines being operated in parallel, they may both receive beam with very different parameters, tailored individually for each experiment. Shortly afterwards, in May 2016, a record self-amplified spontaneous emission (SASE) energy at a wavelength of 21 nm was achieved. The FLASH2 gas monitor detector measured an energy of 1 mJ in a single pulse, corresponding to 10^{14} photons per shot. With the FLASH2 variable-gap undulators, many lasing schemes proposed in the past can finally be tested: linear and quadratic tapering, frequency doubling, harmonic lasing and reverse undulator tapering.

Highlights

For two years now, FLASH has been operating with two beamlines in parallel as a tandem delivering SASE radiation to two experimental halls, called “Albert Einstein” and “Kai Siegbahn”. User operation at FLASH2 officially started on 8 April 2016, with two user teams receiving beam for their experiments at the same time, both with quite different parameters (Fig. 1).

With the variable-gap undulators of FLASH2, several new lasing schemes proposed years ago can now be experimentally tested. One evident technique is the tapering of undulators: since the electrons lose energy to the generated SASE radiation, the resonance condition is kept by slightly changing the gap of downstream undulator sections. With this

procedure, saturation occurs at a higher SASE energy level. In May 2016, a world record SASE energy of 1 mJ was measured at FLASH2 at a wavelength of 21 nm. This corresponds to 10^{14} photons per pulse, never achieved elsewhere.

In a special run, the electron beam energy was pushed to its present limit of 1230 MeV, more than ever reached at FLASH. Using the FLASH2 undulators at their optimum, the wavelength could be reduced from its 4 nm design value to 3.5 nm, the smallest SASE fundamental wavelength achieved so far at the facility. Towards longer wavelengths, the reach was extended to 90 nm.

Besides using the usual third and fifth harmonic of the fundamental, smaller wavelengths can also be generated by



Figure 1
Official start of FLASH2 user operation in April 2016. Two user teams received beam at the same time with different parameters tailored to their specific experiment.

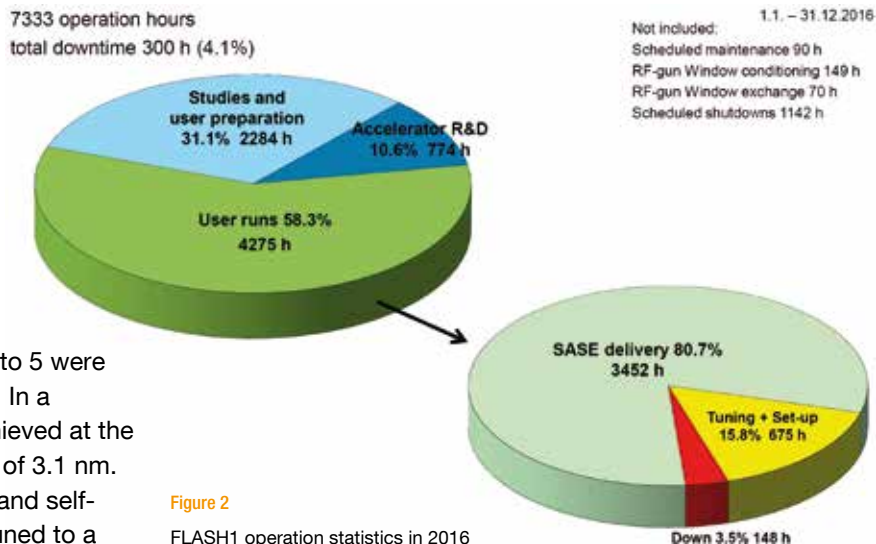


Figure 2

FLASH1 operation statistics in 2016

frequency doubling. As an example, Undulators 1 to 5 were tuned to 6.2 nm and Undulators 6 to 12 to 3.1 nm. In a promising experiment, a few microjoules were achieved at the double frequency, corresponding to a wavelength of 3.1 nm. This scheme can be extended to harmonic lasing and self-seeding, where the first part of the undulators is tuned to a multiple of the wavelength of the last part. To this end, it is important that only harmonics starting independently of the fundamental are amplified, resulting in a bandwidth smaller than the one of the usual third and fifth harmonic. First experiments at FLASH2 did indeed indicate a reduction in bandwidth and an improved longitudinal coherence.

The old beam arrival time monitors of FLASH have the drawback of poor resolution for electron bunch charges smaller than about 250 pC. An upgrade is under way, and first tests are promising. The new electronics was tried out in a user experiment with excellent results. The arrival time stability could be pushed from the usual 20–30 fs to a record 14 fs rms within a bunch train. The new electronics will be fully exploited in 2017, once the new pickup hardware is installed.

FLASH1 operation

In 2016, FLASH1 was operated for 7333 h; 90 h were scheduled for maintenance. The facility was shut down for 1142 h, mainly for installation of the FLASHForward experiment to be realised at the new third beamline, FLASH3. Operation was interrupted for another 70 h to change a leaky radio frequency (RF) window at the RF gun and for a commissioning time of the new window of 149 h. Almost 60% of the beam time was devoted to user experiments, 30% to FLASH studies, beamline commissioning and user run preparation, while 10% was reserved for open accelerator R&D. SASE radiation was delivered to users for 3452 h, i.e. 80.7% of the user beam time. A considerable amount of time (15.8%) was used for tuning the machine to specific user needs; the downtime due to component failures was only 3.5% (Fig. 2).

FLASH2 operation

FLASH2 user operation had a good start. A total of 1570 h was devoted to users, even though the first two experimental beamlines were just ready for use. A large portion of the beamtime, 5440 h, was used for beamline commissioning, photon diagnostics commissioning and various experiments with the variable-gap undulators. During operation time, FLASH2 was on standby for 1645 h. Standby is generated

when FLASH1 operation does not allow beam in FLASH2. This happens for example when FLASH1 requires a change of beam energy to change the wavelength for a FLASH1 user experiment.

Seeding experiments

Seeding experiments at sFLASH, the seeding section of the FLASH1 beamline, continued in 2016 with many improvements, especially regarding the seed laser and the laser beamline. As of December 2016, experiments are concentrating on improving the high-gain harmonic generation method (HGHG). The experiments profit considerably from LOLA, the deflecting structure downstream of the sFLASH undulators, which enables a precise characterisation of the seeded FEL properties. HGHG seeding was performed with a seed wavelength of 266 nm and operating the FEL at the seventh harmonic at 38 nm. At this wavelength, FEL saturation was observed with a maximum pulse energy of 110 μ J. Bunching at the ninth and eleventh harmonic was observed as well, although at reduced FEL output energy.

FLASH refurbishment

FLASH has been operating as a user facility for 11 years now. Many components are reaching the end of their lifetime. In addition, due to extensive user demands, the parameter range of FLASH has been continuously extended towards very short photon pulse duration and thus operation with much lower beam charge than initially designed and towards an arrival time stability goal of 10 fs or less. A refurbishment programme has been launched to address these issues. The plan is to upgrade all diagnostics to achieve a better precision for charge levels down to 20 pC. Furthermore, some of the accelerator modules will be refurbished to allow a better RF regulation and higher energy reach. The FLASH team also plans to develop a new generation of photoinjector lasers.

Contact: Siegfried Schreiber, siegfried.schreiber@desy.de

Successful plasma experiments

In 2016, the PITZ photoinjector test facility at DESY in Zeuthen was operated with a new, more stable radio frequency electron source (RF gun) setup, leading to regular operation at parameters required for the European XFEL X-ray free-electron laser. Thanks to the facility's unique possibilities for longitudinal beam shaping and new electron beam diagnostic techniques, the first successful plasma acceleration experiments at PITZ became possible, leading to the world's first direct observation of self-modulation instability.

RF gun developments

Since March 2016, a new gun setup has been operated at PITZ. Gun 4.6 includes a new, improved cathode spring design and is equipped with two DESY-type RF windows placed at the optimised position to minimise the power load of reflections from the gun. After a conditioning time of several months, the gun is now mainly being operated at the European XFEL goal parameters (6.5 MW power in the gun, 650 μ s RF pulse duration) without major problems – and with increasing reliability.

In spring 2016, a fundamental upgrade of the PITZ cooling system took place. After further improvements in the low-level RF (LLRF) regulation system, the amplitude and phase stability of gun and booster could be significantly improved.

During the 2016 run time, first studies for correcting the always observed beam asymmetry by means of additional quadrupole corrector coils placed within the gun solenoid were successfully carried out. More systematic studies will be performed to directly transfer this know-how to the FLASH and European XFEL user facilities.

In close collaboration with colleagues from DESY in Hamburg, automatic procedures were developed and tested at PITZ, such as fast recovery and cold start-up procedures, which significantly reduce the downtime of the machine after an interruption of the gun operation.

Plasma acceleration experiments

Within the framework of the accelerator R&D programme of the Helmholtz Association, the PITZ group is investigating beam-driven plasma wakefield acceleration mechanisms. In 2016, several weeks of beam time were dedicated to plasma acceleration experiments.

An improved setup with a new heat pipe oven lithium plasma cell – allowing stable operation with a plasma density of $\sim 10^{14}$ cm^{-3} – was built and operated in the PITZ beamline (Fig. 1). Using this plasma cell, the self-modulation of a long electron beam in a plasma wake was directly demonstrated for the first time worldwide. The results of this very successful experiment are of vital importance for the Advanced Wakefield Experiment (AWAKE) at CERN, as they show the feasibility of one of the key concepts this plasma acceleration experiment is based on. A corresponding publication was submitted to *Nature Communications*. Further experiments with the lithium cell for investigating e.g. the influence of the plasma density profile on self-modulation are being prepared for 2017.

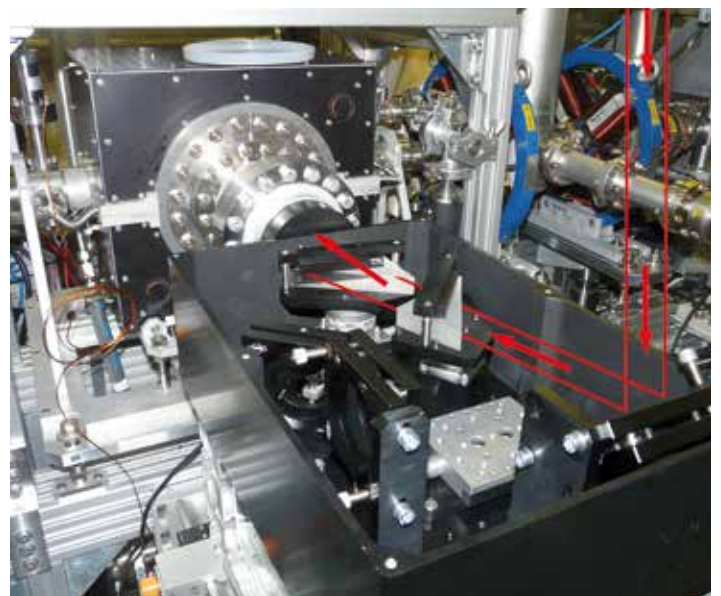


Figure 1
Lithium plasma cell installed at the PITZ beamline. The optical path of the ionisation laser is indicated in red.

In a second experiment, the efficient acceleration of electrons in a plasma at a high transformer ratio (HTR) – that is, the ratio of maximum accelerating field in the witness bunch and maximum decelerating field in the driver bunch – was shown.

In the framework of a PhD thesis, the use of an alternative plasma cell design was successfully explored: a gas discharge plasma cell was designed, built and characterised at DESY in Zeuthen. Compared to the lithium cell, such a plasma cell has the advantage of being easily scalable to longer plasma lengths, but it offers much less flexibility in the plasma shaping than the heat pipe oven design with its transverse coupling of the ionisation laser. In the last run period of 2016, first data was taken with the new plasma cell. Measurements will continue in March 2017 with an upgraded setup.

Longitudinal beam characterisation

The basic diagnostic tool for the demonstration of self-modulation and high transformer ratios, but also for the general characterisation of the time-resolved electron beam properties is the RF deflector (transverse deflecting structure, TDS). Built as a prototype for the European XFEL injector, the TDS at PITZ was put into operation in 2015. In 2016, the system was commissioned and high-resolution measurements became possible, allowing a fine-tuning of the temporal electron beam profile using the flexible photocathode laser system built by MBI in Berlin, Germany. This fine-tuning capability was very important for the self-modulation and HTR studies mentioned above, since both need well-shaped time profiles. For example, a double-triangle shape (Fig. 2) was the precondition for the successful proof of efficient electron acceleration in a plasma for the HTR studies.

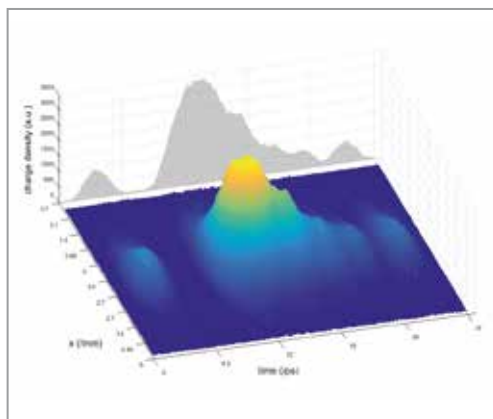


Figure 2
TDS measurement of the temporal double-triangle electron beam shape (driver bunch) and the witness bunch used for the HTR studies

3D ellipsoidal laser system

Good progress was made in 2016 with the commissioning of the 3D ellipsoidal laser system developed at the Institute of Applied Physics in Nizhny Novgorod, Russia. With strong support of the corresponding DESY groups in Hamburg, the new laser system was synchronised to the PITZ RF system, and first synchronised photoelectrons were generated. First measurements of the produced electron beam properties were performed, and the effect of temporal masking was observed with the TDS.

Laser beam shaping has been observed in the infrared (in both the transverse and temporal plane) and is in progress for the ultraviolet. Alignment stability and laser beam transport issues have to be resolved in the near future, and proper electron beam characterisation is anticipated for the PITZ operation periods in 2017.

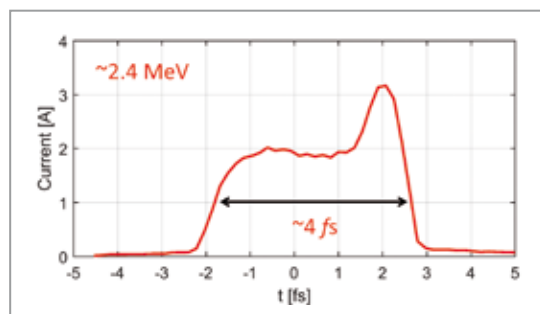


Figure 3
First simulations towards the generation of ultrashort bunches at PITZ

Further studies for PITZ applications

In 2016, the PITZ group continued to investigate possibilities for using a PITZ-like accelerator as a source for pump–probe applications at the European XFEL, namely using the X-ray laser pulses and either THz radiation or electron diffraction. For THz generation, simulations and first measurements at high bunch charges (up to 4 nC) were performed. A first THz generation setup will be installed at the PITZ accelerator in the framework of a PhD thesis in 2017.

The group also started to investigate the possibility to generate MHz-pulsed, ultrashort electron bunches based on the PITZ photoinjector. First simulation results have shown the capability of generating low-charge, sub-10 fs electron bunches in the long electron bunch trains at PITZ (Fig. 3), and further optimisations are ongoing.

Contact: Anne Oppelt, anne.oppelt@desy.de

European XFEL.

Accelerator installation and injector commissioning completed

The linear accelerator complex of the European XFEL X-ray free-electron laser and its comprehensive infrastructure are being constructed by an international Accelerator Consortium of 17 European research institutes under the leadership of DESY, the main shareholder of the facility. In 2016, installation in the main linear accelerator tunnel was finished, and the superconducting part of the accelerator was cooled down in order for operation to start at the beginning of January 2017. Installation work in the other tunnel sections continued. By mid-2016, the injector commissioning, which had begun at the end of 2015, was successfully completed, with all performance goals reached.

Progress in 2016

The accelerator complex of the European XFEL consists of the 40 m long injector, the 1.3 km long cold (i.e. cryogenically cooled) main linear accelerator with altogether 96 superconducting accelerator modules and about 3.3 km of warm (i.e. not cryogenically cooled) beamlines used to transport the electron beam either between successive linear accelerator sections or to the undulators.

The section in the 2 km long main linear accelerator tunnel (XTL) was completed in 2016, and its commissioning started with the cool-down of the superconducting modules. The injector was operated for seven months before it was shut down to finalise the connection of the cryogenic systems.

Linear accelerator installation completed

The production of accelerator modules at CEA in Saclay, France, was concluded with the delivery of Module XM100 at the end of July 2016. For schedule reasons and because a few modules needed sophisticated repair, it was decided to stop the tunnel installation after 96 series modules. This decision was supported by the fact that the excellent performance of the installed 96 modules guarantees an energy reach already well above the European XFEL specification of 17.5 GeV.

The main accelerator in XTL consists of nine cryogenic strings (CS), typically comprising 12 modules with eight cavities each. Only CS1 consists of four modules, which accelerate the electron beam to the intermediate energy needed in the first bunch compressor. As a consequence of the reduction to 96 modules, CS9 includes only eight modules. For the initial commissioning, CS8 and CS9 will remain inactive, as the technical commissioning of CS8 requires some final preparations scheduled for early 2017. Installation of CS9, which suffered an incident during a pressure test of a helium exhaust line just prior to the first cool-down, will be finished in

extended maintenance periods. Most of the damage along CS9 was repaired in late fall 2016, but the radio frequency (RF) waveguide distribution required the procurement of replacement parts. Nevertheless, operation of all cryogenic strings including CS8 will allow a beam energy of 17.5 GeV to be reached in summer 2017.

Following the module installation, the remaining RF power stations – consisting of pulse transformer, klystron and waveguide distribution system – were installed. In addition, electronic cabinets housing low-level RF controls, electron beam diagnostics, and vacuum and cryogenic controls were positioned underneath the linear accelerator sections. Downstream of the cold linear accelerator, the last beamline components were installed, including beamline magnets, vacuum chambers with pumps, kicker magnets to distribute the beam to the different downstream tunnels and electron beam diagnostics. With the cabling of all the components, work in XTL was finished by fall 2016.



Figure 1
Connecting the beam vacuum systems of two superconducting modules of the European XFEL linear accelerator, using a small, localised cleanroom



Figure 2

View along the 80 modules of the linear accelerator section L3 in the European XFEL main tunnel. Underneath the accelerator is a standard RF power station supplying four accelerator modules, followed by shielded electronic cabinets housing a variety of systems.

In December 2016, the cryogenic system was fully commissioned and the first cool-down of the accelerator started. The thorough assembly and installation of the accelerator modules, cryogenic boxes and transfer lines paid off: neither vacuum leaks nor cold leaks (i.e. helium leaks opening at cold temperatures) were found, which constitutes an excellent basis for the future long-term operation of the linear accelerator.

Injector performance goals reached

The 40 m long injector is the first section of the accelerator. All the members of the Accelerator Consortium contributed to its construction. As the injector comprises almost all sub-systems that are also present in the other parts of the accelerator, its commissioning and operation not only posed various electron beam dynamics challenges but also served as an extensive system test.

With the round-the-clock routine operation of the first two superconducting accelerator modules – a standard 1.3 GHz module and a 3.9 GHz higher-harmonic module used to manipulate the longitudinal beam shape – the commissioning team gained valuable experience for the commissioning of the other 96 modules now installed in the tunnel. The geometric properties of the 3.9 GHz system, in particular, proved to be very sensitive to slight variations in helium pressure, and detuning was often observed before a change in pressure was registered in the cryogenic system itself. To resolve the issue, suitable pressure sensors in the main linear accelerator will be included in the regulation loops.

The interplay between the two RF systems and their combined effect on the electron beam can be observed with the help of a transverse deflecting system. To this end, a transverse RF field is applied along the length of the electron bunch, giving the head and the tail of the bunch different transverse offsets. The energy spread along the bunch can

then be observed on a screen after a spectrometer dipole. By adjusting the amplitude and phase of the RF systems with respect to each other, the energy spread can be minimised.

As a measure of the beam phase space volume, the emittance is one of the most important electron beam parameters. It is determined in the injector by means of a sequence of four consecutive beam imaging screens mounted about 4 mm off the nominal beam trajectory. Using fast kicker magnets, individual bunches can be steered onto the screens. This system allows a fast and almost non-invasive emittance measurement even along a bunch train. After careful tuning of the injector parameters, the target value of <math><1\text{ mm mrad}</math> was routinely observed.

The superconducting accelerator can accelerate bunch trains of 2700 electron bunches at a repetition rate of 10 Hz. This mode was successfully established in the injector, entailing the use of the 4 kW high-power beam absorber at the end of the injector. In total, a beam charge of about 3 C was produced during the injector commissioning – that is, about the same order of magnitude as the LCLS X-ray FEL at SLAC in the USA has produced so far since its startup in 2009.

Transition to user operation

The year 2017 will be extremely busy and exciting for the Accelerator Consortium. The technical commissioning of the European XFEL accelerator will lead to the operation of the world's largest superconducting linear accelerator. Under the leadership of DESY, beam commissioning will begin, with the goal to observe first lasing in the SASE1 undulator by early summer.

Contact: Hans Weise, hans.weise@desy.de
 Winfried Decking, winfried.decking@desy.de



Highlights · New technology · Developments.

➤	FLASH starts user operation	32
➤	Novel beam phase monitoring at the European XFEL	34
➤	Photocathodes at FLASH	36
➤	First demonstration of harmonic lasing at FLASH2	38
➤	Reverse undulator tapering at FLASH2	40
➤	Extended FLASH2 operation modes	42
➤	Harmonic footprint	46
➤	Bunch purity at PETRA III	48
➤	Finalisation of the European XFEL main accelerator	50
➤	Accelerator modules for the European XFEL	52
➤	Phase space manipulation in the European XFEL injector	54
➤	Dry-ice cleaning of high-power RF components	56
➤	LUX	58
➤	Taming plasma waves	60
➤	EuPRAXIA	62

FLASH2 starts user operation.

Operation of two beamlines in full swing

The second free-electron laser (FEL) line at DESY's FLASH facility allows two independent experiments to be run simultaneously, both delivering intense, short FEL pulses in the range from XUV to soft X-rays with user-specific parameters. In April 2016, FLASH ran in parallel operation for two user experiments with different FEL pulse requirements for the first time. In May 2016, a record self-amplified spontaneous emission (SASE) of 1 mJ in a single pulse was achieved twice, at a wavelength of 21 nm and 12.6 nm. With the FLASH2 variable-gap undulators, many lasing schemes proposed in the past can finally be tested: linear and quadratic tapering, frequency doubling, harmonic lasing and reverse undulator tapering.

First user operation at FLASH2

The FLASH facility has been delivering FEL pulses in the wavelength range from XUV to soft X-rays since 2005. The extension of FLASH by a second undulator beamline now allows multi-user operation. Both undulator beamlines are driven by the same linear accelerator. A fast kicker system and a Lambertson septum are used to extract a part of the bunch train into the FLASH2 beamline. FLASH2 has variable-gap undulators, which allow the wavelength to be chosen to a certain extent independently of FLASH1. In order to operate FLASH2 almost independently of FLASH1, a second injector laser specifically for FLASH2 and a new flexible low-level RF system were installed. First lasing of FLASH2 was achieved in August 2014 simultaneously to FLASH1 user operation. On 8 April 2016, two user experiments were run in parallel for the first time. In 2016, FLASH2 was operated for 1570 h for users.

The simultaneous user operation entails some challenges. For operation with long pulse trains, the available RF flat-top pulse duration needs to be shared between the FLASH1 and

FLASH2 experiments. Figure 1 shows an example of FLASH1 running with 250 bunches of about 300 pC at 1 MHz repetition rate and FLASH2 running with 50 bunches of about 100 pC at 200 kHz – with both undulator beamlines sharing the available RF pulse duration.

Since FLASH1 is still equipped with fixed-gap undulators, all wavelength changes in FLASH1 require a change of the electron beam energy. In consequence, each change of wavelength in FLASH1 requires a new setup and SASE tuning for FLASH2 as well. For FLASH2, a wavelength change is much easier. The variable-gap undulators allow tuning of the wavelength between the FLASH1 wavelength and three times the FLASH1 wavelength. This was demonstrated by the measured FLASH2 wavelengths achieved so far, as shown in Fig. 2. The black line represents the corresponding wavelength at FLASH1 and the grey line the triple of that value. The red dots indicate the wavelength reached for a given beam energy.

Variable-gap undulators also allow tapering. While travelling through the undulators, the electrons lose energy to the SASE radiation and slip off the resonance condition. This can be compensated by slightly adjusting the gap of the last undulators, keeping the electrons always in resonance. With this “trick”, the SASE energy can be substantially increased by about a factor of two.

Moreover, the variable-gap undulators offer the opportunity to test and implement special lasing schemes, such as frequency doubling and harmonic lasing.

The requirements for the FEL beam depend on the experiments. One major figure of merit is the SASE energy. Figure 3

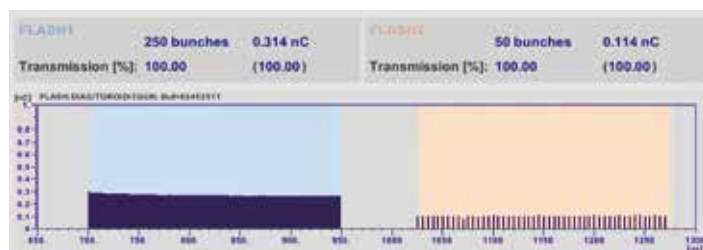


Figure 1

Example of bunch trains with different charges and repetition rates shared between FLASH1 and FLASH2. Here, the repetition rate is 1 MHz for FLASH1 and 200 kHz for FLASH2.

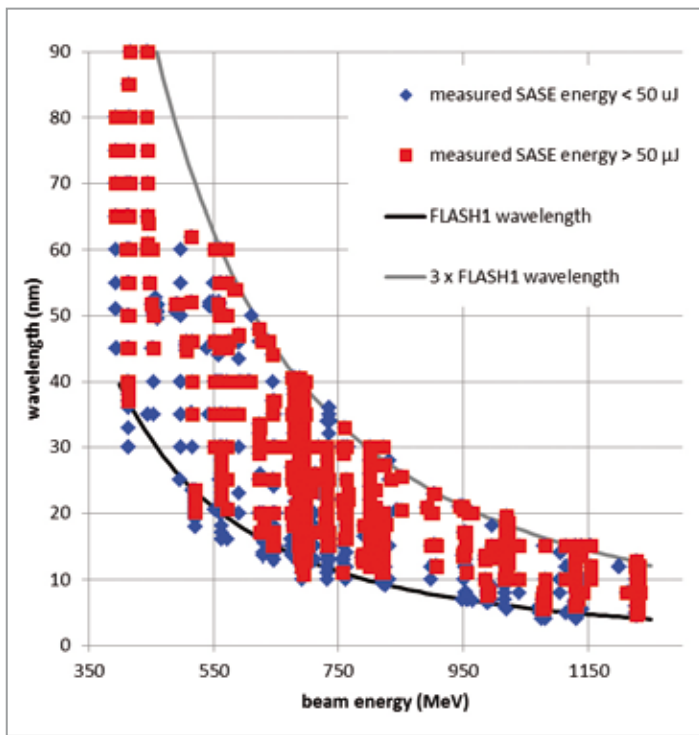


Figure 2

SASE wavelength demonstrated at FLASH2 as a function of the electron beam energy. FLASH2 was designed to reach wavelengths between the FLASH1 wavelength determined by the beam energy (black line) and three times this wavelength (grey line).

shows the achieved SASE energies as a function of the wavelength. The potential of undulator tapering is demonstrated by the generation of SASE at a wavelength of 21 nm with a single-pulse energy of 1 mJ – a record energy that is impossible to realise at FLASH1. This corresponds to 10^{14} photons, a value never reached at this wavelength in a single pulse. Similar results have been achieved at other wavelengths as well, e.g. at 12.6 nm. In general, single-pulse energies above 200 μJ are much easier to realise than at FLASH1 and have been demonstrated for many wavelengths between 7 nm and 90 nm. The different colours in Fig. 3

represent different charge ranges. FLASH2 is typically operated with bunch charges between 20 pC and 350 pC, but higher charges are possible as well.

Some user experiments are not so much interested in maximum pulse energy but more in very short FEL pulses with a duration below 50 fs. Such short pulses are typically generated with bunch charges below 200 pC.

Contact: *Juliane Rönsch-Schulenburg*
juliane.roensch@desy.de

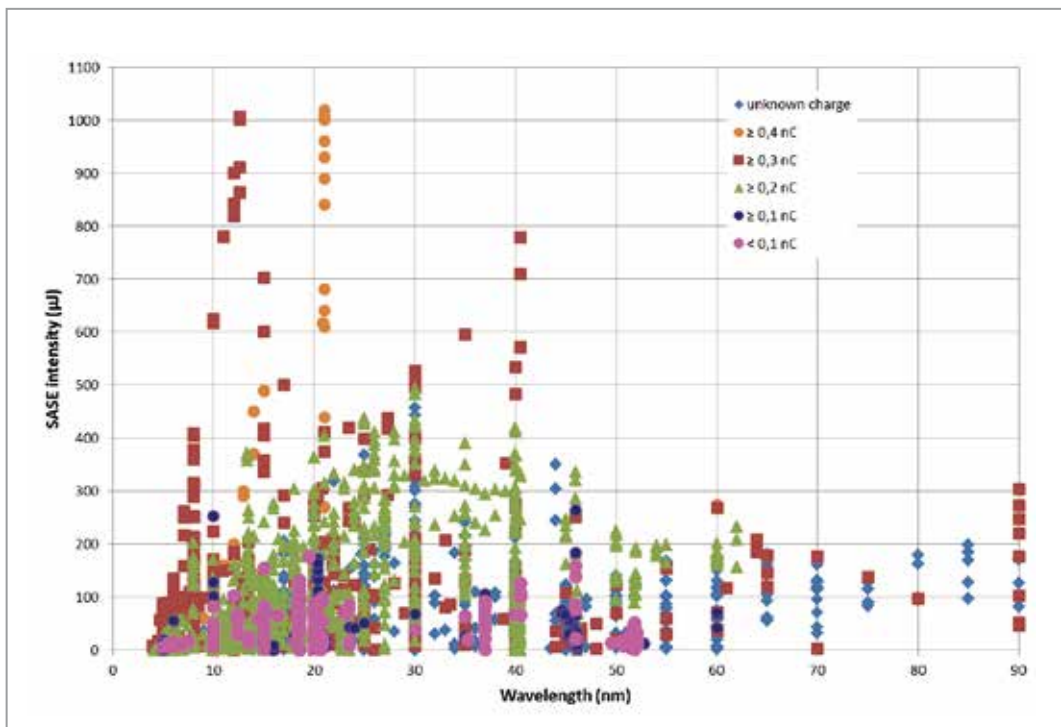


Figure 3

SASE energies as a function of wavelength measured at FLASH2. The different colours represent different charge ranges.

Novel beam phase monitoring at the European XFEL.

Direct online beam-to-RF phase monitoring based on higher-order modes

In order to generate high-quality photon beams at the European XFEL X-ray laser, the radio frequency (RF) field inside the superconducting cavities needs to be controlled with a precision better than 0.01° and 0.01% in phase and amplitude, respectively. To this end, we have developed a method to directly measure the beam phase with respect to the RF accelerating field based on beam-excited higher-order monopole modes. A setup based on a fast oscilloscope for the phase measurement was proposed and implemented, first at DESY's FLASH free-electron laser and then at the European XFEL. The measurements are complemented by a coupled circuit simulation, which quantifies the dependence of the resolution on the signal-to-noise ratio and the sampling frequency. The system can provide independent measurements of the beam phase to the control system. Prototype electronics are currently under construction.

Introduction

The European XFEL will accelerate bunches of electrons to tens of GeV in superconducting cavities. In order to produce the high-quality electron beams required for generating high-power, ultrashort, coherent photon pulses, the accelerating RF field has to be controlled to better than 0.01° in phase and 0.01% in amplitude. Control is performed by a dedicated low-level RF (LLRF) system, which uses the input of various precise beam monitors. We have proposed and tested a new phase monitor based on the inspection of resonant fields excited by the electron bunches in the accelerating cavities.

When a bunch of electrons traverses a cavity, it excites resonant electromagnetic fields called higher-order modes (HOMs). These can seriously degrade the electron beam quality if left unchecked and, in the worst case, cause beam breakup. Therefore, power from these fields has to be extracted out of the cavity by means of special couplers. The extracted HOM signals carry useful information about the beam and can thus be used to infer some of its characteristics. Certain modes, called monopole modes, are independent of the beam offsets and proportional to the beam charge. This property makes them attractive for beam phase monitoring, as illustrated below.

In the TESLA-type cavities employed at FLASH and the European XFEL, the RF field used for acceleration has a frequency of 1.3 GHz , while the frequency of the beam-excited monopole modes used for phase monitoring is around 2.4 GHz . By comparing these modes obtained from the HOM couplers, the beam phase relative to the RF field can be obtained.

Coupled circuit model

A circuit model (similar to the one originally developed by D. Nagle, E. Knapp and B. Knapp in 1967) is used to simulate

the beam phase monitoring. The advantage of the model, which is shown schematically in Fig. 1, is that it is quite time-efficient. As the TESLA-type cavities have nine cells, the model consists of nine coupled circuit units. A Gaussian current source is introduced to simulate the beam. A delay between the current pulses in each cell is used to simulate the propagation of the electron beam. The voltages across the first and ninth cell, denoted HOM1 and HOM2, respectively, are superimposed with a 1.3 GHz signal to simulate the signal at the HOM ports.

The obtained signals are analysed to determine the beam phase with respect to the superimposed RF field. As can be seen from Fig. 2, the resolution depends strongly on the signal-to-noise ratio (SNR) and the sampling frequency. A SNR of at least 35 dB is required to obtain a resolution of 0.01° .

Experimental setup

The experimental setup is presented schematically in Fig. 3, which shows one of the two channels installed at one cavity. The signal from the HOM coupler is split in two for bandpass

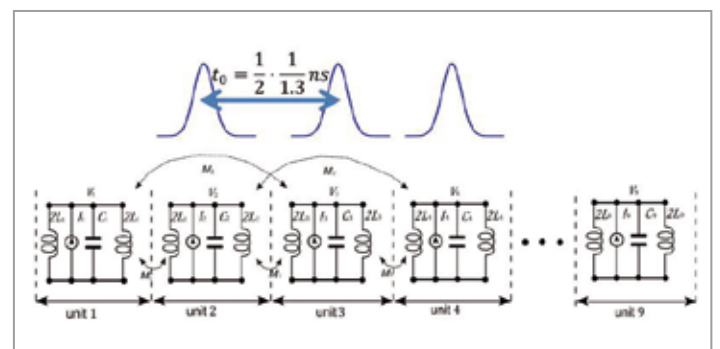


Figure 1
Coupled circuit model with nine units driven by a Gaussian pulse

filtering: one centred at 1.3 GHz, the other at 2.4 GHz. The filtered signals are then combined again before being fed into a fast Tektronix oscilloscope with 20 GS/s sampling rate and 6 GHz bandwidth. The acquired data is transferred to a data acquisition computer via a VX11-LAN link. Data is read from the accelerator control system as well.

Figure 4 shows the spectrum of the measured 1.3 GHz signal and the higher-order monopole band. The last couple of monopole modes in the band delivering stronger signals were chosen for this purpose.

The phase of the beam with respect to the accelerating field can be obtained by comparing the 1.3 GHz and 2.4 GHz signals. The phase obtained is shown in Fig. 5 for an RF phase set to -5° , 0° and 5° . The resolution is 0.12° for a beam charge of 0.5 nC and an accelerating gradient of 22 MV/m. Using this setup, a resolution of ca. 0.1° rms is typically obtained with this beam charge and accelerating gradient for both FLASH and the European XFEL. With a higher SNR, the best resolution observed is 0.03° at FLASH.

Summary and outlook

A resolution of 0.1° of the measurement of the beam phase with respect to the accelerating RF field can be guaranteed based on the current experimental setup, though a higher resolution of up to 0.03° has been observed. The simulation results from the coupled circuit agree well with the experiments, quantifying that a SNR of at least 35 dB is needed to obtain a resolution of 0.01° .

The system can be used for monitoring long-term beam phase drifts and correcting them via the LLRF system. Moreover, it can help to decouple possible phase jitter and drift contributions from the accelerator module, the third-harmonic module and the gun.

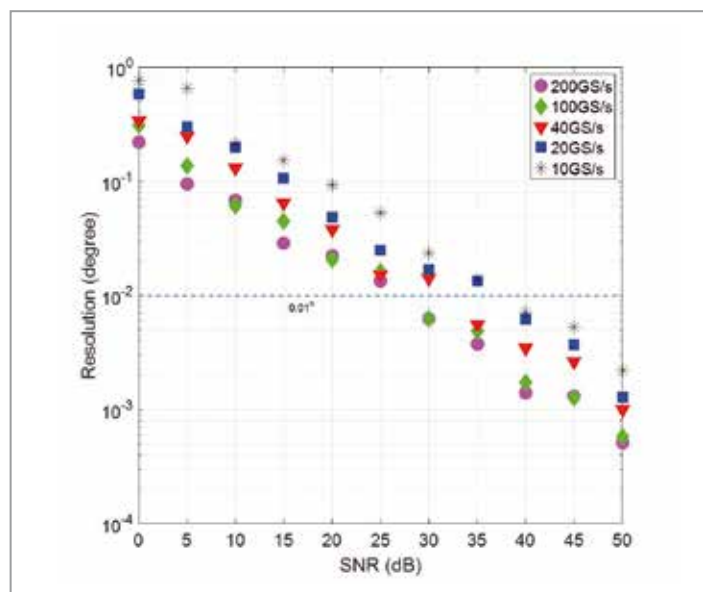


Figure 2
Dependence of the resolution on SNR and sampling frequency

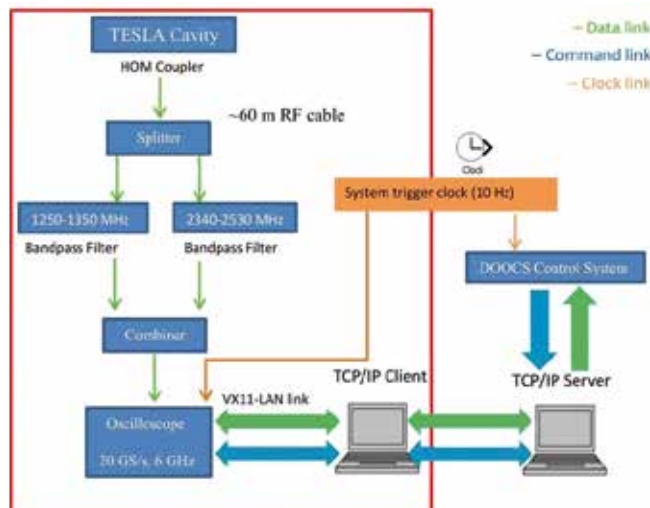


Figure 3
Experimental setup for beam phase determination

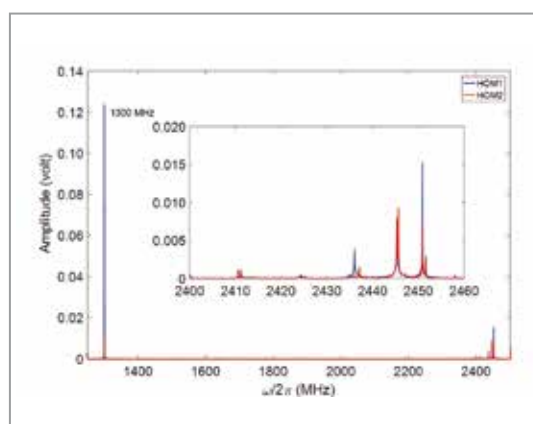


Figure 4
Example of a spectrum measured from both HOM couplers of Cavity 2 in the European XFEL injector module

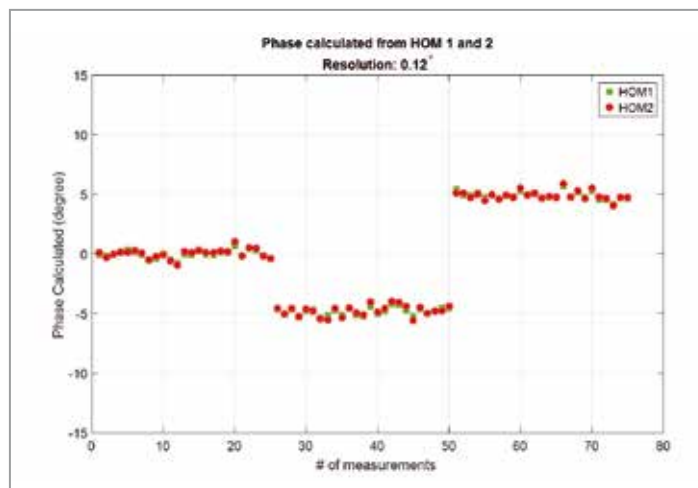


Figure 5
HOM-based beam phase versus change in klystron phase

Prototype electronics based on the MicroTCA standard are being developed, using a direct sampling technique rather than the usual down-converting scheme. The electronics also monitor HOMs around 1.7 GHz for beam position monitoring.

Contact: Liangliang Shi, liangliang.shi@desy.de
Nicoleta Baboi, nicoleta.baboi@desy.de

Photocathodes at FLASH.

An apparently infinite source of bright electrons

Beam at DESY's FLASH soft X-ray free-electron laser facility starts at the photocathode – point zero. The cathode is a thin film of caesium telluride on a molybdenum plug inserted from the back into the radio frequency electron source (RF gun). As a high-duty-cycle machine, FLASH accelerates thousands of electron bunches per second. Only a high-quantum-efficiency cathode can meet this requirement. A special laser system perfectly synchronised to the RF field of the gun sends picosecond-long UV laser pulses to the cathode. The laser photons have just enough energy to liberate electrons into free space, which form a bunch to be accelerated in FLASH. A crucial factor for durable high quantum efficiency (QE) – i.e. the number of electrons liberated per laser pulse – is the vacuum condition in the RF gun. Great care has therefore been taken to keep the RF gun clean and realise permanent ultrahigh-vacuum conditions. The QE is monitored on a regular basis to detect possibly serious drops in efficiency. The present cathode is very stable; it has been in operation for a record time of more than 750 days.

Photocathodes

There are only a few candidates for high-QE cathodes suitable for high-brightness electron sources. Caesium telluride (Cs_2Te) is the choice for FLASH. In cooperation with LASA in Segrate near Milano, Italy, cathodes were already produced in 1997 within the TESLA collaboration for the TESLA Test Facility injector 2. Cathodes are prepared in special chambers: one was set up at LASA and a copy at DESY. The cathode is a thin film deposited on a molybdenum plug. First, a 10 nm thin layer of tellurium is formed with a diameter of 5 mm. Afterwards, caesium is deposited onto the film. Caesium evaporation is stopped once the QE is maximised. As this type of cathode needs to be kept under clean ultrahigh vacuum all the time, a transport chamber powered by a car battery has been developed, which allows the cathodes to be moved around Europe – from Milano to Hamburg, but also to DESY's PITZ photoinjector test facility in Zeuthen. It has been shown that, even after long-time storage, the QE is maintained at its initial value – provided that the vacuum conditions stay perfect.

Quantum efficiency

The QE is defined as the ratio of the number of electrons emitted from the cathode to the number of photons impinging it. The spectral response – i.e. QE as a function of photon energy – has been measured with a high-pressure mercury lamp scanning the photon energy from 3 to 5 eV (Fig. 1). From these measurements, we deduce a work function of 3.5 eV, in agreement with literature. From another measurement – of QE as a function of the accelerating field on the cathode – we get a value of 3.6 eV, consistent with the first one.

From the spectral response, we know that the highest QE is obtained for photon energies around 5 eV. This energy fits well with the fourth harmonic of the wavelength emitted by standard solid-state laser materials. FLASH uses two lasers based on Nd:YLF (1047 nm) and one on Yb:YAG (1030 nm), with the fourth harmonic at 262 nm and 257 nm, respectively, corresponding to about 4.7 eV. From the spectral response shown in Fig. 1, we obtain a QE of 10%, which is sufficient for the high-duty-cycle operation of FLASH. A high QE considerably reduces the cost and complexity of the laser systems. In our case, the average powers of the laser systems are kept below 1 W, which is a reasonable number for robust and reliable laser operation.

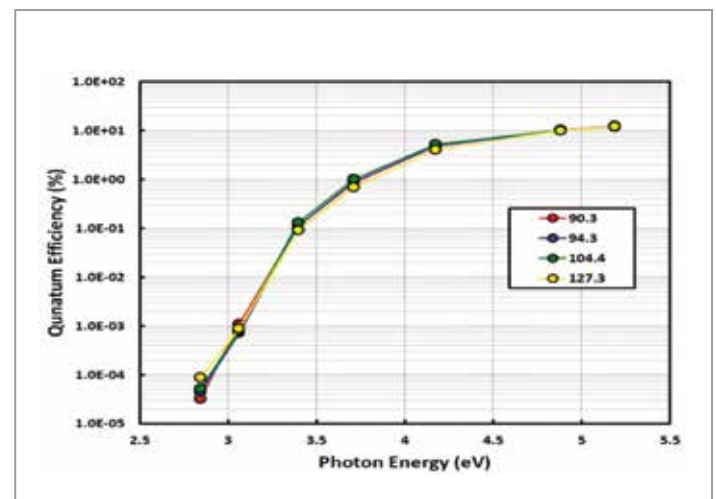


Figure 1
Spectral response of four Cs_2Te cathodes

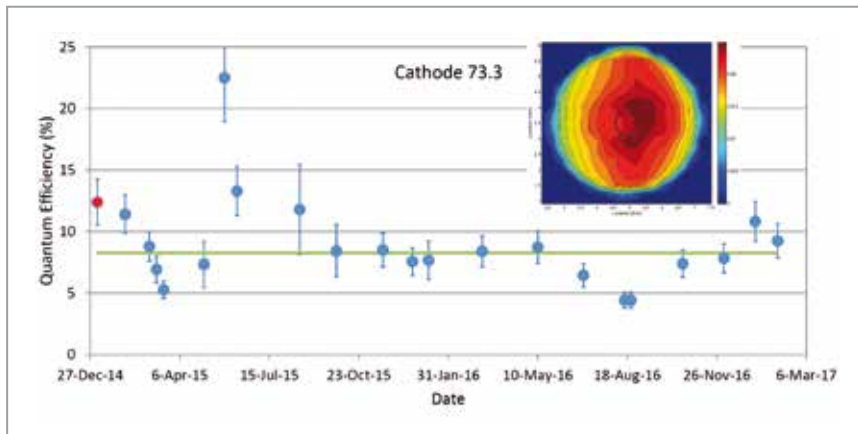


Figure 2
Quantum efficiency of Cathode 73.3 measured at regular intervals during operation at FLASH. The red dot indicates the initial QE just after production at LASA, on 26 June 2013. As of 28 February 2017, the cathode has been in operation for 755 days with a total charge emitted of 12 C. The insert shows a QE map taken in February 2017. The position and approximate size of the laser beam are indicated by a black circle. The QE at this position is 9.2%.

Lifetime

The lifetime of a cathode is a crucial parameter. Whenever the QE falls below a critical value, the lasers will not be able to produce the charge required for beam operation. For the present laser systems, this limit is around 1%. The FLASH cathode load-lock system has four cathodes stored in ultrahigh-vacuum chambers flanged to the RF gun, ready for being used. If a photocathode fails, it can be replaced quickly within two hours. Once all cathodes are used up, a new box with fresh cathodes is installed within a few days. Fortunately, the vacuum conditions in the RF gun remain good, so that we can expect a long cathode lifetime also in the future.

To estimate the lifetime, we measure the QE at intervals of a few weeks. We also scan the cathode with a tiny 100 μm laser beam spot to produce a so-called QE map, which yields two types of information: how homogeneous the electron emission over the cathode is and how well the laser is aligned. What we are actually interested in is the “effective” QE. To this end, we measure the number of electrons accelerated in the gun with a toroidal coil and the number of photons on the cathode with a pyro-electric joulemeter (accuracy 2%).

Figure 2 shows the QE of Cathode 73.3 measured at regular intervals during operation at FLASH. The initial QE just after production at LASA, on 26 June 2013, was 12.3%. As of 28 February 2017, the cathode has been in operation at FLASH for 755 days with a total charge emitted of 12 C. The QE measured in February 2017 was 9.2%.

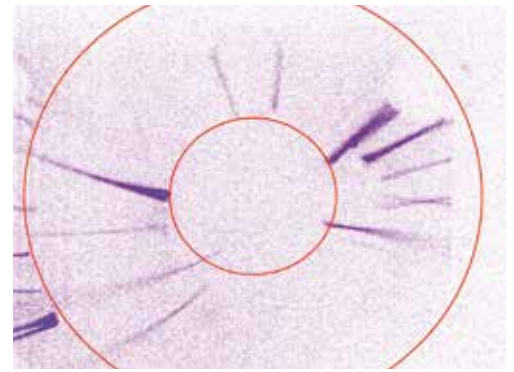


Figure 3
Dark current measured at screen 3GUN (1.5 m downstream of the cathode). The RF gun is operated with 5 MW forward power corresponding to a 53 MV/m field gradient on the cathode and with a solenoid current of 309 A (0.182 T). The total dark current is 6 μA . The circles approximately indicate the rim of the cathode plug (outer circle) and the cathode's Cs_2Te thin film (inner circle).

The insert in Fig. 2 shows a QE map. The position and approximate size of the laser beam are indicated by a black circle. The photocathode diameter is 5 mm, the laser spot diameter usually 1.2 mm. With time, the overall QE degrades slowly. However, the spot where the laser hits degrades faster initially, but recovers again later.

Dark current

Field emitters from particles or surface defects are a source of dark current, i.e. electrons emitted in the presence of a high electric field. This dark current is unwanted; moreover, it is lost in many places along the accelerator due to its large energy spread and is a source of activation of beamline materials. An increase in dark current may also indicate surface damage induced by thermal stress or RF field breakdown events.

Figure 3 shows an image of dark current taken on a YAG powder screen 1.5 m downstream of the cathode. The RF gun is operated with 5 MW forward power corresponding to a 53 MV/m field gradient on the cathode and with a solenoid current of 309 A (0.182 T). The total dark current measured at this location is a stable 6 to 10 μA – a value that is acceptable.

Contact: Siegfried Schreiber, siegfried.schreiber@desy.de
Sven Lederer, sven.lederer@desy.de

First demonstration of harmonic lasing at FLASH2.

Improving temporal coherence and radiation power, providing higher-energy photons

Harmonic lasing is a prospective operation mode of X-ray free-electron laser (FEL) user facilities that allows for generating brighter beams of higher-energy photons and for realising a harmonic lasing self-seeded (HLSS) FEL [1]. In 2016, harmonic lasing was successfully demonstrated at FLASH2, the second undulator line of DESY's FLASH soft X-ray FEL facility, in the wavelength range between 4.5 nm and 15 nm [2,3]. The spectral brightness was improved in comparison with the self-amplified spontaneous emission (SASE) FEL mode by a factor of 6 in the exponential gain regime. A better performance of the HLSS FEL with respect to the SASE FEL in the post-saturation regime with a tapered undulator was observed as well.

The HLSS FEL scheme

The development of X-ray FEL schemes with enhanced spectral brightness is of great practical importance. In addition to well-known seeding and self-seeding techniques, there are also schemes that don't use optical elements. One of them is the HLSS FEL scheme, which is based on the combined lasing on a harmonic in the first part of the undulator, with increased undulator parameter K , and on the fundamental in the second part [1]. In this way, the second part of the undulator is seeded by a narrow-band signal generated through harmonic lasing in the first part (Fig. 1).

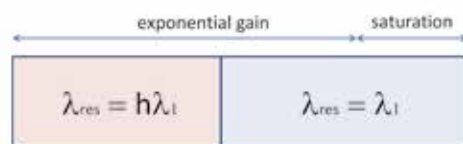


Figure 1
Conceptual scheme of a HLSS FEL

First demonstration

HLSS FEL operation at FLASH2 was successfully demonstrated in several test runs in 2016 at different electron energies and radiation wavelengths [2,3]. The first evidence of harmonic lasing was observed on 1 May. The electron energy was 948 MeV. Initially, we tuned ten undulator sections to standard SASE, operating in the exponential gain regime at a

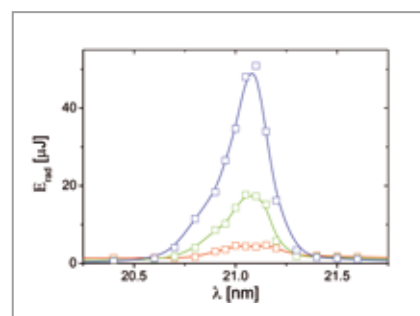


Figure 2
Scan of the resonance wavelength of the first part of the undulator with one undulator section (red), two sections (green) and three sections (blue). The pulse energy is measured after the second part of the undulator, tuned to 7 nm.

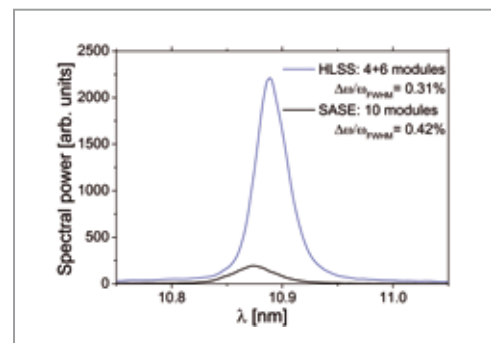


Figure 3
Spectral density of the radiation energy for the HLSS (blue) and SASE (black) configuration

wavelength of 7 nm (the rms K parameter was 0.73); the pulse energy was 12 μJ . Then we gradually tuned the first three sections to the third subharmonic (the rms K parameter was 1.9) and scanned them around 21 nm (Fig. 2). The output pulse energy at 7 nm exhibits a strong non-linear dependence on the length of the seeding section tuned to 21 nm, which happens due to the third-harmonic lasing in the first part. Also, the effect is essentially resonant. When three seeding undulator sections were scanned (blue line), the ratio of the pulse energies at the optimal tune (21.1 nm) and at the 20 nm tune was 51 μJ / 0.3 μJ = 170. This ratio is likely underestimated because of the background radiation at the fundamental at 20 nm.

Further studies

The HLSS FEL studies at FLASH2 continued in June 2016 with the photon beam spectrometer available. Since the electron energy was different (757 MeV), lasing occurred at another wavelength, 11 nm. The undulator settings were similar to the previous case: we used ten undulator sections, and the rms K parameter was 0.73 in the SASE mode and 1.9 in the first part of the undulator in the HLSS mode. The difference with the previous measurements was that we detuned four undulator sections in the HLSS regime. The pulse energies were 11 μJ in the SASE mode and 53 μJ in the HLSS mode. The spectra were measured with the wide-spectral-range XUV spectrometer of FLASH2.

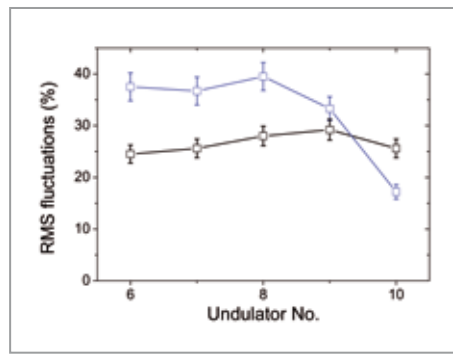
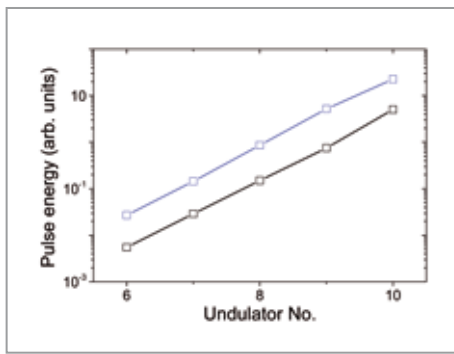


Figure 4

Radiation pulse energy (left) and pulse energy fluctuations (right) in the second part of the undulator for HLSS (blue) and SASE (black). A small aperture in front of an MCP detector is used for this measurement.

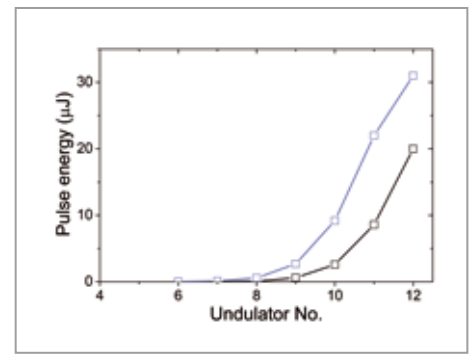


Figure 5

Radiation pulse energy versus position in the undulator for HLSS (blue) and SASE (black). The post-saturation taper was optimised in both cases.

Figure 3 presents averaged spectra for two study cases: SASE FEL with ten undulator sections and HLSS FEL with four sections tuned to 33 nm and six sections tuned to 11 nm. The spectral powers differ by a factor of 6 due to an increase of the pulse energy in the HLSS regime by a factor of 5 and a reduction of the bandwidth by a factor of 1.3 (0.31% for HLSS versus 0.41% for SASE). Our analysis showed that, under the given experimental conditions, the spectrum width was visibly widened due to the energy chirp along the electron beam [3].

We also performed a dedicated measurement proving an increase of the coherence time in the HLSS FEL case. The method is based on statistical measurements of the FEL pulse energy along the undulator length. In the high-gain linear regime, SASE FEL radiation has the statistics of completely chaotic polarised light. Shot-to-shot rms fluctuations of the FEL pulse energy σ after a pinhole are connected to the number of longitudinal modes by a simple relation, $M = 1/\sigma^2$ [4]. For a given FEL pulse length, the coherence length is inversely proportional to the number of longitudinal modes.

Figure 4 presents measurements of the FEL pulse energy and its fluctuations versus undulator length for a small aperture (significantly smaller than the FEL beam size) in front of a multichannel plate (MCP) detector. Measurements between Sections 6 to 8 (9) correspond to the high-gain exponential regime for the HLSS (SASE) configuration. With the data given in Fig. 4 (right), we obtained an estimate of an increase in coherence time at the end of the exponential gain regime by a factor of 1.8 ± 0.3 , which is in good agreement with the theoretical value [1]. Note that this moderate enhancement observed in our experiment is obtained because at FLASH2, we are limited to the application of the third (and no higher) harmonic. In a tuneable-gap undulator with higher K , such as the SASE3 undulator of the European XFEL X-ray laser (with an rms K parameter of about 7), one can in principle use a

much higher harmonic number, which is expected to yield a much higher coherence enhancement factor.

Post-saturation tapering

In November 2016, we set up the HLSS FEL configuration with the first four undulator sections tuned to 45 nm and eight sections tuned to 15 nm. The electron energy was 645 MeV, the charge was 100 pC, and the rms value of K was 1.9 in the first part of the undulator and 0.73 in the second part. We reached FEL saturation in the SASE and HLSS modes, and applied post-saturation taper to improve the FEL efficiency (Fig. 5).

We used quadratic taper, and for each mode (HLSS and SASE), we optimised two parameters: the beginning of tapering and the taper depth. The pulse energy was enhanced in the HLSS configuration from 18 μ J in the non-tapered undulator to 31 μ J when the post-saturation taper was applied. In the SASE configuration, the respective enhancement was from 15 μ J to 20 μ J. Note that a similar efficiency enhancement was previously observed in numerical simulations [2]. The improvement of the post-saturation taper regime is achieved in the HLSS case because of an earlier saturation and a better longitudinal coherence than in the SASE case.

Contact: Evgeny Schneidmiller, evgeny.schneidmiller@desy.de
Mikhail Yurkov, mikhail.yurkov@desy.de

References:

- [1] E.A. Schneidmiller and M.V. Yurkov, Harmonic Lasing in X-ray Free electron Lasers, *Phys. Rev. ST Accel. Beams* 15, 080702 (2012).
- [2] E.A. Schneidmiller and M.V. Yurkov, Studies of Harmonic Lasing Self-seeded FEL at FLASH2, *Proceedings of IPAC2016, Busan, Korea*, p. 725.
- [3] E.A. Schneidmiller and M.V. Yurkov, First operation of a harmonic lasing self-seeded free electron laser, *Phys. Rev. ST Accel. Beams* 20, 020705 (2017).
- [4] E.A. Schneidmiller and M.V. Yurkov, Application of Statistical Methods for Measurements of the Coherence Properties of the Radiation from SASE FEL, *Proceedings of IPAC2016, Busan, Korea*, p. 738.

Reverse undulator tapering at FLASH2.

Paving the way for full polarisation control and attosecond pulses in X-ray FELs

The amplification process in a free-electron laser (FEL) can be effectively controlled by means of changing the resonance properties along the tuneable-gap undulator. An afterburner scheme based on reverse undulator tapering allows for achieving full control of the polarisation properties of the output radiation. The theoretical basis for this scheme was developed at DESY [1] and successfully realised in a proof-of-principle experiment at FLASH2 [2], the second undulator line of DESY's FLASH soft X-ray FEL facility, as well as at the LCLS X-ray laser at SLAC in the USA [3].

Reverse undulator tapering scheme

The baseline design of a typical X-ray FEL undulator assumes a planar configuration, which results in a linear polarisation of the FEL radiation. However, many experiments at X-ray FELs would profit from using circularly polarised radiation. As a cheap upgrade, the installation of a short helical afterburner can be considered, but then an efficient method is needed to suppress the powerful linearly polarised background from the main undulator. A new method for realising this suppression is based on the application of a reverse taper in the main undulator [1] (Fig. 1).

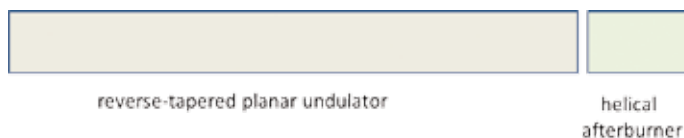


Figure 1
Conceptual scheme for obtaining circular polarisation at X-ray FELs [1]. Saturation is achieved with a strong microbunching and a suppressed radiation power in a tapered main (planar) undulator. Then the modulated beam radiates at full power in an afterburner tuned to the resonance.

It has been discovered that, in a certain range of the taper strength, the density modulation (bunching) at saturation is practically the same as in the case of a non-tapered undulator, while the power of the linearly polarised radiation is suppressed by orders of magnitude. The strongly modulated electron beam then radiates at full power in the afterburner.

Proof-of-principle experiment at FLASH2

Reverse tapering was successfully tested at FLASH2 [2], as shown in Fig. 2 and 3. The signal from the afterburner sections exhibits resonance behaviour and reaches a

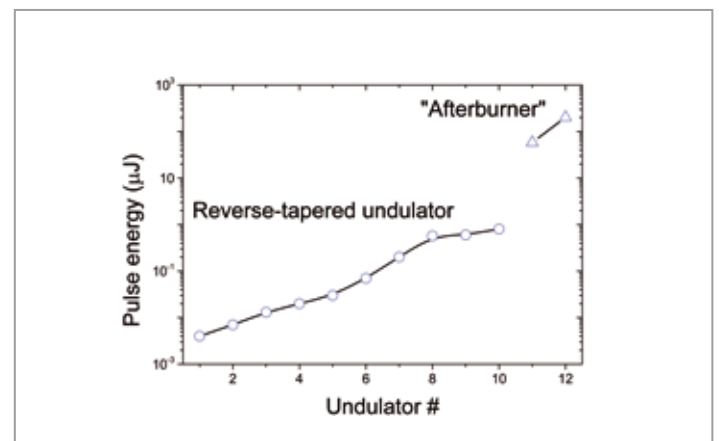


Figure 2
Proof-of-principle experiment at FLASH2 showing the evolution of the radiation pulse energy versus the undulator number. The first ten undulator sections are reverse-tapered (circles). The last two sections (triangles) are tuned to the resonance with the incoming microbunched beam.

maximum value when the resonance frequency of the afterburner matches the frequency of the electron beam modulation in the main undulator. An important figure of merit for the afterburner is the contrast, i.e. the ratio of the radiation powers from the afterburner and from the main undulator. We demonstrated that a contrast of 200 is achievable. For a helical afterburner, the contrast will increase up to 400. This means that the degree of circular polarisation from a helical afterburner will reach 99.8%.

The density modulations of the electron beam driving a self-amplified spontaneous emission (SASE) FEL in the saturation and post-saturation regime contain a rich spectrum of higher harmonics. The radiation of a SASE FEL with a planar

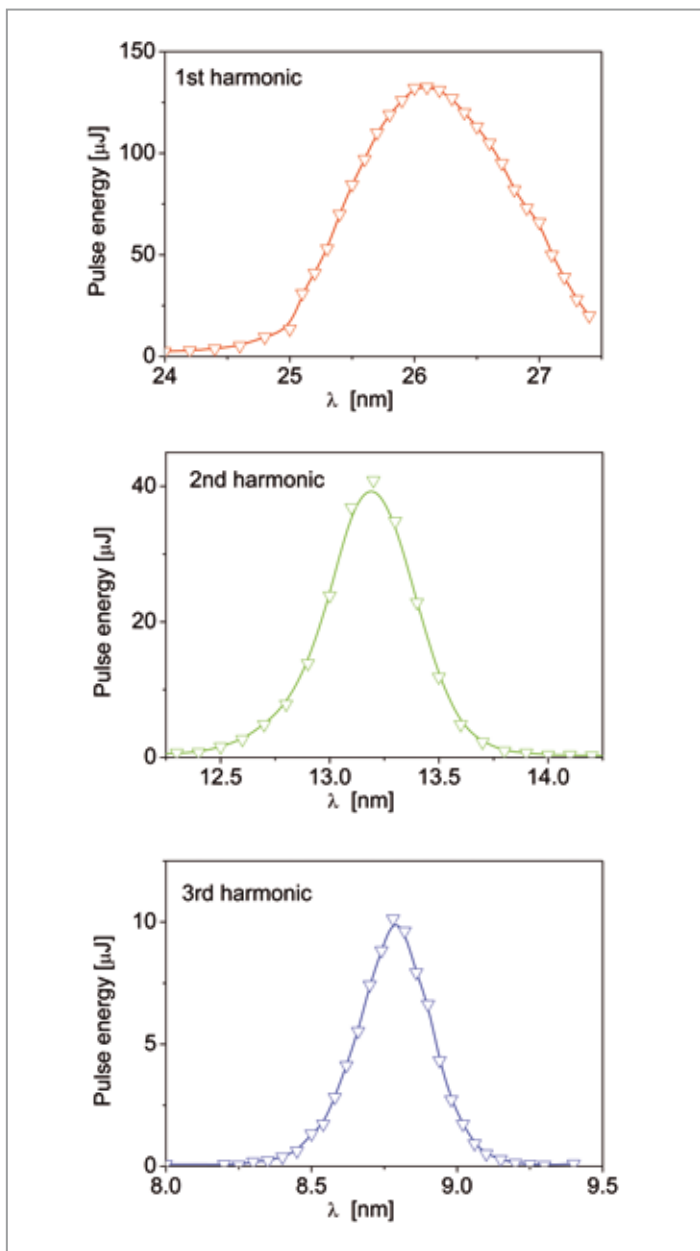


Figure 3
Afterburner at FLASH2. Output pulse energy versus resonance wavelength of two afterburner sections. Scans are performed for the fundamental (top), the second harmonic (middle) and the third harmonic (bottom). The first ten undulator sections are tuned to the resonance wavelength of 26.5 nm with 5% reverse taper. The scan around 26 nm is limited due to the undulator gap limit of 9 mm.

undulator contains higher odd harmonics as well. However, their intensity is pretty low, with the third-harmonic intensity on the percent level and the fifth harmonic on the level of a fraction of a permille of the fundamental. This happens because of debunching of the electron beam at higher harmonics due to the strong interaction of the electron beam with the fundamental. Another important problem is a strong background of radiation from the main undulator.

The application of reverse tapering in the main undulator allows for reaching high values of beam bunching at higher harmonics with very low radiation background from the main undulator. The afterburner tuned to higher harmonics is then capable of generating much higher radiation

intensities than envisaged in the scheme with an untapered main undulator.

Relevant experimental results of the proof-of-principle experiment are presented in Fig. 3. Ten undulator sections of the main undulator were tuned to the radiation wavelength of 26.5 nm, and a reverse undulator tapering of 5% was applied. The two remaining sections were tuned to the maximums of the power around the fundamental harmonic (top), the second harmonic (middle) and the third harmonic (bottom). Radiation pulse energies were 150 μJ for the fundamental, 40 μJ for the second harmonic and 10 μJ for the third harmonic. We note that the pulse energy of the second harmonic is comparable with the pulse energy of the fundamental, and that the pulse energy of the third harmonic exceeds the level of the third harmonic from SASE FEL by an order of magnitude. Thus, the afterburner with reverse tapering scheme holds great potential for extending the operating wavelength range of X-ray FELs in general and FLASH in particular.

Further applications

The realisation of such a scheme in the SASE3 undulator of the European XFEL X-ray laser will allow the generation of X-ray radiation pulses with a peak power in excess of 100 GW and an ultimate high degree of circular polarisation [1]. The proposed technique is universal and can be easily implemented at all beamlines of the European XFEL and other X-ray FEL facilities. Recently, the scheme was successfully realised at LCLS [3].

Another important field of application of the reverse undulator tapering technique is the production of attosecond radiation pulses in X-ray FELs [4]. The attosecond X-ray FEL scheme is conceptually simple and involves two steps. First, the energy of a short slice of an electron bunch is modulated by a few-cycle optical laser. Then the modulated electron bunch passes a reverse-tapered undulator and radiates isolated, ultrashort X-ray pulses. These pulses are precisely synchronised to the optical laser, providing an opportunity to perform pump-probe experiments with sub-femtosecond temporal resolution.

*Contact: Evgeny Schneidmiller, evgeny.schneidmiller@desy.de
Mikhail Yurkov, mikhail.yurkov@desy.de*

References:

- [1] E.A. Schneidmiller and M.V. Yurkov, Obtaining high degree of circular polarization at x-ray free electron lasers via a reverse undulator taper, *Phys. Rev. ST Accel. Beams* 16, 110702 (2013).
- [2] E.A. Schneidmiller and M.V. Yurkov, Reverse undulator tapering for polarization control at XFELs, *Proc. IPAC2016 Conf.*, Busan, Korea, 2016. <http://accelconf.web.cern.ch/AccelConf/ipac2016/papers/mopow008.pdf>
- [3] A. Lutman et al., Polarization control in an X-ray free electron laser, *Nature Photonics* 10, 468 (2016).
- [4] E.L. Saldin, E.A. Schneidmiller and M.V. Yurkov, Self-amplified spontaneous emission FEL with energy-chirped electron beam and its application for generation of attosecond x-ray pulses, *Phys. Rev. ST Accel. Beams* 9, 050702 (2006).

Extended FLASH2 operation modes.

Two-colour mode of operation, reaching shorter wavelengths and higher photon flux

Variable-gap undulators support additional modes of operation beyond the standard self-amplified spontaneous emission (SASE) mode, providing modified radiation features and extending user capabilities. At FLASH2, the second undulator line of DESY's FLASH free-electron laser (FEL) facility, a frequency doubler is capable of producing two-colour pulses (ω , 2ω) with controllable pulse energy ratio. The optimisation of the frequency doubler for operation at shorter wavelengths allowed photon energies above the nitrogen *K*-edge to be reached, which significantly exceeds the original specifications of FLASH2 [1]. Radiation pulse energies in excess of 1 mJ were demonstrated by means of undulator tapering [2,3].

Frequency doubler at FLASH2

Extending the operating range of FLASH into the “water window” (i.e. the range between the *K*-absorption edges of carbon and oxygen at 4.38 nm and 2.34 nm, respectively) is highly desirable for the user community. With the maximum electron energy of 1.25 GeV, it is possible to operate both beamlines, FLASH1 and FLASH2, just a little below the carbon *K*-edge. Higher-order odd harmonics cover the water window, but with low intensities contaminated by a strong background from the fundamental.

With the tuneable-gap undulator of FLASH2, however, it is possible to realise a two-undulator, second-harmonic generation scheme allowing operation at shorter wavelengths [1]. A frequency doubler is also an attractive mode

of operation enabling two colours (ω , 2ω) to be generated simultaneously.

Realising the frequency doubler scheme with a tuneable-gap undulator is conceptually simple (Fig. 1). The first part of the undulator is tuned to the frequency ω . The amplification process develops up to the onset of the saturation regime when a visible beam modulation at the fundamental and at higher harmonics occurs, but the radiation power does not reach saturation. Then the electron beam enters the second part of the undulator tuned to the frequency 2ω , and the beam modulations at the second harmonic seed the amplification process.

The operation of the frequency doubler was successfully demonstrated during several test runs at FLASH2 in 2016. Figure 2 (left) shows the gain curve of the frequency doubler 8 nm \rightarrow 4 nm. The first five undulator sections were tuned to 8 nm and the last seven sections to 4 nm. The red and blue curves show the radiation pulse energies at 8 nm and 4 nm, respectively. The amplification process in the



Figure 1

Schematic layout of the frequency doubler. The first part of the undulator is tuned to the frequency ω , the second part to the frequency 2ω .

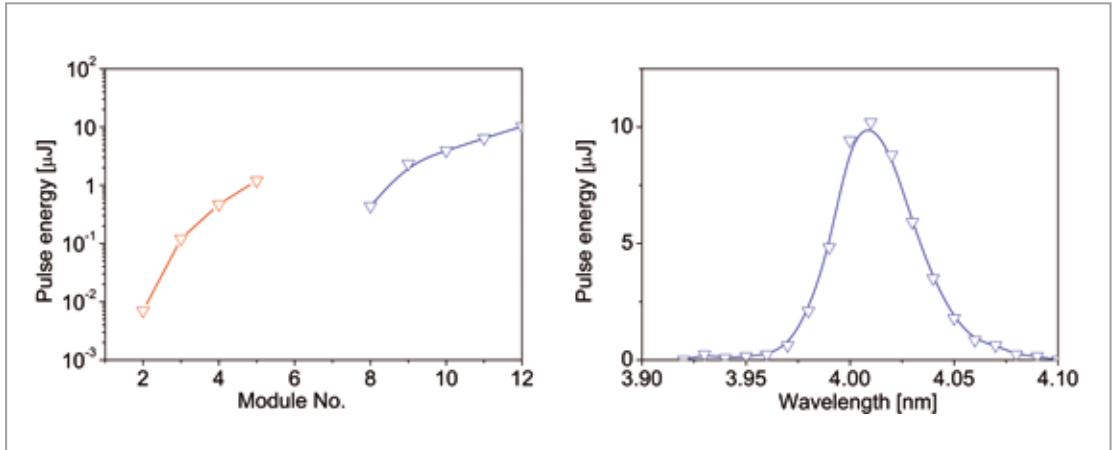


Figure 2
 Frequency doubler at FLASH2.
 Left: Gain curve of the frequency doubler at FLASH2. The first part of the undulator (five sections) is tuned to 8 nm, the second part (seven sections) to 4 nm. The red and blue colours correspond to the radiation wavelengths of 8 nm and 4 nm, respectively. Right: Radiation pulse energy at the second harmonic versus resonance frequency of the second part of the undulator.

second part (frequency doubler) exhibits resonance behaviour on the frequency tuning (Fig. 2 right). Even harmonics of the radiation are strongly suppressed in the

planar undulator, confirming that the beam bunching at the second harmonic seeds the amplification process of the frequency-doubling sections.

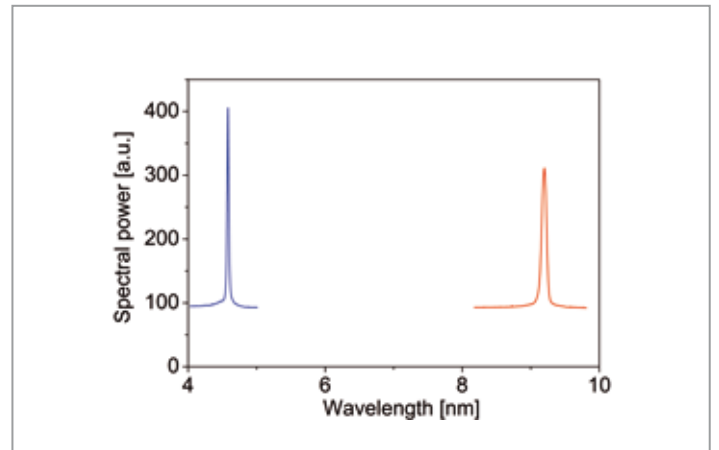
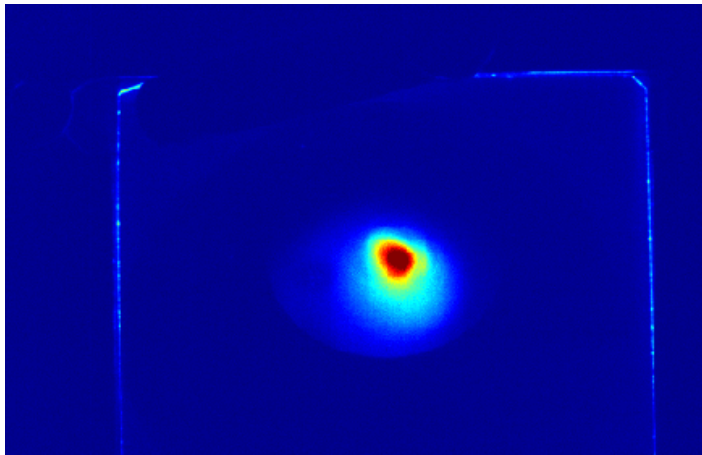


Figure 3
 Frequency doubler at FLASH2. Left: Image of the photon beam in the experimental hall. The small red spot is the 4.5 nm (second harmonic) radiation, the pulse energy is 10 μJ. The larger blue spot is the 9 nm radiation, the pulse energy is 10 μJ. Right: Averaged radiation spectra.

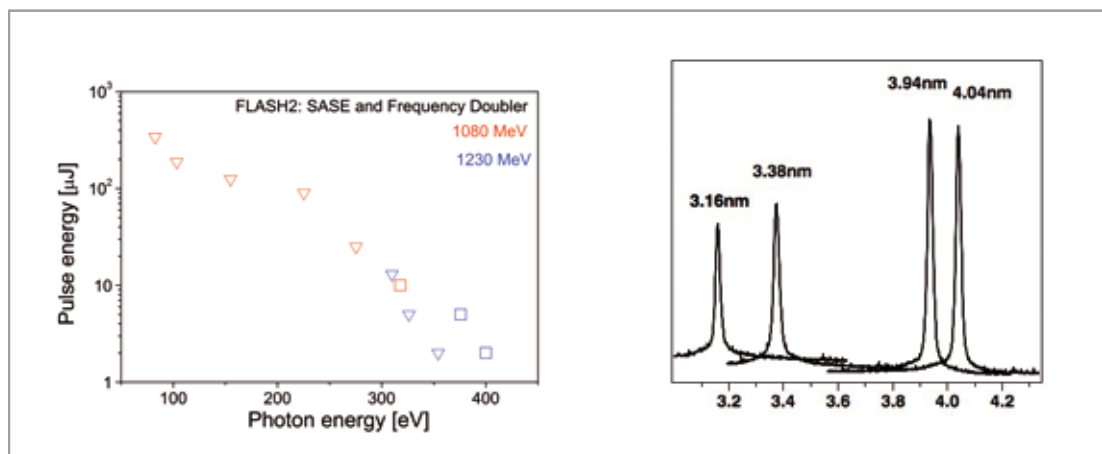


Figure 4

Overview of SASE and frequency doubler operation at electron energies of 1080 MeV and 1230 MeV. Left: Radiation pulse energy versus photon energy. Right: Spectra of frequency doubler. Triangles represent SASE, squares denote the frequency doubler.

Our experience shows that the tuning procedure of the frequency doubler is simple and reproducible. In particular, it is possible to tune the relative intensities of the two colours (ω , 2ω) in a wide range. When tuned to equal intensities, the pulse energies were in the range from a few to 10 μJ . The radiation was transported to the FLASH2 experimental hall for characterisation. Figure 3 shows an example of photon beam images and spectra in the two-colour operation mode. From this first experience, we can state that this operation mode can be proposed to users.

Generating shorter wavelengths

At fixed electron energy, shortening of the radiation wavelength is achieved by opening the undulator gap. The undulator field is then reduced, the FEL gain decreases, and in a uniform undulator, the undulator length is insufficient to reach the saturation regime. In contrast, the frequency doubler scheme is capable of generating shorter-wavelength radiation than the standard SASE FEL mode. Indeed,

the first part of the undulator then operates at twice-longer wavelength, and saturation is obtained at half the full undulator length. The induced beam bunching at the second harmonic is much larger than the shot noise in the electron beam, and it becomes possible to reach saturation on a much shorter length of the doubling section.

For a fair comparison of the two options (SASE and frequency doubler), we performed two dedicated runs at FLASH2 operating with electron energies close to the limit. First, the standard SASE mode was optimally tuned at full undulator length, and the radiation pulse energy was scanned versus the radiation wavelength. Then the frequency doubler scheme was optimally tuned with the same electron beam, and the pulse energy was scanned. Results of the pulse energy measurements are compiled in Fig. 4. As can be seen, visibly shorter wavelengths were reached with the frequency doubler. In particular, photon energies above the nitrogen *K*-edge were demonstrated, which significantly exceeds the original specifications of FLASH2.

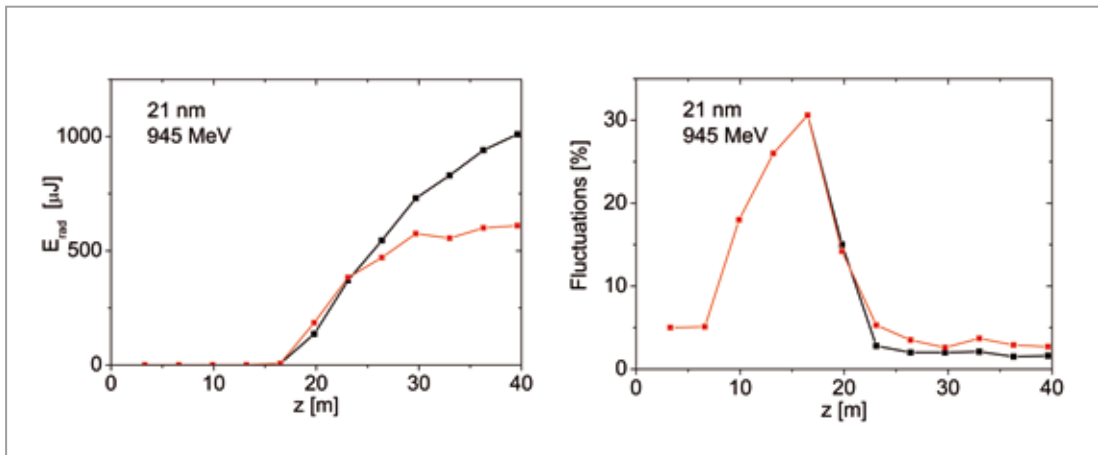


Figure 5

Pulse energy (left) and fluctuations of the radiation pulse energy (right) versus undulator length measured at FLASH2. The electron energy is 945 MeV, the radiation wavelength 21 nm, the bunch charge 400 pC. The colour red denotes the untapered case, black the optimum undulator tapering.

Increasing the pulse energy

Another attractive feature of FLASH2 operation is the increase of the pulse energy by means of undulator tapering, for which we developed the relevant theory and experimental techniques [2,3]. Optimum conditions for undulator tapering assume the starting point to be two field gain lengths before the saturation point, corresponding to the maximum brilliance of the SASE FEL radiation.

The saturation point on the gain curve is defined by the condition that fluctuations decrease by a factor of 3 with respect to their maximum value at the end of the exponential regime. Then the quadratic law of tapering is applied (optimal for moderate increase of the extraction efficiency at the initial stage of tapering [3]).

This experimental technique was successfully tested at FLASH2 (Fig. 5). Saturation occurred at an undulator length of 20 m, and the saturation energy was about 150 μJ. Optimised tapering increased the pulse energy by a factor of 6, up to 1000 μJ. The untapered undulator delivered only

610 μJ at the full undulator length of 40 m. Thus, the tapering of the FLASH2 undulator demonstrated a great benefit in increasing the radiation pulse energy.

Contact: Evgeny Schneidmiller, evgeny.schneidmiller@desy.de
Mikhail Yurkov, mikhail.yurkov@desy.de

References:

- [1] M. Kuhlman, E.A. Schneidmiller and M.V. Yurkov, Operation of frequency doubler at FLASH2, to be published.
- [2] E.A. Schneidmiller and M.V. Yurkov, Optimization of a high efficiency free electron laser amplifier, *Phys. Rev. ST Accel. Beams* 18, 030705 (2015).
- [3] E.A. Schneidmiller and M.V. Yurkov, Proc. IPAC2016 Conf., Busan, Korea, 2016. <http://accelconf.web.cern.ch/AccelConf/ipac2016/papers/mopow013.pdf>

Harmonic footprint.

FEL seeding at FLASH

In free-electron lasers (FELs) such as DESY's FLASH soft X-ray facility, ultrashort high-intensity radiation pulses are generated by highly relativistic electron bunches travelling through periodic magnetic structures, the undulators. The fundamental physical process of radiation emission in combination with a high charge density of the electron bunches leads to an exponential build-up of radiation power along the undulator. In order to precisely initiate or "seed" this process, new modes of operation for FELs have been invented and developed over the last years. At FLASH, an experimental setup to study different seeding options is implemented and currently operated in the high-gain harmonic generation mode. A worldwide unique feature of this setup, among others, is the availability of a transverse deflecting structure located behind the seeded FEL beamline, which enables the precise characterisation of the seeded FEL properties.

High-gain harmonic generation

One of the key features of radiation from FELs is the high spectral brightness in combination with a high degree of coherence for each kind of interferometric application.

FELs operated in the self-amplified spontaneous emission mode (SASE) feature a high degree of transverse coherence, but lack longitudinal coherence because the electron pulses are typically much longer than the coherence length of the radiation. One way to improve the longitudinal coherence is to externally imprint the coherence properties of an external, fully coherent radiation pulse onto the FEL; in other words, to seed the electron pulse with an external laser. Since there are no lasers available in the soft and hard X-ray spectral range that can overcome the background noise of the FEL amplifier (except the FEL itself), techniques have been developed to seed the electron beam at much longer wavelengths and then convert the frequencies to higher harmonics.

In the high-gain harmonic generation (HGHG) mode, the external laser imprints a periodic energy modulation at the laser wavelength onto the electron beam through the interaction of

the radiation field of the laser with the electron pulse in an undulator. A subsequent magnetic chicane allows the conversion of the energy into a density modulation, leading to a modulation of the electron beam current. Loosely speaking, the electron pulses are "sliced" at the wavelength of the seed laser. By sending the sliced beam through a subsequent undulator, it is possible to amplify radiation pulses at higher harmonics of the seed wavelength and therefore to operate the FEL at much smaller wavelengths than the initial seed laser.

At FLASH, an experimental setup has been implemented to test different seeding schemes, among them the HGHG mode. Figure 1 illustrates the key elements of the electron beamline. Two short five-period undulators enable the interaction of the seed laser radiation with the electron beam. The chicanes depicted by the green dipole magnets are used to manipulate the microstructure of the electron pulses. A 10 m long undulator is used to amplify the FEL radiation in the extreme-ultraviolet spectral range. An additional chicane after the FEL allows the extraction of the FEL radiation for characterisation and experimental applications, while letting the electron beam travel further down the beamline. Here, a

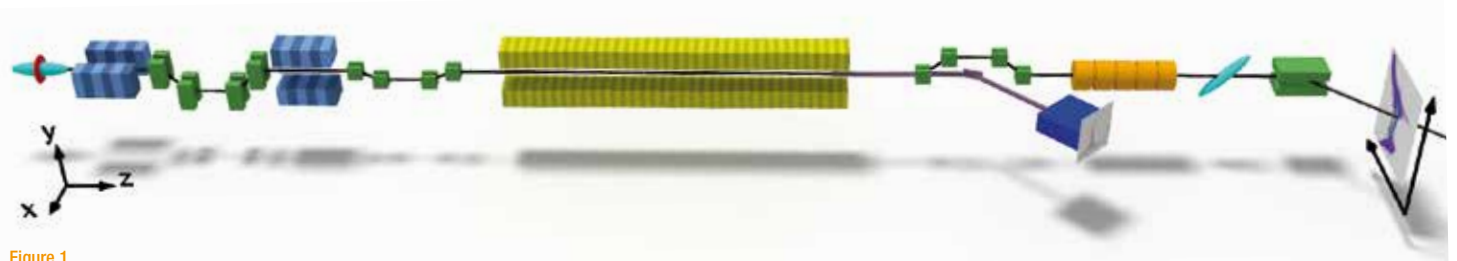


Figure 1

Illustration of the experimental seeding setup at FLASH. The electron and laser pulses travel from left to right through short five-period undulators (blue) and two magnetic chicanes (green dipole magnets) to modify the microstructure of the electron pulses. The 10 m long undulator (yellow) is used to amplify radiation pulses in the extreme-ultraviolet spectral range. In a third magnetic chicane, the electron pulses bypass a mirror used to extract the FEL radiation. The electrons are then deflected vertically in a transverse deflecting structure (orange) and steered horizontally by a dipole onto a screen for diagnostic purposes.

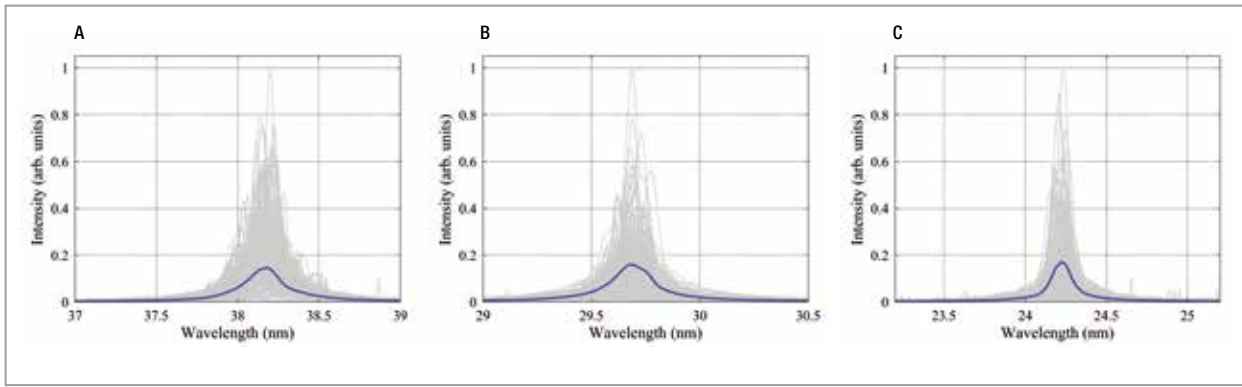


Figure 2
Radiation spectra at the seventh (A), ninth (B) and eleventh (C) harmonic of the seed laser wavelength of 266 nm

Figure 3

Photoelectron spectra for different time delays between FEL and THz radiation. The increase and decrease of the kinetic energy of the photoelectrons is caused by the electric field of the THz pulses. (Courtesy: Armin Azima)

special diagnostic tool – a transverse deflecting structure and a dipole magnet – measures the electron beam energy temporally resolved, enabling the identification of the region inside the electron pulse that has generated the FEL pulse.

In 2016, FEL seeding in the HGHG mode was performed with a seed wavelength of 266 nm and the FEL operating at the seventh harmonic at 38 nm. At this wavelength, FEL saturation was observed with a maximum pulse energy of 110 μ J. Bunching at the ninth and eleventh harmonic was also observed, although at reduced FEL output energy. Figure 2 shows spectra at the seventh, ninth and eleventh harmonic of the 266 nm seed laser. The spectral width $\Delta\lambda/\lambda$ was measured to be below 0.14%, currently limited by the resolution of the installed spectrometer. The stability of the central wavelength was measured to be $\sigma_\lambda/\lambda = 0.038\%$.

FEL pulse characterisation

One of the goals of the seeding experiment at FLASH is to demonstrate the improved longitudinal coherence properties of the seeded FEL in contrast to an unseeded FEL. To this end, the generated FEL radiation can be guided to a dedicated diagnostic hutch adjacent to the FLASH1 accelerator tunnel, which allows the installation of additional hardware for photon diagnostics.

A tool commonly known as THz streaking has been installed and commissioned in 2016 and will allow the temporal characterisation of the FEL radiation. Up to now, the interaction of a single-cycle THz pulse with the FEL pulse has been demonstrated. Figure 3 shows the trace of photoelectron spectra generated by the interaction of the FEL radiation with argon gas and for different time delays between the THz pulses and the FEL pulses. The THz pulses are generated from the same

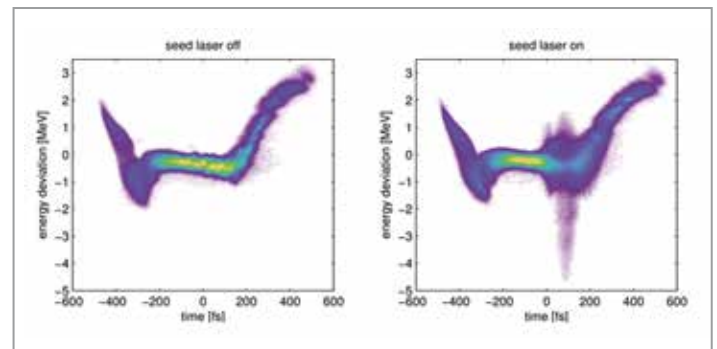
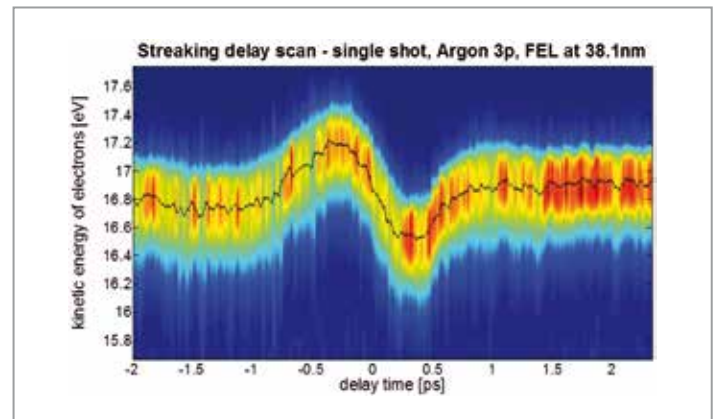


Figure 4

Longitudinal phase space distribution of an unseeded (left) and seeded (right) electron bunch. The analysis of such images allows information to be extracted about the emitted photon pulse as well as the electron beam properties.

laser system that is used to seed the FEL, and therefore these two signals are intrinsically synchronised.

Time-resolved electron bunch diagnostics

A unique feature of the experimental seeding setup at FLASH is the possibility to diagnose the electron pulses after the emission of seeded FEL radiation has taken place. This allows for, on the one hand, gaining indirect information about the radiation pulse and, on the other hand, further characterising the electron bunch properties. Figure 4 shows the longitudinal phase space distribution of an unseeded and seeded electron bunch. The signature of the seeded part is clearly visible at +100 fs.

Contact: Jörn Bödeewadt, joern.boedewadt@desy.de

Bunch purity at PETRA III.

Requirements, measurements, impurity sources and cleaning

For nearly 50% of the time, DESY's PETRA III synchrotron radiation source is operated in a dedicated "timing mode" to allow time-resolved measurements. In this mode, the longitudinal "purity" of the fill is of great importance. Parasitic bunches influencing this purity can be caused by different mechanisms in the pre-accelerator chain and in PETRA III itself. During the 2016 user run, the multibunch feedback system was routinely used to automatically remove all impurities.

User requirements

PETRA III is a third-generation synchrotron light source, providing hard X-rays from a 6 GeV beam of typically 100 mA of stored electrons. For improved thermal stability, the machine is operated in top-up mode with periodical injections every few minutes, to keep the beam intensity constant within 1%. Mainly two fill patterns are used at PETRA III: the "continuous mode" with 960 bunches at 8 ns bunch spacing and the "timing mode" with 40 bunches 192 ns apart.

PETRA III is operated in the timing mode for nearly 50% of the time. About half of all beamlines make use of this mode for time-resolved measurements. One of the requirements is that the intensity of any unwanted bunch in between the 40 main bunches is less than 10^{-5} with respect to the main bunch intensity. Nuclear resonant scattering experiments at Beamline P01 have the highest purity demands of 10^{-8} .

Measurement

To achieve the needed precision, it is unavoidable to use a single-photon counting technique with quite long integration times. For this purpose, an avalanche photodiode (APD) installed at Beamline P01 has been used. Amplified APD signals start a time-to-digital converter (TDC), which is stopped by the next bunch trigger. The TDC histogram of the photon arrival times is a direct measure of the time structure of the beam. The count rate has to be a small fraction of the bunch repetition frequency, otherwise the measurement is affected by the recovery time of the APD and by pile-up from multiphoton events. A typical TDC histogram measured during top-up operation is shown in Fig. 1.

The data taking stops automatically when a preselected number of counts is reached. Before cleaning the histogram and restarting the measurement, the parasitic bunch contents

relative to the main bunch are calculated and archived together with the raw data.

Sources of impurities

A well-known source of parasitic bunches are the pre-accelerators of PETRA III. In the Positron Electron Accumulator (PIA), ± 8 ns bunches are generated by a longitudinal compression phase shortly before extraction. A dedicated chopper system in the following transport line removes most of the impurities, but not all. Several other production mechanisms have been identified and removed in the last years, such as dark current from the LINAC II linear accelerator, electrons left over in the DESY II synchrotron from the preceding transfer or a mismatch between the energy of the injected beam at injection into DESY II.

Such parasitic bunches are injected into PETRA III at a constant fraction together with the main bunches. During top-up mode, they can accumulate up to a significant level.

Independently of that, initially empty buckets following the main bunches get populated even when PETRA III is running with a stored beam without top-up. Simulations and measurements of parasitic bunch growth rates proved that the mechanism is based on Touschek scattering and recapture of scattered particles in subsequent buckets if they lose enough energy due to radiation damping.

Cleaning

Achieving a bunch purity of less than 10^{-5} during top-up mode in PETRA III is rather challenging and requires an active cleaning technique. Owing to its capability of broadband signal processing and generating, the multibunch feedback system was extended to provide the needed cleaning

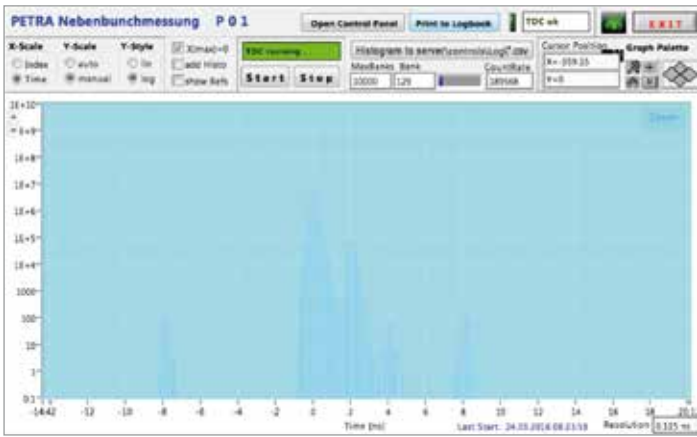


Figure 1
Screenshot of a TDC histogram, no cleaning active; counts versus time to the main bunch

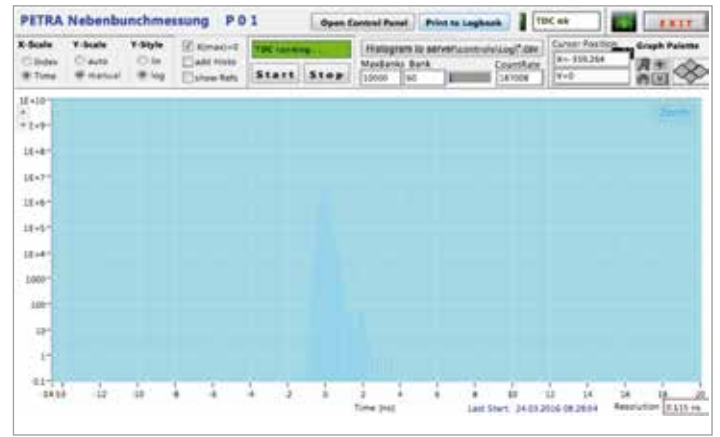


Figure 2
Screenshot of a TDC histogram with active bunch cleaning; counts versus time to the main bunch

functionality. Hereby, the parasitic particles can be excited resonantly on their betatron tune frequency without affecting the main bunches. This is achieved by an active decoupling of the excitation signal from the main bunches. A further decoupling between parasitic and main bunches is caused by a difference in betatron tune frequency, typically on the order of a few kHz, due to the beam intensity dependence on the betatron tune frequency. Because of the machine's small vertical aperture, the cleaning excitation is only applied in this plane.

Since parasitic bunches are not affected by active damping, their resonances are narrow, and therefore a slow frequency sweep within 500 ms slightly above the vertical tune of the main bunches is sufficient to remove them completely from the machine.

Since the beginning of the 2016 user run, this cleaning has been routinely done directly after every top-up injection. The small remaining excitation of the main bunches during

cleaning can be minimised by carefully optimising the time span and the amplitude of the excitation. A TDC histogram measured a few minutes later than Fig. 1, just after one single cleaning sweep, is shown in Fig. 2.

One should bear in mind that a measurement needs some minutes, collecting counts from the +2 ns parasitic bunch re-populated after cleaning. An example of the history of parasitic bunch contents is shown in Fig. 3 (with cleaning roughly once per hour). The blue line shows the growth and removal by cleaning of the +2 ns parasitic bunch, the green line the corresponding content of the parasitic +4 ns bunch. In routine operation, all relative parasitic bunch populations are less than 10^{-5} .

Using an active cleaning technique, PETRA III is thus able to meet the given bunch purity specification.

Contact: Heiko Ehrlichmann, heiko.ehrlichmann@desy.de
Jens Klute, jens.klute@desy.de

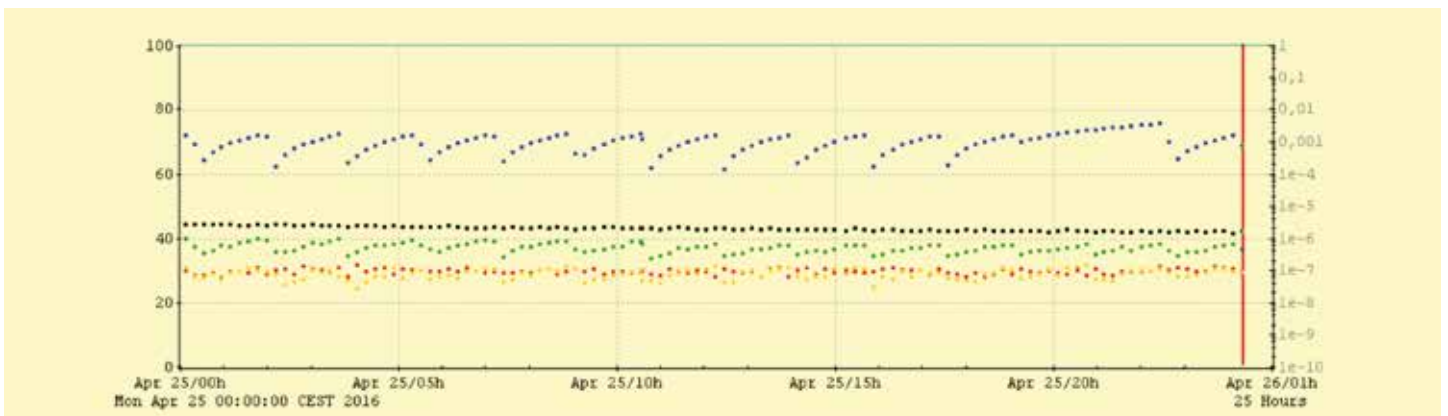


Figure 3
History of relative parasitic bunch contents (right y-axis); the different coloured traces correspond to different parasitic bunches.

Finalisation of the European XFEL main accelerator.

Increasing installation speed through process management

In August 2014, the first superconducting accelerator module for the European XFEL X-ray free-electron laser was installed in the tunnel. At the beginning of 2015, it became obvious that an increase in installation speed was required to meet the European XFEL time schedule. Therefore, in mid-2015, the cooperation of the 13 involved work packages was optimised in order to ensure the completion of the main accelerator in 2016. To this end, process management methods were applied to create a better work sequence plan, and an operative installation management was established in the tunnel to control the workflow (see *DESY Accelerators 2015*). This article presents the installation procedure and the process optimisation, which resulted in the finalisation of the European XFEL main accelerator in 2016.



Figure 1
European XFEL main accelerator ready for cool-down at the beginning of December 2016

Work sequence

In total, 96 accelerator modules were installed on the whole accelerator length of about 1.5 km (Fig. 1). The installation was divided into subsections called cryostrings. Each cryo-string typically contains 12 modules fed by three RF stations.

The work sequence is presented in Fig. 2. First of all, the modules were mounted on the tunnel ceiling and welded together (“Installation of 12 Modules”). Then, the racks were brought into position and the RF stations including infrastructure were built up (“RF Stations and Utilities”). In parallel, the copper cables (“Cable MDI”), the “Optical Fibers” and the “Ethernet” cable were laid. After that, the subsystems required for the personnel interlock approval (“Preparation Personnel Interlock”) were put into operation.

The personnel interlock approval by the German Technical Inspection Association TÜV was followed by the preparation of coupler conditioning (“Preparation Conditioning”). The arrows pointing from “Installation of 12 Modules” to “RF Stations and Utilities” are marked with the date when the process step “Global Helium Leak Test of Insulating Vacuum” was finished and the following process steps could start. The block length shown in Fig. 2 corresponds to the planned duration. The real duration deviated from this value.

Accelerating the installation speed

To accelerate the overall progress, the work was organised in such a way that up to three cryostrings could be processed in different stages (see Cryostrings 3 to 5 in Fig. 2). As of 25 February 2016, the period from one “Global Helium Leak Test of Insulating Vacuum” to the next was reduced from 12 to 6 weeks. This increase in installation speed was possible thanks to the assignment of an additional welding and wave-guide installation team. The project management had requested the welding team after the initial process analysis in 2015 had shown the potential for increased installation speed.

Each block in Fig. 2 contains 4 to 24 process steps, which were visualised in a process map including their dependencies. A reasonable work sequence was developed in cooperation with the work package leaders (see *DESY Accelerators 2015*) and optimised from one cryostring installation to the next (Plan # 1 to 4). After the third iteration, an optimised sequence was found (Plan # 4) that did not require further change. Plan # 5 was only made to take into account some process steps omitted in Cryostrings 8 and 9 that were not necessary for the cool-down. This dynamic optimisation of

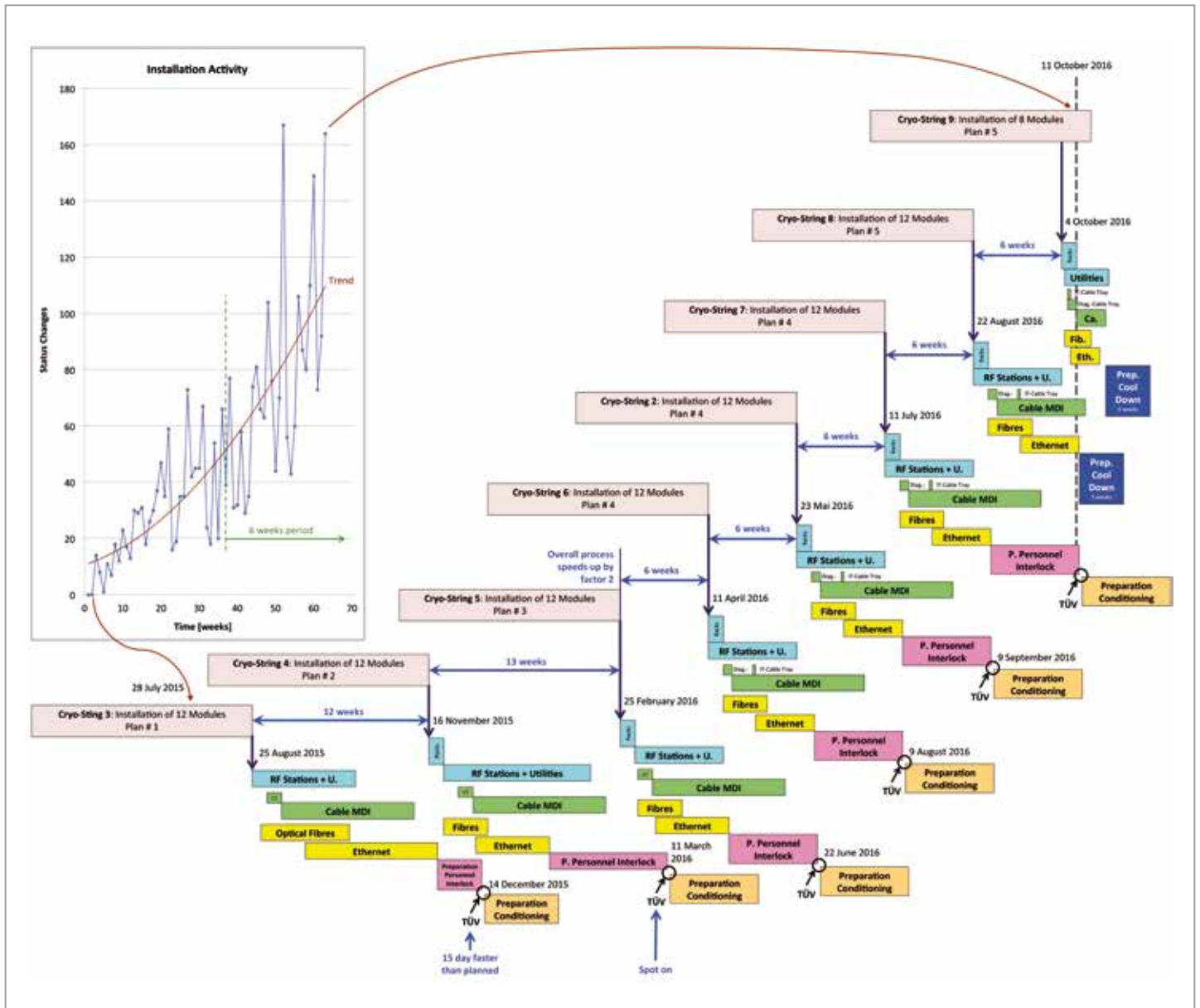


Figure 2 Installation process from 28 July 2015, when the installation management took effect, to 11 October 2016. In this period of just over 15 months, 84% of the main accelerator was installed. The trend line indicates the increase in installation speed.

the work sequence was another essential reason for the permanent acceleration of the installation process.

To measure the installation speed, the number of status changes per week was monitored. This status recording was primarily done to get an overview of the installation state of the main accelerator. Weekly documentations recorded which process steps were started or finished. The graph in Fig. 2 shows how many process steps were started or finished per week. This number fluctuated in a wide range. Therefore, a trend line was added that corresponds approximately to the average installation speed.

From 28 July 2015 to 11 October 2016, the installation speed was increased by a factor of 10. In this period of just over

15 months, 84% of the main accelerator was installed – meaning that, if this increased speed could have been achieved from the beginning, the main accelerator could have been installed in 1.5 years.

An unexpected interruption caused by a failed pressure test on 11 October 2016 delayed the scheduled installation finalisation by several weeks. Nevertheless, the main accelerator was prepared for cool-down at the beginning of December 2016.

Contact: Michael Bousonville, michael.bousonville@desy.de
 Frank Eints, frank.eints@desy.de
 Stefan Choroba, stefan.choroba@desy.de

Accelerator modules for the European XFEL.

Performance tests of 102 superconducting modules

For the main linear accelerator and the injector of the European XFEL X-ray free-electron laser, 102 accelerator modules were constructed and tested by an international consortium led by DESY. Each module houses eight superconducting cavities manufactured by companies in Germany and Italy under the supervision of DESY and INFN/LASA in Milano, Italy. With an average usable accelerating gradient of about 30 MV/m in the individual cavity acceptance tests, the required average design gradient of 23.6 MV/m could be significantly exceeded. The assembly of the over 12 400 individual parts for each module took place at the French partner institute CEA in Saclay. After transport of the modules to DESY, a team from the Polish partner institute IFJ-PAN in Krakow performed comprehensive tests of each individual module in the Accelerator Module Test Facility (AMTF) at DESY. After successful tests, 96 modules were installed in the main linear accelerator and one module in the injector.

Cryomodule construction and testing

The superconducting linear accelerator of the European XFEL, which has a design electron beam energy of 17.5 GeV, is currently being commissioned. Of the 102 accelerator cryomodules constructed, 96 were installed in the main accelerator tunnel after successfully passing the performance test in the dedicated test facility AMTF.

The cryomodule development started in the 1990s within the TESLA Test Facility collaboration. In total, eleven cryomodules with iterative improvements were constructed, tested and used in the FLASH accelerator at DESY before the design for the European XFEL was finished. The operation temperature of 2 K (-271.15°C), together with high-level requirements for vacuum cleanliness, low residual magnetic field and robustness for a lifetime of about 20 years, requires a complex and advanced design as well as the use of appropriate materials. The main components of each cryomodule are:

- Eight superconducting 1.3 GHz niobium cavities for accelerating the electron beam
- Eight RF power couplers, motor-driven frequency tuners and magnetic shields (one each per cavity)
- One unit including a quadrupole magnet (for focusing the beam) and a beam position monitor (BPM-quad-unit)
- Many metres of cryogenic and vacuum piping, bellows and valves, including the 300 mm gas return pipe, which forms the mechanical backbone of the module
- Many metres of different current leads and signal cabling
- Many square metres of cryogenic shields
- The outer (yellow) vacuum vessel

In total, 9422 different components and over 12 400 individual parts are needed to complete one cryomodule. The parts were contributed by many partners of the international European XFEL consortium. The integration of all 102 cryo-

modules took place over a 2.5-year period at the French partner institute CEA in Saclay. The about 12 m long modules were then transported by road from Saclay to Hamburg, where they were immediately prepared for the performance test at the AMTF (Fig. 1).

A team from the Polish partner institute IFJ-PAN in Krakow performed all the cryomodule tests in close collaboration with several DESY groups. The performance tests followed a well-defined procedure, starting with an extensive incoming inspection for functioning and conformity with respect to mechanics, RF, electronics and vacuum.

Afterwards, the cryomodules were mounted onto the cryogenic and high-power RF test stand (Fig. 2). Before cool-down to 2 K for the first time, the RF power couplers were operated at room temperature with short (<1.4 ms) pulses up to 800 kW to check their response and performance. During this operation, a significant improvement in performance



Figure 1
Accelerator cryomodules in the AMTF in front of the test stands



Figure 2
Cryomodule mounted on the test stand with RF power couplers connected to the waveguide distribution, ready for closing the cryogenic connection

(“conditioning”) could often be observed. After cool-down to 2 K, the key performance parameters of each individual cavity were measured, namely maximum accelerating gradient and dark-current-induced X-rays (if any). Next, the cryogenic heat loads with all cavities powered on (dynamic) and off (static) were measured. In addition, the functionality of other important subsystems, such as mechanical frequency tuners and the quadrupole magnet, were tested. After warm-up and disassembly from the test stand, each cryomodule was equipped with its individually adjusted RF waveguide distribution and finally transported into the accelerator tunnel.

RF performance

With a few exceptions, all cryomodules achieved or exceeded the nominal average design gradient of 23.6 MV/m (Fig. 3). The average performance across all modules was 27.5 MV/m (with an rms of 4.8 MV/m). By comparison, the average performance expected from the vertical cavity acceptance test results was 28.3 MV/m, corresponding to an overall reduction of less than 3% after cryomodule assembly. Several modules even achieved (and possibly would have exceeded) 31 MV/m on average – the maximum allowed by the power limitations of the test stand.

Closer inspection of Fig. 3 shows that the individual cryomodule performance exhibited a large relative degradation in

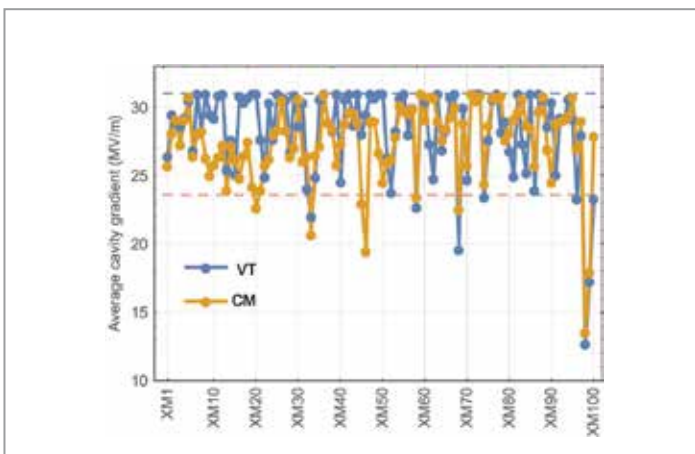


Figure 3
Average operational gradient of all cryomodules (CM, orange data points). The blue data points show the average expected performance from the vertical tests (VT, clipped at 31 MV/m). The red and blue dashed lines represent the nominal European XFEL gradient (23.6 MV/m) and the administrative limit in the cryomodule test (31 MV/m), respectively.

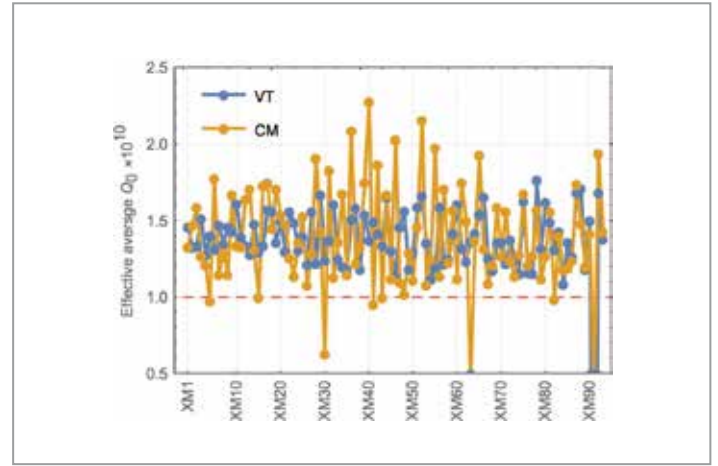


Figure 4
Effective cavity quality factor Q_0 of the cryomodules (CM, orange data points). The blue data points are the estimates from the vertical cavity tests (VT). The red dashed line represents the European XFEL specification (1×10^{10}).

many cryomodules at the start of the production, but that the later production performed much better. This has been attributed to overall better practises during the cryomodule assembly. The degradation quantified in this way is essentially zero for a large fraction of the modules in the later production period. Regarding the measured cryomodule operational gradient, approximately 18% of the cavities were limited by X-rays (dark current), 36% by quenching, with the remaining cavities being administratively limited to 31 MV/m (46%).

Figure 4 shows the average cryomodule cavity quality factor Q_0 as measured at AMTF (CM, orange data points). The quality factor Q_0 is directly proportional to the cryogenic RF heat load. With the exception of three cases, all cryomodules exceeded the specification of 1×10^{10} . The orange data points show an estimate based on the Q_0 values of the cavities as measured in the cold vertical test (VT). While the average over all modules is approximately the same for CM and VT ($\sim 1.4 \times 10^{10}$), the spread from the VT estimates is higher and there appears to be little correlation. Given the very different nature of the measurements (continuous-wave single-cavity RF versus pulsed cryomodule cryogenic heat load measurement for VT and CM, respectively), as well as the expected large uncertainty in both (up to 20%), little can be inferred over a change in Q_0 between vertical test and cryomodule test.

Thanks to the very close and successful collaboration of all the participating institutes and industrial companies, the achieved cryomodule performance lies well above the design values.

The installation of the cryomodules in the European XFEL linear accelerator was finished in October 2016. The cool-down to cryogenic temperature was completed in January 2017, and the commissioning will take place in the first two quarters of 2017.

Contact: Detlef Reschke, detlef.reschke@desy.de
Nicholas Walker, nicholas.walker@desy.de

Phase space manipulation in the European XFEL injector.

Third-harmonic system exceeds nominal performance

The injector of the European XFEL X-ray free-electron laser comprises a special superconducting module operating at 3.9 GHz, i.e. three times the frequency of the main linear accelerator, for beam phase space manipulation before the three bunch compression stages downstream along the facility. This third-harmonic system is a crucial component for achieving the nominal beam parameters needed for lasing at extremely short wavelengths. The system was installed in the tunnel in September 2015 and operated above specification during the injector run from December 2015 to July 2016.

European XFEL injector

The European XFEL consists of the injector, the main linear accelerator (linac) with altogether 96 superconducting accelerator modules and a number of warm beamlines used to transport the electron beam either to successive accelerator sections or to the undulators.

The injector is the first section of the accelerator. It is about 40 m long and located on the seventh underground floor of the injector building on the DESY-Bahrenfeld site. Here, the electrons are extracted through the photoelectric effect from a cathode exposed to an ultraviolet laser. After acceleration to relativistic energies in a normal-conducting 1.6 cell cavity, the electrons enter the first two superconducting accelerator modules: a standard 1.3 GHz module (A1) similar to all the other modules installed in the accelerator tunnel and a special higher-harmonic module operating at 3.9 GHz (AH1, Fig. 1).

This third-harmonic section is needed to manipulate the longitudinal phase space of the electron beam after the first acceleration stage, in order for the linac to deliver high-current beams with sufficiently low emittance for the production of 1 Å FEL light for user experiments. The beam properties can subsequently be measured with several devices in an extensive diagnostic section.



Figure 1
AH1 module in the tunnel, equipped with its RF distribution and coupler vacuum lines

The beam-based injector commissioning took place from December 2015 to July 2016. The AH1 module was technically commissioned in December 2015 within one day of the “cryo OK” permission to feed RF to the cold modules and operated well above its nominal performance during the injector run from January to July 2016. Operation of the third-harmonic system will continue in January 2017 with the start-up of the whole European XFEL facility, when the system will be used to achieve the design beam specifications after the bunch compression (BC) stages.

Need for a third-harmonic module

By superimposing a higher-harmonic component onto the main accelerating field and properly setting their relative phases and amplitudes, the system can be used to manipulate the longitudinal beam phase space and control the current profile along the bunch so as to allow short-wavelength FEL lasing. These goals are achieved by:

- Removing the RF curvature of the 1.3 GHz RF field of the A1 module, caused by the long bunch length at the injector. This is required to minimise detrimental space charge effects at low energies.
- Compensating for non-ideal effects further down the linac, such as wakefields, non-linear optics in the BC stages and space charge effects in the rest of the accelerator.

Control of the energy chirp, curvature and skewness (first-, second- and third-order correlations in the longitudinal beam phase space) allows for proper tuning of the relative setting of the harmonic and fundamental fields in order to optimise the beam current profile after the BC stages.

AH1 milestones and commissioning

AH1 is functionally identical to a standard module of the main linac. It contains eight cavities operating at 3.9 GHz (i.e. three

times the main linac frequency, therefore the structures are 1/3 of the size) and a magnet package at the upstream end of the module.

The AH1 cavities were produced as an in-kind contribution to the European XFEL by INFN in Milano, Italy, and tested at the LASA laboratory in Italy before being shipped to DESY (between September 2014 and February 2015). The performance of all the cavities in terms of accelerating gradient and quality factor Q_0 at the operational temperature of 2 K was well above the European XFEL specifications (Fig. 2).

The cleanroom rollout of the cavity string at DESY took place in July 2015. After assembly, the AH1 module was ready to be installed in the tunnel in September 2015. Several final preparation steps were performed in the tunnel, such as the assembly of the RF distribution and the integration into the injector cryogenic string. The injector cool-down started on 10 December 2015, and AH1 was ready on 16 December: operating it at nominal gradients was possible from the first day of commissioning.

During the technical commissioning in December 2015, AH1 operation was achieved at the nominal European XFEL pulse structure, with an overall module gradient well above the nominal requirements. In January 2016, the final calibration activity started, i.e. the tuning of the loaded quality factor Q_L of the individual cavities and the proper alignment of the relative phases, to allow for correct beam operation under the vector sum control of the eight cavities. For AH1, these operations are performed differently from those for the standard 1.3 GHz accelerating modules, as the power coupler has a fixed antenna. A combination of three-stub tuners at each cavity and waveguide spacers allows the combined quality factor tuning and phase alignment.

This preparation was performed in parallel to the regular beam commissioning of the other components of the injector,

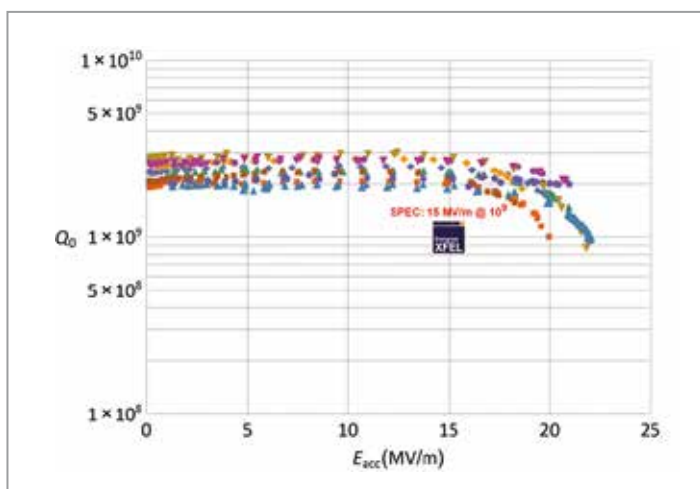


Figure 2 Vertical test results for all ten cavities needed for the AH1 module (eight cavities in the module plus two spares). The cavity quality factor Q_0 is plotted as a function of the accelerating gradient.

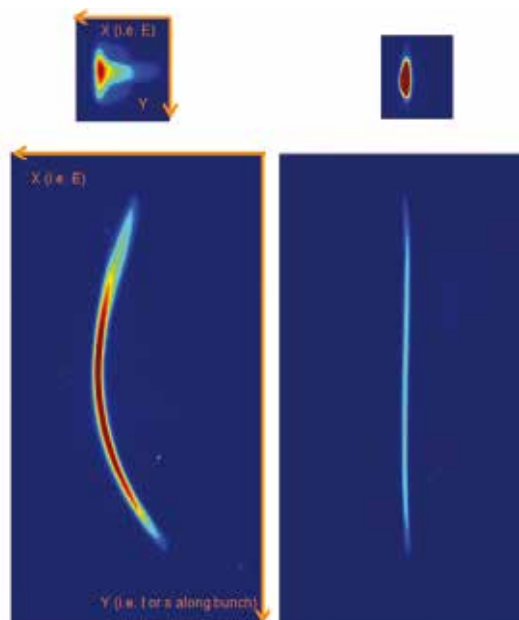


Figure 3 Beam image on the screen in the spectrometer beamline with the TDS off (top plots) and TDS on (bottom plots). In the top plots, the X coordinate reflects the beam energy in the dispersive line and Y is the vertical beam coordinate. In the bottom plots, the Y coordinate is transformed into a longitudinal coordinate along the bunch by the action of the TDS, allowing the energy–position correlation to be visualised. The figures on the left were obtained with AH1 off, showing the RF curvature of the 1.3 GHz RF field on the bunch. The figures on the right were obtained by properly setting the AH1 RF parameters so as to achieve the cancellation of the RF curvature.

since the RF pulse was shifted with respect to the beam. AH1 was then put into operation with beam in February 2016 to assess its phase space manipulation performance.

During the technical commissioning and RF characterisation, a 10% agreement of the cavity quench gradients with respect to the vertical test characterisation was achieved, and dedicated temperature stability measurements at the highest voltage set points of the module were performed, confirming the possibility to reach all foreseen design scenarios. Temperatures were extremely stable even in the most critical parts of the cavities, i.e. the conductively cooled higher-order mode regions at each end.

An important confirmation of the effect of AH1 on the beam came with the availability of the transverse deflecting structure (TDS) in the injector beamline: the beam image on the screen in the dispersive spectrometer beamline shows a clear linearisation effect (Fig. 3).

The control of the voltage sum of the RF fields of the two modules (the standard 1.3 GHz module A1 and the 3.9 GHz module AH1) allows the longitudinal beam shape parameters (e.g. chirp, curvature, skewness) to be set so as to achieve the phase space linearisation required for proper matching to the compression stages downstream along the linac.

Contact: Cecilia Giovanna Maiano,
cecilia.giovanna.maiano@desy.de

Dry-ice cleaning of high-power RF components.

Performance of RF photo guns at FLASH, PITZ and REGAE

Complex copper radio frequency (RF) structures are used as electron sources (RF guns) based on the photoemission effect. In the past, the performance of these copper RF resonators was often limited by dark currents, which could reach several thousand μA in resonators cleaned with conventional methods, such as high-pressure water rinsing or alcohol rinsing. Nowadays, carbon dioxide dry-ice snow cleaning has become a well-established method to reduce harmful dark currents emitted from particles polluting the inner surface of the copper structures. Compared with conventional methods, dry-ice cleaning was found to reduce dark currents in RF guns at DESY's FLASH free-electron laser and the PITZ photoinjector test facility at DESY in Zeuthen by an order of magnitude. These very good achievements were also demonstrated for RF guns for DESY's REGAE facility, where RF conditioning was performed in a very short time.

Introduction

Carbon dioxide (CO_2) snow cleaning or blasting is a well-known cleaning method used in industry for various applications, especially for removing surface contaminations such as hydrocarbons, grease or even paint. Its major advantage is the non-abrasive and dry cleaning process. Dry ice removes particles without altering the surface and, since frozen CO_2 sublimates, the surface will keep dry after cleaning.

The DESY MHF-SL group uses the CO_2 snow cleaning method, where liquid CO_2 streams through a specially built nozzle, generating a mixture of gas and CO_2 snow at the outlet. Compared with high-pressure water rinsing (HPWR), where the mechanical effect from the high water pressure is the major cleaning agent, dry-ice cleaning additionally includes thermal and chemical cleaning effects. Relaxation of liquid CO_2 in a nozzle results in a snow/gas mixture with approximately 45% snow at a temperature of 194 K.

To ensure acceleration and focusing of the CO_2 stream, it is surrounded by a near-supersonic N_2 jet, which at the same time prevents condensation of humidity on the resonator surface. The absence of liquids during cleaning is a big advantage when handling ultrahigh-vacuum components.

The thermal cleaning effect is based on shock-freezing of the contaminations, strong impact of the snow crystals and a 500-fold increase in volume after sublimation. Contaminations become brittle and start to flake off the surface. The chemical cleaning effect occurs when snow crystals hit the surface and melt at the point of impact. Liquid CO_2 is a good solvent, especially for hydrocarbons and silicones.

Technical layout

To ensure a particle-free environment, the entire cleaning setup is located in an ISO 5 cleanroom. Figure 1 shows the cleaning device with a 1.3 GHz RF gun, mounted on a traverse that moves in the vertical direction. The RF gun is turning while moving up and down over the cleaning lance and the nozzle. To guarantee that every part of the complex inner surface of the resonator is cleaned, the nozzle itself can be moved steplessly from the horizontal to the vertical direction to realise various jet angles (Fig. 2).



Figure 1
Dry-ice cleaning device for RF guns at DESY, with a 1.3 GHz gun installed



Figure 2
Lance with moveable nozzle. The nozzle can be moved steplessly from horizontal to vertical to realise various jet angles. It is used for 1.3 GHz RF guns with an iris diameter of 50 mm.

RF guns with an RF frequency higher than 1.3 GHz and therefore much smaller inner diameters, such as the RF gun for REGAE ($f = 3$ GHz, $D_i = 21.6$ mm), require smaller lances with a maximum diameter of 18 mm. As it is not possible to install moveable nozzles in such a small housing, four different lances and nozzles with fixed jet angles are used in this case (Fig. 3).

All used nozzles are designed as follows: A specially formed Venturi nozzle (designed and manufactured by the Fraunhofer Institute for Manufacturing Engineering and Automation IPA in Stuttgart, Germany) with an inner diameter of not more than 0.2 mm expands the liquid CO₂ at the outlet, where a gas/snow mixture is created. A high-pressure (16 bar) N₂ jet surrounds the CO₂ jet and accelerates the complete jet to nearly supersonic speed. The formed jet has an effective usable length of 4–7 cm, since it starts to widen with increasing

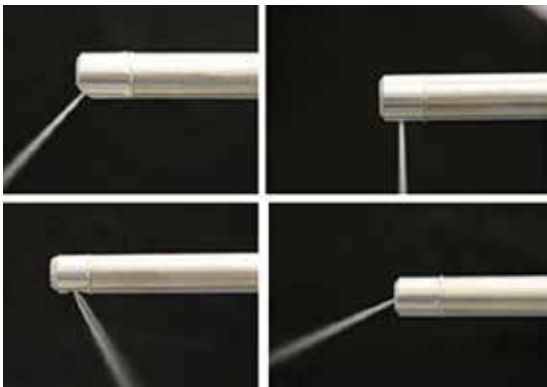


Figure 3
Small lances with nozzles in a fixed position at different angles, used for cleaning 3 GHz REGAE RF guns with an iris diameter of 21.6 mm

length. A maximum jet diameter of 5 mm is the limit for optimal cleaning conditions. The N₂ jet can also be used separately for cleaning and drying purposes.

Cleaning and results

Each RF gun is cleaned in several steps with different jet angles. After each step, the cleaning lance is kept inside, blowing N₂ only, to avoid condensation of humidity from the ambient air on the clean inner surface. The motion speeds of moving parts are chosen in such a way that the jet streaks each part of the inner surface for a given amount of time.

For the FLASH RF gun, dry-ice cleaning was found to reduce dark currents by an order of magnitude. The present dark current of the RF Gun 3.1 installed in FLASH is about 5 μ A while running at operating parameters, whereas the limiting value is 20 μ A. At PITZ, several RF guns were tested in the last years, with dry-ice cleaning reducing dark currents by about a factor of 10 compared to cleaning with liquids. Figure 4 shows a plot of dark current as a function of RF power in guns cleaned using HPWR and dry-ice cleaning.

The REGAE guns were never cleaned with liquids such as water or alcohol, so the two cleaning methods cannot be compared in this case. In tests, RF conditioning could be done very quickly. It took only two weeks to reach an accelerating gradient of 100 MV/m, which can only be achieved if the dark current is low enough.

Tests are ongoing to also apply this cleaning method to other ultrahigh-vacuum RF components. Expectations are high, especially for the cleaning of superconducting resonators.

Contact: Arne Brinkmann, arne.brinkmann@desy.de
Jörg Ziegler, joerg.ziegler@desy.de

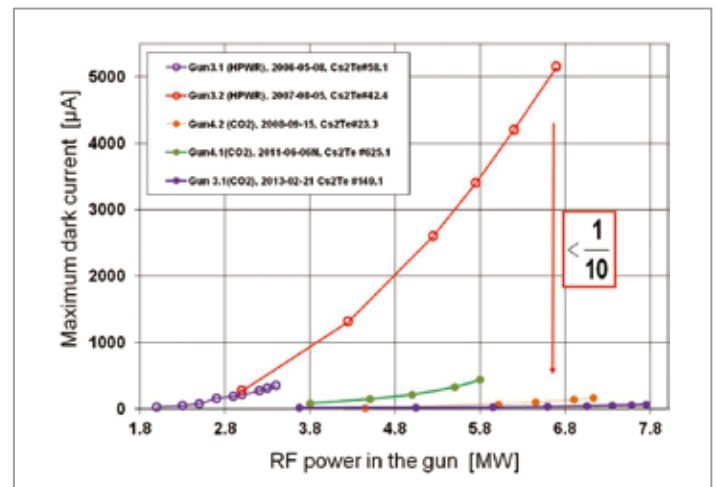


Figure 4
Comparison of dark currents of 1.3 GHz RF photo guns cleaned with high-pressure water rinsing (HPWR) and dry-ice cleaning (Courtesy of Igor Isaev, PITZ)

First plasma-accelerated electrons generated on the DESY campus

LUX is a laser plasma wakefield accelerator driving an undulator beamline for the generation of few-femtosecond X-ray pulses at compact scales and with unprecedented time resolution for pump-probe experiments. The accelerator, which is built and operated by DESY and the University of Hamburg, was first commissioned in 2016 and demonstrated electron beams with up to 400 MeV energy at a repetition rate of 5 Hz. Currently, the beamline is being upgraded for generating first undulator radiation.

Overview

The Laser-Plasma Driven Undulator X-Ray Source (LUX) beamline is built and operated within the LAOLA collaboration of DESY and its strategic partner, the University of Hamburg. It is an integral part of DESY's long-term vision to advance plasma accelerator technology towards first applications.

In a laser plasma wakefield accelerator, an ultrashort, high-intensity laser pulse is focused into a millimetre-scale plasma target, typically a 300 μm diameter capillary milled into a sapphire crystal (Fig. 1). In the hydrogen-filled capillary, the laser excites a travelling plasma wave, which sustains large electric field gradients. Electrons injected from the plasma background can be accelerated to giga-electronvolt-scale beam energies over very short distances (Fig. 2).

Laser plasma wakefield accelerators are expected to drive a next generation of light sources, offering intrinsic synchronisation of the infrared driver laser – including any secondary synthesised infrared or THz beams – to the generated X-ray pulses, and thus temporal resolution on a single-femtosecond scale. Its unique timing properties in combination with the reduced size and cost of such a laser-driven setup could be of great benefit for a variety of applications.

The workhorse of the LUX beamline is the 200 TW ANGUS laser system (Fig. 3), which provides very energetic laser pulses of 5 J in 25 fs pulse duration, at a repetition rate of 5 Hz, to the LUX electron accelerator. The LUX beamline is located right next to the laser lab within an old DESY tunnel.

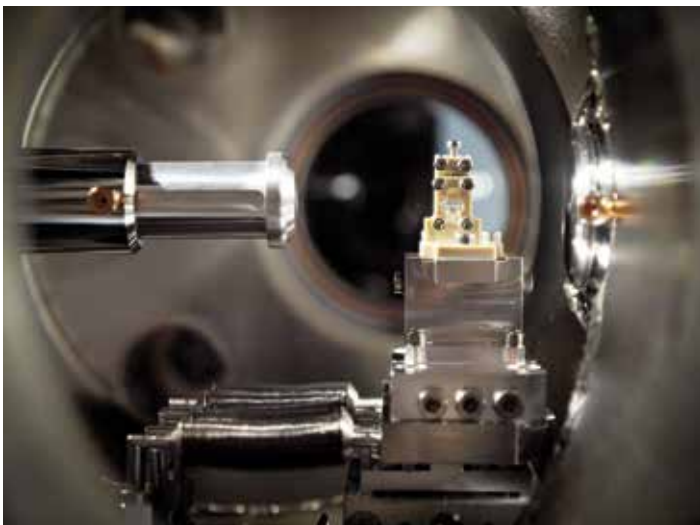


Figure 1
Four-millimetre-long sapphire plasma target used for laser plasma acceleration in the LUX beamline. The high-power laser pulses enter the target chamber from the left and are focused onto the entrance of the plasma capillary to accelerate electrons to high energies over few-millimetre distances.

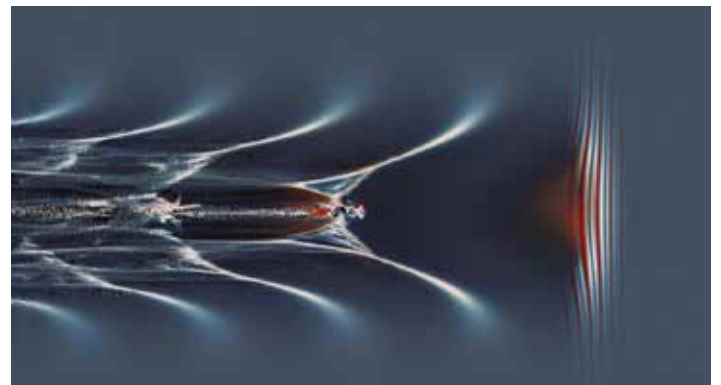
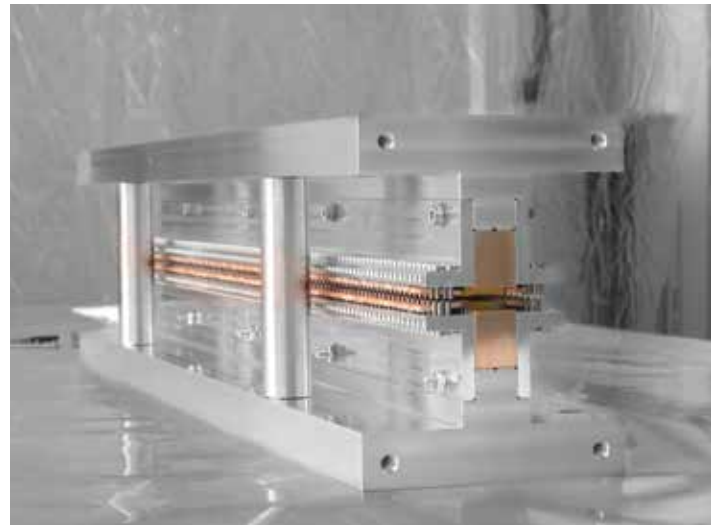


Figure 2
Particle-in-cell simulation of a laser-driven plasma wave. The intense laser travels to the right and induces a charge separation by pushing plasma background electrons to the side. A bubble-like plasma cavity is formed, in which an electron bunch can be trapped and accelerated.

Figure 4

The BEAST II in-vacuum undulator:
With only 5 mm magnet period,
it is optimised for generating
X-ray pulses using laser plasma-
accelerated electrons.



Here, the laser is focused into the plasma target to generate electron beams. Those beams are then transported to a diagnostics section followed by a short, specially designed undulator – dubbed BEAST II – to generate very short X-ray pulses.

One of the major challenges faced by the plasma acceleration community is to gain precise control over the highly sensitive acceleration process. From the beginning, the LUX project was designed and optimised for stability and reproducibility, with a focus on stable laser operation. The project uniquely combines state-of-the-art accelerator concepts, accelerator technology and diagnostics with the new concepts and developments of laser plasma wakefield acceleration.

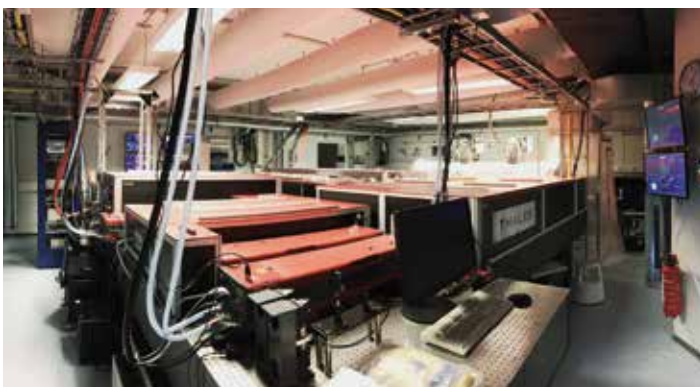


Figure 3

The 200 TW ANGUS laser system. The complete laser infrastructure was upgraded with advanced diagnostics and integrated into the accelerator controls systems.

Commissioning of the LUX experiment

With great support from the technical groups at DESY, the first phase of commissioning was completed in mid-2016, followed by the successful demonstration of first plasma-accelerated electrons, with the LUX accelerator generating high-energy beams of up to 400 MeV at 5 Hz repetition rate. Those first experiments proved the full operability of the LUX accelerator beamline at its design specifications. This was the first time that plasma-accelerated electrons were generated on the DESY campus.

The LUX beamline is currently being upgraded to include the undulator and the X-ray diagnostics sections. After the upgrade, it will thus feature the highly compact, in-vacuum permanent-magnet BEAST II undulator, which has been specifically designed to operate with plasma-driven electron beams (Fig. 4). Thanks to the undulator period length of only 5 mm, the electron beams demonstrated at LUX will already be sufficient to reach water-window photon energies.

Future developments

Future upgrades of the LUX beamline are foreseen to include a second laser transport beamline to enable advanced diagnostics and synchronised pump–probe experiments, as well as a 2 m long cryocooled undulator, specifically designed for a first demonstration of free-electron laser (FEL) amplification with plasma-generated electron beams.

The demonstration of a laser plasma-driven FEL is extremely challenging, as the quality and control of the plasma-driven beams are still limited. To relax the constraints on the electron beam quality, tailored electron transport and undulator concepts are currently being developed.

Contact: *Andreas Maier*, andreas.maier@desy.de

Project webpage: lux.desy.de

Taming plasma waves.

Start-to-end simulations reveal how to suppress hose instability in plasma wakefield accelerators

The FLASHForward project will employ electron beams from the accelerator of DESY's FLASH free-electron laser facility to drive a plasma wakefield accelerator (PWFA). Extreme wakefields on the order of GV/m enable a highly compact acceleration scheme, but also entail large growth rates for beam-plasma instabilities, most importantly the hose instability. If not sufficiently controlled, the hose instability can crucially limit the applicability of PWFAs. We recently generalised the mathematical description of the hose instability and obtained an improved understanding of the governing dynamics and of mitigation mechanisms. In addition, a newly established start-to-end simulation framework led to the important insight that an increase of the beam emittance can stabilise the beam propagation in plasma. These results are vital to enhance the stability of current and future PWFAs.

FLASHForward experiment

Plasma wakefield acceleration is a novel technology that delivers ultrahigh fields suitable for the acceleration of electrons to GeV energies over distances of much less than a metre. The FLASHForward experiment at DESY [1] is designed to generate such high accelerating fields in the wake of FLASH electron beams interacting with a plasma. The system will effectively operate as a transformer, in which the energy from the drive beam is transferred to the electrons of a trailing beam via the plasma wake. The technique is promising, but before beams suitable for relevant applications are generated, some challenges need to be overcome.

Hose instability

One of the most critical issues in beam-driven PWFAs is the hose instability [2,3]. This instability is seeded by an initial transverse asymmetry of the charge distribution of the beam (beam centroid deviation), which couples to the plasma wave and causes an asymmetry of the accelerating structure. This couples back to the beam centroid and thereby amplifies the initial asymmetry during the propagation, resulting in unstable acceleration and transport of trailing beams.

We were recently able to show in theoretical and numerical studies that this instability does not grow exponentially as predicted by the state-of-the-art description, but is mitigated after some beam propagation in the plasma target [4]. This is due to a decoherence of the individual electron oscillations stemming from the varying energy loss along the beam, intrinsically occurring as the beam drives the plasma wave, and from a possible initial correlated and/or uncorrelated energy spread. In addition, we found in theoretical studies that vacuum-to-plasma density tapers can reduce the hosing seed. However, for beams with a substantial initial beam

centroid deviation, hosing can still lead to an unstable acceleration process and/or a degraded beam quality.

Start-to-end simulations

Intra-beam structures can have a crucial impact on the performance of a PWFA. Hence, realistic, three-dimensional start-to-end simulations of the complete accelerator and the beam-plasma interaction are vital to understand and control undesired instabilities.

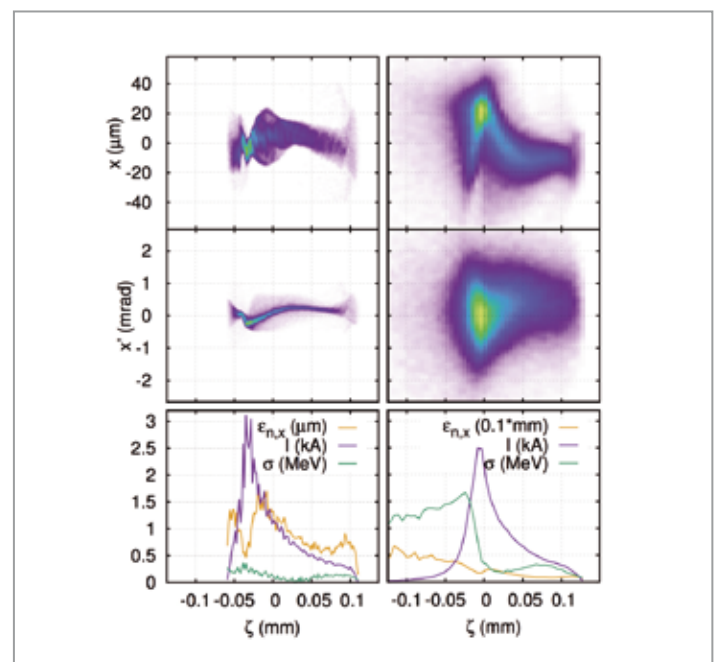


Figure 1

Simulated FLASH beams at the entrance to the FLASHForward plasma cell, without (left) and with (right) emittance spoiler. Top and middle panels: Horizontal charge projection. Bottom panels: Current profile, emittance and energy spread.

Particle tracking simulations

Simulations on beam optimisation and transport within the FLASH linear accelerator and the FLASHForward extraction are performed using the tracking code ELEGANT [5]. By tuning the ratio between the voltages and phases of the various accelerating modules, triangular beam current profiles can be produced during the compression in the chicanes [6]. Such profiles are optimal for the energy transfer from drive beam to plasma wave in the plasma accelerator. During the compression of the beam, coherent synchrotron radiation (CSR) is generated, causing the centroid deviations that seed the hose instability. CSR effects are enhanced with an, in principle, desired higher beam current. Hence, a balance between strong beam compression and small centroid deviations needs to be found. Figure 1 (left) shows such a balanced-case beam at the plasma cell entrance.

Particle-in-cell (PIC) simulations

The phase space (6D) distributions of the beams simulated with particle-tracking codes up to the plasma cell entrance are subsequently imported into the PIC code OSIRIS [7] for the computation of the beam–plasma interaction. Hereby, a plasma density profile with a smooth vacuum-to-plasma transition and a uniform plateau with a density of $n_0 = 10^{16} \text{ cm}^{-3}$ is considered (Fig. 2(e)). The charge density of the beam and the plasma is shown for two cases with 2 kA and 3 kA peak current in Fig. 2(a) and (c), respectively. It can be seen that the hose instability leads to a beam centroid displacement from head to tail, as well as an according deformation of the plasma cavity. The centroid evolution at the tail of the beam for the different cases is depicted in Fig. 2(f). The amplitudes of the beam-centroid and channel-centroid oscillations grow owed to hosing and impede the stable acceleration of a trailing beam.

Emittance spoiling

Since hosing is enhanced when beam electrons oscillate coherently, we exploit the following effect occurring for large-emittance beams. The non-linearity of the wakefields for large radii results in a decoherence of the transverse beam electron motion if the beam is sufficiently large. We therefore propose to spoil the emittance by inserting a thin slab of material into the beamline. Due to scattering of the beam electrons with the atoms of the material, the transverse momentum distribution of the beam is broadened. The beam acquires a greater emittance and becomes wider in the transverse direction after being rematched into the beamline.

Figure 2 shows PIC simulation results for beams with 2 kA and 3 kA peak current without (cases (a) and (c)) and with (cases (b) and (d)) usage of an emittance spoiler. Cases (c) and (d) correspond to the beams shown in Fig. 1 (left and right, respectively). We observe significantly reduced centroid oscillations during the beam propagation in the plasma in

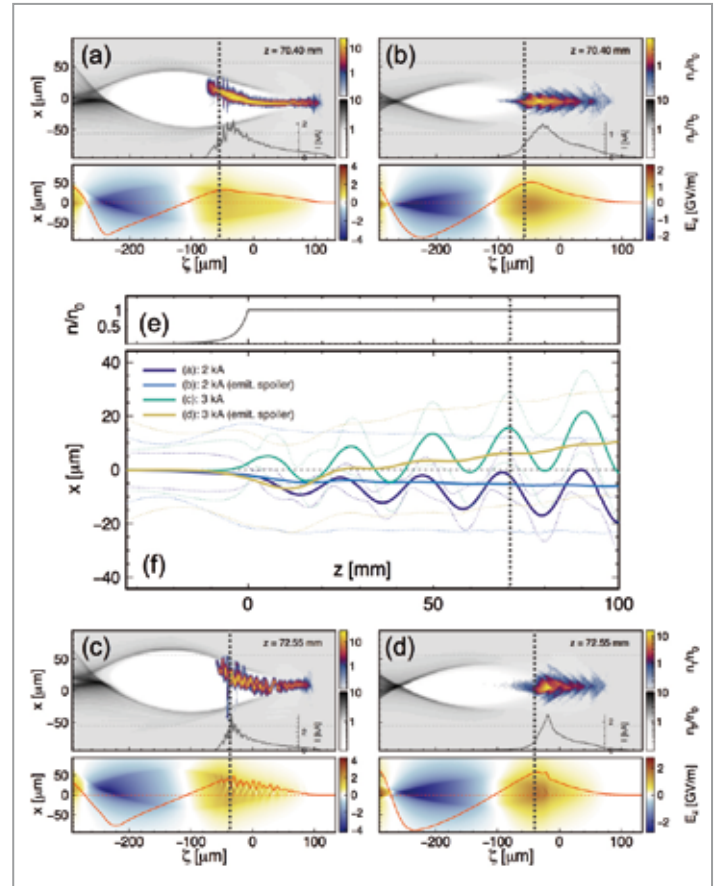


Figure 2

Results from PIC simulations for the centroid oscillations of the beam (f) for four different cases (a), (b), (c) and (d). Beams sent through a thin slab of aluminium ((b) and (d)) show an enhanced stability.

PIC simulations for the emittance-spoiled beams (cases (b) and (d) in Figure 2(f)). A rigorous explanation of the observed phenomena is currently being developed.

In conclusion, we gained an improved understanding of the hose instability, proposed a novel method to reduce the hosing seed in vacuum-to-plasma tapers and found that emittance-spoiled beams can suppress the hose instability. Hence, these results are crucial to enable PWFAs with enhanced stability.

References:

- [1] A. Aschikhin et al., Nucl. Instrum. Methods A806, 175 (2016).
- [2] D.H. Whittum et al., Phys. Rev. Lett. 67, 991 (1991).
- [3] C. Huang et al., Phys. Rev. Lett. 99, 255001 (2007).
- [4] T. Mehrling et al., Submitted (2016).
- [5] M. Borland et al., Advanced Photon Source LS-287 (2000).
- [6] P. Piot et al., Phys. Rev. Lett. 108, 034801 (2012).
- [7] R.A. Fonseca et al., Plas. Phys. Contr. Fusion 55, 124011 (2013).

Contact: Timon Mehrling, timon.mehrling@desy.de

The Horizon2020 project “European Plasma Research Accelerator with eXcellence In Applications” (EuPRAXIA) is funded by the European Union and started working in November 2015. EuPRAXIA aims at producing a conceptual design report for a highly compact and cost-effective European research infrastructure that produces multi-GeV electron beams and X-rays.

Introduction

EuPRAXIA will use highly innovative laser, beam and plasma technologies in order to achieve ultrahigh accelerating gradients. The accelerator facility will enable pilot applications for photon science, high-energy physics and other fields, such as medicine or materials processing. It will promote and apply world-leading laser technology from European industry.

The EuPRAXIA collaboration consists of 16 European partner institutes and an additional 22 associated partners, including leading laboratories from Europe, Asia, the USA as well as international organisations. As the coordinating institute, DESY plays a central role in the project. EuPRAXIA is structured into 14 work packages, ranging from plasma and laser research through advanced beam physics to outreach activities. Industry partners, such as Amplitude, Thales and TRUMPF Scientific Lasers, are participating through workshops and the Scientific Advisory Committee. The project goal is the delivery of a conceptual design report to the EU in October 2019.

100 cube challenge

The EuPRAXIA “100 cube challenge” for laser technology was defined in early 2016 by the “Laser design and optimisation” work package members, together with colleagues from Thales and Amplitude. The aim is to produce laser pulses of 100 J, with 100 fs duration and at 100 Hz repetition rate.

This goal is expected to be achievable by the mid-2020s but is sufficiently challenging to promote progress in the scientific laser and plasma communities as well as in industry. New and scalable materials for reliable operation at high repetition rates will need to be developed. Higher repetition rates are a key factor for achieving higher stability and relevance for applications.



Figure 1
Participants of the June 2016 meeting on EuPRAXIA, a European plasma accelerator facility, in Pisa, Italy

European plasma accelerator workshop

The complete collaboration and interested scientists from around the world convened for three days at the end of June 2016 in Pisa, Italy, the place where Galileo Galilei defined acceleration some 500 years earlier. The more than 120 registered delegates (Fig. 1) discussed the parameters and technical specifications required at the interfaces between radio frequency (RF) beam injectors, lasers, plasmas, beam transport systems and pilot user areas. Requirements from applications were reviewed, among them free-electron lasers (FELs), table-top electron beams for high-energy physics detector tests, ultracompact X-ray devices for medicine or materials research and other ideas. The meeting concluded with a draft parameter set for the EuPRAXIA facility.

In October 2016, the first yearly EuPRAXIA meeting took place at École polytechnique in Paris; work progress was reviewed and the first study version of the facility was formally defined. In addition, the EuPRAXIA collaboration board was formed and six new associated partners from Germany, Italy, Russia and Israel were admitted into the growing collaboration.

Outlook

In 2017, the collaboration will refine the technical details of the project design and discuss the results at dedicated collaboration meetings in several member states. Comparative simulations will assess the performance reach of various design options. A first layout of the accelerator research facility will be defined, including first preliminary cost estimates for technical units such as lasers, RF equipment, plasma technology, beam transport and FEL undulators. Discussions on possible European sites for EuPRAXIA will continue.

Contact: Paul Andreas Walker, andreas.walker@desy.de



References.

>	Committees	66
>	Memberships	67
>	Publications	68

DESY Board of Directors

R. Brinkmann

(Accelerator division)

H. Dosch

(Chairman of the DESY Board of Directors)

J. Mnich

(High-energy physics and astroparticle physics)

C. Harringa

(Administrative division)

E. Weckert

(Photon science division)

C. Stegmann

(Representative of the directorate in Zeuthen)

Machine Advisory Committee (MAC)

Riccardo Bartolini (Univ. Oxford, UK)

Michael Borland (ANL, USA)

Oliver Brüning (CERN, CH, Chair)

Angeles Faus-Golfe (Univ. Valencia, E)

Massimo Ferrario (INFN, I)

Zhirong Huang (SLAC, USA)

Pantaleo Raimondi (ESRF, F)

Andrzej Wolski (Univ. Liverpool, UK)

DESY Scientific Board

M. Aldaya Martin (DESY)

R. Aßmann (DESY)

F. Beckmann (HZG)

T. Behnke (DESY)

M. Bieler (DESY)

I. Bloch (DESY)

K. Borras (DESY)

A. Burkhardt (DESY)

K. Büßer (DESY)

F. Calegari (DESY)

H. Chapman (DESY)

M. Diehl (DESY)

R. Döhrmann (DESY)

J. Dreyling Eschweiler (DESY)

W. Drube (DESY)

S. Fiedler (EMBL)

T. Finnern (DESY)

B. Foster (DESY)

A. Frey (KET)

E. Gallo (DESY)

H. Graafsma (DESY)

I. M. Gregor (DESY)

C. Grojean (DESY)

G. Grübel (DESY)

W. Gülzow (DESY)

J. Haller (Univ. Hamburg)

B. Heinemann (DESY)

M. Hempel (DESY)

K. Honkavaara (DESY)

K. Jansen (DESY)

F. Kärtner (DESY)

R. Kammering (DESY)

M. Kasemann (DESY)

C. Kluth (DESY)

M. Kowalski (DESY)

M. Krause (DESY)

G. Kube (DESY)

K. Lipka (CMS)

A. Maier (KfB)

N. Meyners (DESY)

K. Mönig (DESY)

B. Murphy (KfS)

A. Mußgiller (DESY)

T. Naumann (DESY)

C. Niebuhr (DESY)

D. Nölle (DESY)

K. Peters (DESY)

E. Plönjes-Palm (DESY)

M. Pohl (DESY)

D. Reuther (DESY)

R. Röhlsberger (DESY)

R. Santra (DESY)

M. Schmitz (DESY)

T. Schörner-Sadenius (DESY)

V. Schomerus (DESY)

S. Schreiber (DESY)

C. Schroer (DESY)

H. Schulte-Schrepping (DESY)

A. Schulz (DESY)

C. Schwanenberger (DESY)

U. Schwanke (H U Berlin)

A. Schwarz (DESY)

G. Servant (DESY)

A. Stierle (DESY)

K. Tackmann (DESY)

S. Techert (DESY)

M. Tischer (DESY)

R. Treusch (DESY)

T. Tschentscher

(European XFEL)

Y. Umhey (DESY)

J. Viefhaus (DESY)

M. Vogt (DESY)

N. Walker (DESY)

P. Wegner (DESY)

G. Weiglein (DESY)

H. Weise (DESY)

H. C. Wille (DESY)

K. Wittenburg (DESY)

W. Wurth (DESY)

H. Yan (DESY)

Memberships.

ACHIP Consortium Advisory Board (Moore Foundation)
Reinhard Brinkmann

ACHIP Executive Board
Ralph Aßmann

AMICI EU Project Steering Committee
Hans Weise

ANKA Machine Advisory Committee
Klaus Balewski

Apollon/CILEX Technical Advisory Committee
Ralph Aßmann

AREAL Project, Armenia, International Technical Advisory Committee
Klaus Flöttmann

Accelerator Test Facility (ATF) Programme Advisory Committee
Ralph Aßmann

AWAKE Experiment CERN Collaboration Board
Ralph Aßmann

BerlinPro Machine Advisory Committee
Holger Schlarb, Siegfried Schreiber

BESSY Machine Advisory Committee
Winfried Decking

CERN Accelerator School Advisory Committee
Winfried Decking, Kay Wittenburg

CERN Accelerator School on FELs and ERLs (CAS 2016) Programme Committee and Local Chair
Kay Wittenburg

CERN Accelerator School Introductory (2016) and Advanced Level (2017) Programme Committee
Kay Wittenburg

CERN Accelerator School on Vacuum Systems and Technologies Programme Committee
Lutz Lilje

CERN Scientific Policy Committee
Reinhard Brinkmann

DEELS Workshop 2016 Local Chair
Gero Kube

European Plasma Research Accelerator with eXcellence In Applications (EuPRAXIA) - Collaboration Board
Ralph Aßmann, Reinhard Brinkmann

European Plasma Research Accelerator with eXcellence In Applications (EuPRAXIA) - Coordinator
Ralph Aßmann

ESRF Machine Advisory Committee
Ralph Aßmann

European Advanced Accelerator Concepts Workshop (EAAC2017) Organising Committee
Ralph Aßmann

European Advanced Accelerator Concepts Workshop (EAAC2017) Co-Chair
Ralph Aßmann

European Physical Society Accelerator Group (EPS-AG)
Ralph Aßmann

European Coordination for Accelerator R&D (EuCARD2) Deputy Coordinator
Ralph Aßmann

European Coordination for Accelerator R&D (EuCARD2) Steering Board
Ralph Aßmann

European Coordination for Accelerator R&D (EuCARD2) Governing Board
Ralph Aßmann

European Coordination for Accelerator R&D (EuCARD2) Coordinator
Ralph Aßmann

European Network for Novel Accelerators (EuroNNAc) Coordinator
Ralph Aßmann

European Coordination for Accelerator R&D (EuCARD2) Deputy Coordinator WP12
Nicoleta Baboi

European Physical Society Accelerator Group (EPS-AG)
Ralph Aßmann

European Spallation Source (ESS) Technical Advisory Committee
Hans Weise

European Synchrotron Radiation Facility (ESRF) Machine Advisory Committee
Ralph Aßmann

FAIR Machine Advisory Committee
Kay Wittenburg

FEL 2017 Scientific Programme Committee
Frank Stephan, Siegfried Schreiber

FLAC Machine Advisory Committee SwissFEL
Holger Schlarb

Future Circular Collider (FCC) Collaboration Board
Ralph Aßmann

HBB Workshop (Cuba 2016) Organising Committee
Ralph Aßmann

Helmholtz Think Tank
Hans Weise

ICALEPCS International Scientific Advisory Committee (ISAC)
Reinhard Bacher

IBIC International Programme Committee (IBIC 2016)
Kay Wittenburg

ICFA Beam Dynamics Panel
Rainer Wanzenberg

ICFA Mini Workshop on High Order Modes in Superconducting Cavities 2016 Scientific Programme Committee
Nicoleta Baboi

ILC European Action Plan Working Group
Nicholas Walker

International Conference on RF Superconductivity International Programme Committee
Wolf-Dietrich Möller

IPAC 2016 and 2017 Organising Committee
Ralph Aßmann

IPAC 2017 Scientific Advisory Board
Lutz Lilje

IVEC2017 Technical Programme Committee
Stefan Choroba

John Adams Institute Advisory Board
Reinhard Brinkmann

Joint University Accelerator School Advisory Board
Winfried Decking

Komitee für Beschleunigerphysik
Hans Weise

LINAC 2016 International Organising Committee
Hans Weise

LINAC 2016 Conference Scientific Programme Committee
Stefan Choroba, Hans Weise

LCLS-II Directors Review
Winfried Decking, Lutz Lilje

LCLS-II Vacuum System Review
Lutz Lilje

MAX IV Machine Advisory Committee
Klaus Balewski

NRC-ACOT Advisory Committee on TRIUMF
Hans Weise

OLAV-V (Operation of Large Vacuum Systems) Organising Committee
Lutz Lilje, Sven Lederer

PCaPAC Programme Committee
Philip Duval, Reinhard Bacher

PIP-II Machine Advisory Committee Fermilab
Hans Weise

PHIL Scientific Committee
Frank Stephan

Physical Review Special Topics - Accelerator and Beams - Editor
Klaus Flöttmann

POHANG Accelerator Laboratory International Advisory Committee
Winfried Decking

QRC-KAERI World Class Institute International Advisory Committee
Klaus Flöttmann

STFC Accelerator Strategy Board
Reinhard Brinkmann

Super KEKB Machine Advisory Committee
Ralph Aßmann

TIARA Council DESY Deputy
Ralph Aßmann

TIARA Governing Board
Reinhard Brinkmann

TTC Executive Committee
Hans Weise

TTC Technical Board
Wolf-Dietrich Möller, Detlef Reschke

UK/ESS High Beta Cavity Project Board
Detlef Reschke

Workshop Wakefields 2017 International Advisory Committee
Rainer Wanzenberg

XFEL Detector Advisory Committee
Kay Rehlich

Publications

K. Bane, G. Stupakov and I. Zagorodnov.

Analytical formulas for short bunch wakes in a flat dechirper.
Physical review accelerators and beams, 19(8):084401, and PUBDB-2016-03381, SLAC-PUB-16497; DESY-16-056; LCLS-II-TN-16-08; arXiv:1603.07411.
doi: 10.1103/PhysRevAccelBeams.19.084401.

J. Beckmann et al.

Optical Constants of Harmful and Highly Energetic Liquids and their Application to THz Screening Systems.
IEEE transactions on terahertz science and technology, 6(3):396, and PUBDB-2016-05500.
doi: 10.1109/TTHZ.2016.2547319.

M. Bertucci et al.

Defect detection inside superconducting 1.3 GHz cavities by means of x-ray fluorescence spectroscopy.
Review of scientific instruments, 87(1):013103, and PUBDB-2017-00299.
doi: 10.1063/1.4939611.

S. Bettoni et al.

Preservation of Low Slice Emittance in Bunch Compressors.
Physical review accelerators and beams, 19(3):034402, and PUBDB-2016-06323.
doi: 10.1103/PhysRevAccelBeams.19.034402.

H. Brueck et al.

Results of the Magnetic Measurements of the Superconducting Magnets for the European XFEL.
IEEE transactions on applied superconductivity, 26(4):4902204, and PUBDB-2017-00389.
doi: 10.1109/TASC.2016.2520489.

A. Caldwell et al.

Path to AWAKE: Evolution of the concept.
Nuclear instruments & methods in physics research / A, 829:3, and PUBDB-2016-06463.
doi: 10.1016/j.nima.2015.12.050.

M. Dohlus and C. Henning.

Periodic Poisson Model for Beam Dynamics simulation.
Physical review accelerators and beams, 19(3):034401, and PUBDB-2016-02056, DESY-15-071; arXiv:1505.01330.
doi: 10.1103/PhysRevAccelBeams.19.034401.

U. Dorda et al.

SINBAD—The accelerator R&D facility under construction at DESY.
Nuclear instruments & methods in physics research / A, 829:233, and PUBDB-2016-01462.
doi: 10.1016/j.nima.2016.01.067.

I. Dornmair et al.

Plasma-Driven Ultrashort Bunch Diagnostics.
Physical review accelerators and beams, 19(6):062801, and PUBDB-2017-00226.
doi: 10.1103/PhysRevAccelBeams.19.062801.

W. Drube et al.

The PETRA III Extension.

Proceedings of the 12th International Conference on Synchrotron Radiation Instrumentation, New York (NY USA), 6 Jul 2015 - 10 Jul 2015.
Inst., Melville, NY.
doi: 10.1063/1.4952814.

B. Faatz et al.

Simultaneous Operation of Two Soft X-Ray Free-Electron Lasers Driven by One Linear Accelerator.
New journal of physics, 18(6):062002, and PUBDB-2016-02922.
doi: 10.1088/1367-2630/18/6/062002.

G. Geloni, V. Kocharyan and E. Saldin.

Brightness of synchrotron radiation from wigglers.
Nuclear instruments & methods in physics research / A, 807:13, and PUBDB-2015-04824, DESY-14-235; arXiv:1412.2648.
doi: 10.1016/j.nima.2015.10.004.

V. Gharibyan and K. Balewski.

Planck-Scale Gravity Test at PETRA.
Journal of modern physics, 7(9):964, and PUBDB-2016-04302, DESY-16-029.
doi: 10.4236/jmp.2016.79088.

E. Gschwendtner et al.

AWAKE, The Advanced Proton Driven Plasma Wakefield Acceleration Experiment at CERN.
Nuclear instruments & methods in physics research / A, 829:76, and PUBDB-2017-00331, arXiv:1512.05498.
doi: 10.1016/j.nima.2016.02.026.

M. Hachmann and K. Flöttmann.

Measurement of Ultra Low Transverse Emittance at REGAE.
Nuclear instruments & methods in physics research / A, 829:318, and PUBDB-2017-00332.
doi: 10.1016/j.nima.2016.01.065.

M. Hachmann et al.

Design and characterization of permanent magnetic solenoids for REGAE.
Nuclear instruments & methods in physics research / A, 829:270, and PUBDB-2017-00396.
doi: 10.1016/j.nima.2016.02.033.

F. Kaertner et al.

AXSIS: Exploring the frontiers in attosecond X-ray science, imaging and spectroscopy.
Nuclear instruments & methods in physics research / A, 829:24, and PUBDB-2016-01314.
doi: 10.1016/j.nima.2016.02.080.

B. Ketenoğlu et al.

Transfer of the Magnetic Axis of an Undulator to Mechanical Fiducial Marks of a Laser Tracker System.
Nuclear instruments & methods in physics research / A, 808:135, and PUBDB-2017-00362.
doi: 10.1016/j.nima.2015.11.055.

- O. Lishilin et al.
First Results of the Plasma Wakefield Acceleration Experiment at PITZ.
2nd European Advanced Accelerator Concepts Workshop, La Biodola, Isola d'Elba (Italy), 13 Sep 2015 - 19 Sep 2015.
North-Holland Publ. Co., Amsterdam.
doi: 10.1016/j.nima.2016.01.005.
- A. Lüdeke et al.
Common Operation Metrics for Storage Ring Light Sources.
Physical review accelerators and beams, 19(8):082802, and PUBDB-2016-05539.
doi: 10.1103/PhysRevAccelBeams.19.082802.
- A. A. Lutman et al.
Fresh-Slice Multicolour X-Ray Free-Electron Lasers.
Nature photonics, 10(11):745, and PUBDB-2016-06123.
doi: 10.1038/nphoton.2016.201.
- B. Marchetti et al.
Electron-Beam Manipulation Techniques in the SINBAD Linac for External Injection in Plasma Wake-Field Acceleration.
2nd European Advanced Accelerator Concepts Workshop, La Biodola, Isola d'Elba (Italy), 13 Sep 2015 - 19 Sep 2015.
North-Holland Publ. Co., Amsterdam.
doi: 10.1016/j.nima.2016.03.041.
- F. Massimo, S. Atzeni and A. Marocchino.
Comparisons of Time Explicit Hybrid Kinetic-Fluid Code Architect for Plasma Wakefield Acceleration with a full PIC code.
Journal of computational physics, 327:841, and PUBDB-2016-04600.
doi: 10.1016/j.jcp.2016.09.067.
- S. Y. Mironov et al.
Generation of 3D ellipsoidal laser beams by means of a profiled volume chirped Bragg grating.
Laser physics letters, 13(5):055003, and PUBDB-2016-06346.
doi: 10.1088/1612-2011/13/5/055003.
- S. Y. Mironov et al.
Shaping of cylindrical and 3D ellipsoidal beams for electron photoinjector laser drivers.
Applied optics, 55(7):1630, and PUBDB-2016-06342.
doi: 10.1364/AO.55.001630.
- Y. Nie et al.
Potential Applications of the Dielectric Wakefield Accelerators in the SINBAD Facility at DESY.
2nd European Advanced Accelerator Concepts Workshop, La Biodola, Isola d'Elba (Italy), 13 Sep 2015 - 19 Sep 2015.
North-Holland Publ. Co., Amsterdam.
doi: 10.1016/j.nima.2016.01.038.
- T. Plath et al.
Free-Electron Laser Multiplex Driven by a Superconducting Linear Accelerator.
Journal of synchrotron radiation, 23(5):1070, and PUBDB-2016-02918.
doi: 10.1107/S1600577516009620.
- R. Pompili et al.
Beam Manipulation with Velocity Bunching for PWEA Applications.
Nuclear instruments & methods in physics research / A, 829:17, and PUBDB-2017-00443.
doi: 10.1016/j.nima.2016.01.061.
- A. Saa Hernandez et al.
Generation of Large-Bandwidth X-Ray Free-Electron-Laser Pulses.
Physical review accelerators and beams, 19(9):090702, and PUBDB-2016-06322.
doi: 10.1103/PhysRevAccelBeams.19.090702.
- T. Schietinger et al.
Commissioning Experience and Beam Physics Measurements at the SwissFEL Injector Test Facility.
Physical review accelerators and beams, 19(10):100702, and PUBDB-2016-06324.
doi: 10.1103/PhysRevAccelBeams.19.100702.
- G. van der Schot et al.
Open data set of live cyanobacterial cells imaged using an X-ray laser.
Scientific data, 3:160058, and PUBDB-2016-04881.
doi: 10.1038/sdata.2016.58.
- N. Simos et al.
Radiation Damage and Thermal Shock Response of Carbon-Fiber-Reinforced Materials to Intense High-Energy Proton Beams.
Physical review accelerators and beams, 19(11):111002, and PUBDB-2016-05505.
doi: 10.1103/PhysRevAccelBeams.19.111002.
- W. Singer et al.
Production of Superconducting 1.3-GHz Cavities for the European X-Ray Free Electron Laser.
Physical review accelerators and beams, 19(9):092001, and PUBDB-2017-00386.
doi: 10.1103/PhysRevAccelBeams.19.092001.
- M. Weikum et al.
Generation of Attosecond Electron Bunches in a laser-plasma Accelerator Using a Plasma Density Up-ramp.
2nd European Advanced Accelerator Concepts Workshop, La Biodola, Isola d'Elba (Italy), 13 Sep 2015 - 19 Sep 2015.
North-Holland Publ. Co., Amsterdam.
doi: 10.1016/j.nima.2016.01.003.
- G. Xia et al.
Plasma Wakefield Acceleration at CLARA facility in Daresbury Laboratory.
Nuclear instruments & methods in physics research / A, 829:43, and PUBDB-2017-00524.
doi: 10.1016/j.nima.2016.01.007.
- I. Zagorodnov, G. Feng and T. Limberg.
Corrugated Structure Insertion for Extending the SASE Bandwidth up to 3% at the European XFEL.
Nuclear instruments & methods in physics research / A, 837:69, and PUBDB-2016-04948, DESY-16-138; arXiv:1607.07642.
doi: 10.1016/j.nima.2016.09.001.

J. Zhu et al.
Sub-fs Electron Bunch Generation with Sub-10-fs Bunch Arrival-Time Jitter via Bunch Slicing in a Magnetic Chicane.
Physical review accelerators and beams, 19(5):054401, and PUBDB-2016-05891.
doi: 10.1103/PhysRevAccelBeams.19.054401.

J. Zhu et al.
Matching Sub-fs Electron Bunches for Laser-Driven Plasma Acceleration at SINBAD.
2nd European Advanced Accelerator Concepts Workshop, La Biodola, Isola d'Elba (Italy), 13 Sep 2015 - 19 Sep 2015.
North-Holland Publ. Co., Amsterdam.
doi: 10.1016/j.nima.2016.01.066.

Preprints and Internal Reports

P. Amstutz et al.
Confining Continuous Manipulations of Accelerator Beamline Optics.
PUBDB-2016-01896, DESY-16-071; arXiv:1604.06658.

K. Bane, G. Stupakov and I. Zagorodnov.
Analytical Formulas for Short Bunch Wakes in a Flat Dechirper.
PUBDB-2016-01534, SLAC-PUB-16497; DESY-16-056; LCLS-II-TN-16-08; arXiv:1603.07411.

G. Geloni, V. Kocharyan and E. Saldin.
Evidence of Wigner Rotation Phenomena in the Beam Splitting Experiment at the LCLS.
PUBDB-2016-02655, DESY-16-128; arXiv:1607.02928.

G. Geloni, V. Kocharyan and E. Saldin.
Misconception Regarding Conventional Coupling of Fields and Particles in XFEL Codes.
PUBDB-2016-00846, DESY 16-017.

G. Geloni, V. Kocharyan and E. Saldin.
On the Coupling of Fields and Particles in Accelerator and Plasma Physics.
PUBDB-2016-04359, DESY-16-194; arXiv:1610.04139.
doi: 10.3204/PUBDB-2016-04359.

V. Gharibyan.
Experimental Hint for Gravitational CP Violation.
PUBDB-2016-01182, DESY 16-014.

V. Gharibyan and K. Balewski.
Planck-scale Gravity test at PETRA - Letter of Intent.
PUBDB-2016-03273, arXiv:1602.06251; DESY-16-029.

C. Hernandez-Garcia et al.
Studies on charge production from Cs₂Te photocathodes in the PITZ L-band normal conducting radio frequency photo injector.
PUBDB-2016-06432, arXiv:1607.00295.
doi: 10.3204/PUBDB-2016-06432.

M. Holz et al.
The OTR Vessel Issues.
PUBDB-2016-04769, MDI/WP17 Internal Report 1.

E. A. Schneidmiller et al.
First Operation of a Harmonic Lasing Self-Seeded Free Electron Laser.
PUBDB-2016-06533, DESY-16-243; arXiv:1612.03635.
doi: 10.3204/PUBDB-2016-06533.

I. Zagorodnov, G. Feng and T. Limberg.
Corrugated Structure Insertion for Extending the SASE Bandwidth up to 3% at the European XFEL.
PUBDB-2016-02746, DESY-16-138; arXiv:1607.07642.

Conference Contributions

PCaPAC 2016

R. Bacher.
Augmented User Interaction.
11th International Workshop on Personal Computers and Particle Accelerator Controls, Campinas (Brazil), 25 Oct 2016 - 28 Oct 2016.
doi: 10.3204/PUBDB-2016-06410.

P. Duval, M. Lomperski and bobnar.
Control System Evolution and the Importance of Trial and Error.
11th International Workshop on Personal Computers and Particle Accelerator Controls, Campinas (Brazil), 25 Oct 2016 - 28 Oct 2016.
doi: 10.3204/PUBDB-2016-06433.

P. Duval et al.
Automated Availability Statistics.
11th International Workshop on Personal Computers and Particle Accelerator Controls, Campinas (Brazil), 25 Oct 2016 - 28 Oct 2016.
doi: 10.3204/PUBDB-2016-06437.

L. Froehlich et al.
High Level Software for the Commissioning of the European XFEL.
11th International Workshop on Personal Computers and Particle Accelerator Controls, Campinas (Brazil), 25 Oct 2016 - 28 Oct 2016.

M. C. Hierholzer et al.
Software Tests and Simulations for Control Applications Based on Virtual Time.
11th International Workshop on Personal Computers and Particle Accelerator Controls, Campinas (Brazil), 25 Oct 2016 - 28 Oct 2016.
doi: 10.3204/PUBDB-2016-05319.

G. K. Sahoo, F. Brinker and F. Wedtstein.
Orbitkorrektur, a Java Client for Transverse Orbitcorrection in PETRA-III.
11th International Workshop on Personal Computers and Particle Accelerator Controls, Campinas (Brazil), 25 Oct 2016 - 28 Oct 2016.
doi: 10.3204/PUBDB-2016-05647.

RT2016

M. C. Hierholzer, G. Varghese and M. Killenberg.
Software Tests and Simulations for Realtime Applications Based on Virtual Time.

20th IEEE-NPSS Real Time Conference, Padua (Italy), 5 Jun 2016 - 10 Jun 2016.

doi: 10.3204/PUBDB-2016-05847.

M. Killenberg et al.

Integrating Real-Time Control Applications into Different Control Systems.

20th IEEE-NPSS Real Time Conference, Padua (Italy), 5 Jun 2016 - 10 Jun 2016.

doi: 10.3204/PUBDB-2016-05840.

T. Kozak et al.

Fast Intra Bunch Train Charge Feedback for FELs based on Photo Injector Laser Pulse Modulation.

20th IEEE-NPSS Real Time Conference, Padua (Italy), 5 Jun 2016 - 10 Jun 2016.

doi: 10.3204/PUBDB-2016-05853.

T. Leśniak et al.

RTM RF Backplane Extensions for MicroTCA.4 Crates –Concept and Performance Measurements.

20th IEEE-NPSS Real Time Conference, Padua (Italy), 5 Jun 2016 - 10 Jun 2016.

IEEE.

doi: 10.1109/RTC.2014.7097413.

D. Makowski et al.

Automated Testing of MicroTCA.4 Modules.

20th IEEE-NPSS Real Time Conference, Padua (Italy), 5 Jun 2016 - 10 Jun 2016.

J. Piekarski et al.

Phase and Amplitude Drift Calibration of the RF Detectors in FELs LLRF Systems.

20th IEEE-NPSS Real Time Conference, Padua (Italy), 5 Jun 2016 - 10 Jun 2016.

K. Przygoda et al.

MicroTCA.4 based RF and Laser Cavities Regulation Including Piezo Controls.

20th IEEE-NPSS Real Time Conference, Padua (Italy), 5 Jun 2016 - 10 Jun 2016.

T. Rohlev et al.

Production and Testing of the LO and CLK Generation Module Built in MicroTCA.4 Form Factor.

20th IEEE-NPSS Real Time Conference, Padua (Italy), 5 Jun 2016 - 10 Jun 2016.

L. Rota et al.

An Ultra-fast Linear Array Detector for MHz Line Repetition Rate Spectroscopy.

20th IEEE-NPSS Real Time Conference, Padua (Italy), 5 Jun 2016 - 10 Jun 2016.

doi: 10.3204/PUBDB-2016-05885.

R. Rybaniec et al.

FPGA Based RF and Piezo Controllers for SRF Cavities in CW Mode.

20th IEEE-NPSS Real Time Conference, Padua (Italy), 5 Jun 2016 - 10 Jun 2016.

doi: 10.1109/RTC.2016.7543112.

N. Shehzad et al.

Modular Software for MicroTCA.4 Based Control Applications.

20th IEEE-NPSS Real Time Conference, Padua (Italy), 5 Jun 2016 - 10 Jun 2016.

doi: 10.3204/PUBDB-2016-05842.

G. Varghese et al.

Implementing a ReboT Server on a Microblaze.

20th IEEE-NPSS Real Time Conference, Padua (Italy), 5 Jun 2016 - 10 Jun 2016.

doi: 10.3204/PUBDB-2016-05889.

M. Żukociński et al.

Universal High-Performance LO and CLK Generation Module for LLRF System Receivers.

20th IEEE-NPSS Real Time Conference, Padua (Italy), 5 Jun 2016 - 10 Jun 2016.

doi: 10.3204/PUBDB-2016-05845.

LINAC2016

A. Brinkmann and J. Ziegler.

Dry-Ice Cleaning of RF-Structures at DESY.

28th Linear Accelerator Conference, East Lansing (USA), 25 Sep 2016 - 30 Sep 2016.

doi: 10.3204/PUBDB-2016-05804.

H. Weise.

Status of the European XFEL.

28th Linear Accelerator Conference, East Lansing (USA), 25 Sep 2016 - 30 Sep 2016.

EAAC2015

M. Hachmann and K. Floettmann.

Measurement of Ultra Low Transverse Emittance at REGAE.

2nd European Advanced Accelerator Concepts Workshop, La Biodola, Isola d'Elba (Italy), 13 Sep 2015 - 19 Sep 2015.

M. Hachmann et al.

Design and Characterization of Permanent Magnetic Solenoids for REGAE.

2nd European Advanced Accelerator Concepts Workshop, La Biodola, Isola d'Elba (Italy), 13 Sep 2015 - 19 Sep 2015.

IPAC16

V. Balandin, W. Decking and N. Golubeva.

Notes on Steffen Parameters of Extended Fringe-Field Quadrupoles.

7th International Particle Accelerator Conference, Busan (Korea), 8 May 2016 - 13 May 2016.

JACoW, Geneva, Switzerland.

doi: 10.18429/JACoW-IPAC2016-THPMB005.

- V. Balandin, W. Decking and N. Golubeva.
Numerical Computation of Transport Matrices of Axisymmetric RF Cavities for Online Beam Dynamics Applications.
7th International Particle Accelerator Conference, Busan (Korea), 8 May 2016 - 13 May 2016.
JACoW, Geneva, Switzerland.
doi: 10.18429/JACoW-IPAC2016-THPMB007.
- V. Balandin, W. Decking and N. Golubeva.
Unclosed Lattice Dispersions as a Tool for Partial Removal of Transverse to Longitudinal Beam Correlations.
7th International Particle Accelerator Conference, Busan (Korea), 8 May 2016 - 13 May 2016.
JACoW, Geneva, Switzerland.
doi: 10.18429/JACoW-IPAC2016-THPMB006.
- V. Balandin et al.
Operation of Free Electron Laser FLASH Driven by Short Electron Pulses.
7th International Particle Accelerator Conference, Busan (Korea), 8 May 2016 - 13 May 2016.
- M. Bousonville, F. Eints and S. Choroba.
Planning and Controlling of the Cold Accelerator Sections Installation in XFEL.
7th International Particle Accelerator Conference, Busan (Korea), 8 May 2016 - 13 May 2016.
CERN, Geneva.
doi: 10.3204/PUBDB-2016-05302.
- O. Brovko et al.
Measurements of Ultrasmall Charges with MCP Detector in FLASH Accelerator.
7th International Particle Accelerator Conference, Busan (Korea), 8 May 2016 - 13 May 2016.
[CERN], [Genf].
doi: 10.3204/PUBDB-2016-06263.
- F. Christie, M. Vogt and B. Schmidt.
Compensation of Steerer Crosstalk Between FLASH1 and FLASH2.
7th International Particle Accelerator Conference, Busan (Korea), 8 May 2016 - 13 May 2016.
doi: 10.3204/PUBDB-2016-05326.
- P. Echevarria et al.
First LLRF Tests of BERLinPro Gun Cavity Prototype.
7th International Particle Accelerator Conference, Busan (Korea), 8 May 2016 - 13 May 2016.
- M. Fakhari et al.
Thermal Simulation of an Energy Feedback Normal Conducting RF Cavity.
7th International Particle Accelerator Conference, Busan (Korea), 8 May 2016 - 13 May 2016.
JACoW, Geneva, Switzerland.
doi: 10.18429/JACoW-IPAC2016-MOPMW003.
- N. Joshi et al.
Simulation of Electromagnetic Scattering Through the E-XFEL Third Harmonic Cavity Module.
7th International Particle Accelerator Conference, Busan (Korea), 8 May 2016 - 13 May 2016.
JACoW, Geneva.
- J. Keil and H. Ehrlichmann.
Bunch Purity Measurements at PETRA III.
7th International Particle Accelerator Conference, Busan (Korea), 8 May 2016 - 13 May 2016.
- B. Marchetti et al.
Technical Design Considerations About the SINBAD-ARES Linac.
7th International Particle Accelerator Conference, Busan (Korea), 8 May 2016 - 13 May 2016.
- K. Przygoda et al.
MTCA.4-based Beam Line Stabilization Application.
7th International Particle Accelerator Conference, Busan (Korea), 8 May 2016 - 13 May 2016.
- K. Przygoda et al.
MicroTCA.4 based Single Cavity Regulation including Piezo Controls.
7th International Particle Accelerator Conference, Busan (Korea), 8 May 2016 - 13 May 2016.
doi: 10.3204/PUBDB-2016-02682.
- D. Reschke.
Performance of Superconducting Cavities for the European XFEL.
7th International Particle Accelerator Conference, Busan (Korea), 8 May 2016 - 13 May 2016.
Jacow, CERN.
doi: 10.3204/PUBDB-2016-05788.
- E. A. Schneidmiller and M. Yurkov.
Application of Statistical Methods for Measurements of the Coherence Properties of the Radiation from SASE FEL.
7th International Particle Accelerator Conference, Busan (Korea), 8 May 2016 - 13 May 2016.
doi: 10.3204/PUBDB-2016-06315.
- E. A. Schneidmiller and M. Yurkov.
Reverse undulator tapering for polarization control at XFELs.
7th International Particle Accelerator Conference, Busan (Korea), 8 May 2016 - 13 May 2016.
doi: 10.3204/PUBDB-2016-06312.
- E. A. Schneidmiller and M. Yurkov.
Studies of Harmonic Lasing Self-Seeded FEL at FLASH2.
7th International Particle Accelerator Conference, Busan (Korea), 8 May 2016 - 13 May 2016.
doi: 10.3204/PUBDB-2016-06313.
- E. A. Schneidmiller and M. Yurkov.
Transverse Coherence and Fundamental Limitation on the Pointing Stability of X-ray FELs.
7th International Particle Accelerator Conference, Busan (Korea), 8 May 2016 - 13 May 2016.
doi: 10.3204/PUBDB-2016-06314.
- L. Shi et al.
Measurement of Beam Phase at FLASH using HOMs in Accelerating Cavities.
7th International Particle Accelerator Conference, Busan (Korea), 8 May 2016 - 13 May 2016.
JACoW, Geneva.
doi: 10.3204/PUBDB-2016-04882.

- M. Vogt et al.
The Superconducting Soft X-ray Free-Electron Laser User Facility FLASH.
7th International Particle Accelerator Conference, Busan (Korea), 8 May 2016 - 13 May 2016.
doi: 10.3204/PUBDB-2017-00262.
- Y. Yamamoto, W.-D. Moeller and D. Reschke.
Error Estimation in Cavity Performance Test for the European XFEL at DESY.
7th International Particle Accelerator Conference, Busan (Korea), 8 May 2016 - 13 May 2016.
doi: 10.3204/PUBDB-2016-05948.
- J. Zhu et al.
Dogleg Design for the SINBAD Linac.
7th International Particle Accelerator Conference, Busan (Korea), 8 May 2016 - 13 May 2016.
JACoW, Geneva, Switzerland.
doi: 10.18429/JACoW-IPAC2016-THPMB010.
- DPG-Frühjahrstagung: Arbeitskreis Beschleunigerphysik**
- P. Boonpornprasert et al.
First Characterization of 4 nC Electron Beams for THz Studies at PITZ.
DPG-Frühjahrstagung: Arbeitskreis Beschleunigerphysik, Darmstadt (Germany), 14 Mar 2016 - 18 Mar 2016.
doi: 10.3204/PUBDB-2016-06529.
- M. Gross et al.
Argon Gas Discharge Plasma for PWA-Experiments at PITZ.
DPG-Frühjahrstagung: Arbeitskreis Beschleunigerphysik, Darmstadt (Germany), 14 Mar 2016 - 18 Mar 2016.
doi: 10.3204/PUBDB-2016-06537.
- M. Gross et al.
Electron windows studies for Self-Modulation Experiments at PITZ.
DPG-Frühjahrstagung: Arbeitskreis Beschleunigerphysik, Darmstadt (Germany), 14 Mar 2016 - 18 Mar 2016.
doi: 10.3204/PUBDB-2016-06541.
- C. Saisa-ard, M. Krasilnikov and G. Vashchenko.
Evaluation of the Photocathode Laser Transverse Distribution : Core + Halo Models.
DPG-Frühjahrstagung: Arbeitskreis Beschleunigerphysik, Darmstadt (Germany), 14 Mar 2016 - 18 Mar 2016.
doi: 10.3204/PUBDB-2016-06534.
- IBIC2016**
- H. Delsim-Hashemi.
Single Shot Transversal Profile Monitoring of Ultra Lowcharge Relativistic Electron Bunches at REGAE.
International Beam Instrumentation Conference, Barcelona (Spain), 11 Sep 2016 - 15 Sep 2016.
doi: 10.3204/PUBDB-2016-05708.
- E. Janas et al.
Temperature and Humidity Drift Characterization of Passive RF Components for a Two-Tone Calibration Method.
International Beam Instrumentation Conference, Barcelona (Spain), 11 Sep 2016 - 15 Sep 2016.
doi: 10.3204/PUBDB-2016-04366.
- P. N. Juranic et al.
PALM Concepts and Considerations.
International Beam Instrumentation Conference, Barcelona (Spain), 11 Sep 2016 - 15 Sep 2016.
- G. Kube.
Performance Studies of Industrial CCD Cameras Based on Signal-To-Noise and Photon Transfer Measurements.
International Beam Instrumentation Conference, Barcelona (Spain), 11 Sep 2016 - 15 Sep 2016.
JACoW, Geneva.
- G. Kube et al.
Status of the Two-Dimensional Synchrotron Radiation Interferometer at PETRA III.
International Beam Instrumentation Conference, Barcelona (Spain), 11 Sep 2016 - 15 Sep 2016.
JACoW, Geneva.
- D. Lipka et al.
First Experience with the Standard Diagnostics at the European XFEL Injector.
International Beam Instrumentation Conference, Barcelona (Spain), 11 Sep 2016 - 15 Sep 2016.
JACoW, Geneva.
- K. Przygoda et al.
MicroTCA.4 Based Optical Frontend Readout Electronics and its Applications.
International Beam Instrumentation Conference, Barcelona (Spain), 11 Sep 2016 - 15 Sep 2016.
- L. Rota et al.
KALYPSO: A Mfps Linear Array Detector for Visible to NIR Radiation.
International Beam Instrumentation Conference, Barcelona (Spain), 11 Sep 2016 - 15 Sep 2016.
doi: 10.3204/PUBDB-2016-04365.
- C. Simon et al.
Design and Beam Test Results of the Reentrant Cavity BPM for the European XFEL.
International Beam Instrumentation Conference, Barcelona (Spain), 11 Sep 2016 - 15 Sep 2016.
JACoW, Geneva.
- NAPAC16**
- R. Wichmann.
Accelerator Technical Progress and First Commissioning Results from the European XFEL.
North American Particle Accelerator Conference 2016, Chicago (USA), 9 Oct 2016 - 14 Oct 2016.
doi: 10.3204/PUBDB-2016-05689.

I. Zagorodnov.

Computation of Electromagnetic Fields Generated by Relativistic Beams in Complicated Structures.

North American Particle Accelerator Conference 2016, Chicago (USA), 9 Oct 2016 - 14 Oct 2016.

doi: 10.3204/PUBDB-2016-05810.

I. Zagorodnov, G. Feng and T. Limberg.

Corrugated Structure Insert to Extend SASE Bandwidth Up to 3% at the European XFEL.

North American Particle Accelerator Conference 2016, Chicago (USA), 9 Oct 2016 - 14 Oct 2016.

doi: 10.3204/PUBDB-2016-05813.

Other Conference Contributions

M. Felber.

MicroTCA.4 Usage in the Femtosecond-Synchronization System at European XFEL - Enabling the XFEL for Femtosecond Precision User Experiments.

5th MicroTCA workshop for industry and research, Hamburg (Germany), 7 Dec 2016 - 8 Dec 2016.

doi: 10.3204/PUBDB-2016-06055.

F. Makowski et al.

Design and Implementation of LLRF Station Software Suite in Distributed Control System Used in E-XFEL.

23rd International Conference Mixed Design of Integrated Circuits and Systems, Lodz (Poland), 23 Jun 2016 - 25 Jun 2016.

doi: 10.1109/MIXDES.2016.7529706.

A. Nawaz et al.

Self-Organized Critical Control for the European XFEL Using Black Box Parameter Identification for the Quench Detection System.

3rd Conference on Control and Fault-Tolerant Systems, Barcelona (Spain), 7 Sep 2016 - 9 Sep 2016.

doi: 10.3204/PUBDB-2016-06014.

M. Schloesser.

Coordinate Database at DESY.

14th International Workshops on Accelerator Alignment, Grenoble (France), 3 Oct 2016 - 7 Oct 2016.

doi: 10.3204/PUBDB-2016-06681.

S. Vilcins-Czvitkovits et al.

The Influences of Material Properties to Micro Damages on Vacuum Chamber CF Flanges.

Mechanical Engineering Design of Synchrotron Radiation Equipment and Instrumentation conference, Barcelona (Spain), 11 Sep 2016 - 16 Sep 2016.

JACoW, Geneva.

doi: 10.3204/PUBDB-2016-04878.

H. Weise.

The European XFEL – Status and Commissioning.

Russian Particle Accelerator Conference 2016, Saint Petersburg (Russia), 21 Nov 2016 - 25 Nov 2016.

doi: 10.3204/PUBDB-2017-00511.

Conference Presentations

LINAC2016

A. Brinkmann and J. Ziegler.

Dry-Ice Cleaning of RF-Structures at DESY.

28th Linear Accelerator Conference, East Lansing (USA), 25 Sep 2016 - 30 Sep 2016.

doi: 10.3204/PUBDB-2016-05282.

S. Choroba, V. Katalev and E. Apostolov.

Series Production of the RF Power Distribution for the European XFEL.

28th Linear Accelerator Conference, East Lansing (USA), 25 Sep 2016 - 30 Sep 2016.

doi: 10.3204/PUBDB-2016-05297.

C. Gruen, S. Schreiber and T. Schulz.

A Laser Pulse Controller for the Injector Laser at FLASH and European XFEL.

28th Linear Accelerator Conference, East Lansing (USA), 25 Sep 2016 - 30 Sep 2016.

doi: 10.3204/PUBDB-2017-00381.

M. Krasilnikov et al.

Investigations on Electron Beam Imperfections at PITZ.

28th Linear Accelerator Conference, East Lansing (USA), 25 Sep 2016 - 30 Sep 2016.

doi: 10.3204/PUBDB-2016-06464.

V. Vogel et al.

Summary of the Test and Installation of 10 MW MBKS for the XFEL Project.

28th Linear Accelerator Conference, East Lansing (USA), 25 Sep 2016 - 30 Sep 2016.

doi: 10.3204/PUBDB-2016-05793.

N. J. Walker et al.

Performance Analysis of the European XFEL SRF Cavities, from Vertical Test to Operation in Modules.

28th Linear Accelerator Conference, East Lansing (USA), 25 Sep 2016 - 30 Sep 2016.

H. Weise.

Status of the European XFEL.

28th Linear Accelerator Conference, East Lansing (USA), 25 Sep 2016 - 30 Sep 2016.

2nd general meeting of the Helmholtz programs Matter and Technologies

P. Boonpornprasert et al.

First Experimental Characterization of Electron Beams for THz Options at PITZ.

2nd general meeting of the Helmholtz programs Matter and Technologies, Karlsruhe (Germany), 8 Mar 2016 - 10 Mar 2016.

doi: 10.3204/PUBDB-2016-06522.

M. Gross et al.
First experimental results towards demonstrating the self-modulation instability at PITZ.
2nd general meeting of the Helmholtz programs Matter and Technologies, Karlsruhe (Germany), 8 Mar 2016 - 10 Mar 2016.
doi: 10.3204/PUBDB-2016-06518.

5th MicroTCA workshop for industry and research

J. Branlard.
LLRF System Installation for the European XFEL.
5th MicroTCA workshop for industry and research, Hamburg (Germany), 7 Dec 2016 - 8 Dec 2016.
doi: 10.3204/PUBDB-2016-06156.

K. Przygoda, M. Fenner and H. Laufkoetter.
High Voltage Power Module Pluggable to NAT RTM Power Supply Carrier.
5th MicroTCA workshop for industry and research, Hamburg (Germany), 7 Dec 2016 - 8 Dec 2016.
doi: 10.3204/PUBDB-2017-00011.

IPAC16

M. Bousonville, F. Eints and S. Choroba.
Planning and Controlling of the Cold Accelerator Sections Installation in XFEL.
7th International Particle Accelerator Conference, Busan (Korea), 8 May 2016 - 13 May 2016.

F. Brinker and X. c. team.
Commissioning of the European XFEL Injector.
7th International Particle Accelerator Conference, Busan (Korea), 8 May 2016 - 13 May 2016.
doi: 10.3204/PUBDB-2016-05971.

F. Christie, M. Vogt and B. Schmidt.
Compensation of Steerer Crosstalk Between FLASH1 and FLASH2.
7th International Particle Accelerator Conference, Busan (Korea), 8 May 2016 - 13 May 2016.
doi: 10.3204/PUBDB-2016-05329.

M. Gross et al.
Upgrades of the Experimental Setup for Electron Beam Self-modulation Studies at PITZ.
7th International Particle Accelerator Conference, Busan (Korea), 8 May 2016 - 13 May 2016.
doi: 10.3204/PUBDB-2016-06450.

J. Keil and H. Ehrlichmann.
Bunch Purity Measurements at PETRA III.
7th International Particle Accelerator Conference, Busan (Korea), 8 May 2016 - 13 May 2016.

G. Loisch et al.
A High Transformer Ratio Scheme for PITZ PWA Experiments.
7th International Particle Accelerator Conference, Busan (Korea), 8 May 2016 - 13 May 2016.
doi: 10.3204/PUBDB-2016-06456.

Y. Renier et al.
High Average RF Power Tests With 2 RF Vacuum Windows at PITZ.
7th International Particle Accelerator Conference, Busan (Korea), 8 May 2016 - 13 May 2016.
doi: 10.3204/PUBDB-2016-06454.

Y. Renier et al.
Latest News on High Average RF Power Operation at PITZ.
7th International Particle Accelerator Conference, Busan (Korea), 8 May 2016 - 13 May 2016.
doi: 10.3204/PUBDB-2016-06466.

D. Reschke.
Performance of Superconducting Cavities for the European XFEL.
7th International Particle Accelerator Conference, Busan (Korea), 8 May 2016 - 13 May 2016.
doi: 10.3204/PUBDB-2016-05790.

M. Vogt et al.
The Superconducting Soft X-Ray Free-Electron Laser User Facility FLASH.
7th International Particle Accelerator Conference, Busan (Korea), 8 May 2016 - 13 May 2016.
doi: 10.3204/PUBDB-2017-00263.

HOMSC16

N.-I. Baboi.
HOM Characterization for Beam Diagnostics at the European XFEL.
ICFA Mini Workshop on High Order Modes in Superconducting Cavities 2016, Warnemünde (Germany), 22 Aug 2016 - 24 Aug 2016.
doi: 10.3204/PUBDB-2016-05751.

N.-I. Baboi et al.
Higher Order Modes Based Beam Phase Study : Simulations and Measurements.
ICFA Mini Workshop on High Order Modes in Superconducting Cavities 2016, Warnemünde (Germany), 22 Aug 2016 - 24 Aug 2016.
doi: 10.3204/PUBDB-2016-05749.

T. Hellert.
HOM-based Cavity Alignment Measurement at FLASH.
ICFA Mini Workshop on High Order Modes in Superconducting Cavities 2016, Warnemünde (Germany), 22 Aug 2016 - 24 Aug 2016.
doi: 10.3204/PUBDB-2016-05806.

I. Zagorodnov and M. Dohlus.
Direct time-domain computation of wake fields at third harmonic module of the European XFEL.
ICFA Mini Workshop on High Order Modes in Superconducting Cavities 2016, Warnemünde (Germany), 22 Aug 2016 - 24 Aug 2016.
doi: 10.3204/PUBDB-2016-05808.

IBIC2016

H. Delsim-Hashemi.

Single Shot Transversal Profile Monitoring of Ultra Lowcharge Relativistic Electron Bunches at REGAE.

International Beam Instrumentation Conference, Barcelona (Spain), 11 Sep 2016 - 15 Sep 2016.
doi: 10.3204/PUBDB-2016-05706.

H. Huck et al.

Progress on the PITZ TDS.

International Beam Instrumentation Conference, Barcelona (Spain), 11 Sep 2016 - 15 Sep 2016.

LAOLA 2016

M. Gross.

Status of LAOLA@PITZ.

Laboratory for Laser- and beam-driven plasma Acceleration workshop, Wismar (Germany), 21 Jun 2016 - 22 Jun 2016.
doi: 10.3204/PUBDB-2016-06545.

G. Loisch et al.

Preparations for High Transformer Ratio PWEA Experiments at PITZ.

Laboratory for Laser- and beam-driven plasma Acceleration workshop, Wismar (Germany), 21 Jun 2016 - 22 Jun 2016.
doi: 10.3204/PUBDB-2016-06551.

S. Philipp et al.

Technical updates for the next generation lithium plasma cell at PITZ.

Laboratory for Laser- and beam-driven plasma Acceleration workshop, Wismar (Germany), 21 Jun 2016 - 22 Jun 2016.
doi: 10.3204/PUBDB-2016-06555.

NAPAC16

M. Turner et al.

Compact Ring-Based X-Ray Source With on-Orbit and on-Energy Laser-Plasma Injection.

North American Particle Accelerator Conference 2016, Chicago (USA), 9 Oct 2016 - 14 Oct 2016.

R. Wichmann.

Accelerator Technical Progress and First Commissioning Results from the European XFEL.

North American Particle Accelerator Conference 2016, Chicago (USA), 9 Oct 2016 - 14 Oct 2016.
doi: 10.3204/PUBDB-2016-05745.

I. Zagorodnov.

Computation of Electromagnetic Fields Generated by Relativistic Beams in Complicated Structures.

North American Particle Accelerator Conference 2016, Chicago (USA), 9 Oct 2016 - 14 Oct 2016.
doi: 10.3204/PUBDB-2016-05811.

I. Zagorodnov, G. Feng and T. Limberg.

Corrugated Structure Insertion to Extend SASE Bandwidth Up to 3% at the European XFEL - Beam Dynamics and FEL Simulations.

North American Particle Accelerator Conference 2016, Chicago (USA), 9 Oct 2016 - 14 Oct 2016.
doi: 10.3204/PUBDB-2016-05812.

TTC

D. Kostin.

Improvement / Deterioration of Module Performance Due to RF Conditioning at AMTF.

TESLA Technology Collaboration Meeting 2016, Saclay (France), 5 Jul 2016 - 8 Jul 2016.
doi: 10.3204/PUBDB-2016-05287.

D. Reschke.

EU-XFEL Summary of Performance Degradation.

TESLA Technology Collaboration Meeting 2016, Gif-sur-Yvette (France), 5 Jul 2016 - 8 Jul 2016.
doi: 10.3204/PUBDB-2016-05780.

D. Reschke.

Retreatment of Superconducting Cavities for the European XFEL.

TESLA Technology Collaboration Meeting 2016, Gif-sur-Yvette (France), 5 Jul 2016 - 8 Jul 2016.
doi: 10.3204/PUBDB-2016-05785.

Other Conference Presentations

R. Bacher.

Beyond Mouse-Based User Interaction.

Workshop on Accelerator Operations, Shanghai (China), 19 Sep 2016 - 23 Sep 2016.
doi: 10.3204/PUBDB-2016-06409.

B. Beutner.

European XFEL Injector Commissioning.

4th ARD ST3 Workshop - Matter and Technology, Berlin (Germany), 13 Jun 2016 - 15 Jun 2016.

L. Butkowski et al.

Model Based Fast Protection System for High Power RF Tube Amplifiers Used at European XFEL Accelerator.

20th IEEE-NPSS Real Time Conference, Padua (Italy), 5 Jun 2016 - 10 Jun 2016.
doi: 10.3204/PUBDB-2016-06264.

S. Choroba and V. Katalev.

Construction of the RF System for the European XFEL.

Ninth Continuous Wave and High Average Power RF Workshop, Grenoble (France), 21 Jun 2016 - 24 Jun 2016.
doi: 10.3204/PUBDB-2016-05298.

K. Floettmann.

Generation of Ultra-Short Bunches.

Physics and Applications of High Brightness Beams, Havana (Cuba), 28 Mar 2016 - 1 Apr 2016.

J. Keil.
PETRA IV Lattice Studies.
2nd Workshop on Low Emittance Ring Lattice Design, Lund (Sweden), 1 Dec 2016 - 2 Dec 2016.
doi: 10.3204/PUBDB-2016-06016.

M. Killenberg et al.
ChimeraTK: A Toolkit for Modular Control Applications.
11th International Workshop on Personal Computers and Particle Accelerator Controls, Campinas (Brazil), 25 Oct 2016 - 28 Oct 2016.
doi: 10.3204/PUBDB-2016-06461.

J. Osterhoff.
Considerations for a Beam-Driven EuPRAXIA Accelerator of High Average Power.
EuPRAXIA WP 9 Meeting, Frascati (Italy), 3 Oct 2016 - 4 Oct 2016.

J.-P. Schwinkendorf et al.
FLASHForward - Beam-driven plasma wakefield acceleration at DESY.
17th Advanced Accelerator Concepts Workshop, National Harbor (Maryland, USA), 31 Jul 2016 - 5 Aug 2016.

H. Weise.
Status of the European XFEL.
Russian Particle Accelerator Conference 2016, Saint Petersburg (Russia), 21 Nov 2016 - 25 Nov 2016.
doi: 10.3204/PUBDB-2017-00507.

Thesis

Ph.D. Thesis

M. Fakhari.
Design of Radio-Frequency Cavities and Tera-Hertz Electron Injectors for Advanced Applications.
Universität Hamburg, Hamburg, 2016.

M. Yan.
Online Diagnostics of Time-Resolved Electron Beam Properties with Femtosecond Resolution for X-Ray FELs.
Universität Hamburg, Hamburg, 2016.

Master Thesis

F. Christie.
Compensation of Steerer Crosstalk between FLASH1 and FLASH2.
University of Hamburg, 2015.

Bachelor Thesis

D. Dettmann.
Abschätzung des Einflusses von realen Feldprofilen der Elektronenquelle auf simulierte Strahlparameter bei PITZ.
Technische Hochschule Wildau, 2016.

A. Mufti.
Verbesserung und Charakterisierung der ArF Laser Beamline des Plasmabeschleunigungsexperiments bei PITZ.
Technische Hochschule Wildau, 2016.

Photographs and graphics

DESY

Fred Dott/European XFEL

European XFEL

W. Ronny Huang/CFEL/DESY/MIT

Marta Mayer/DESY

Heiner Müller Elsner/DESY/European XFEL

Dirk Nölle/DESY

N. Delbos/UHH

I. Dornmair/UHH

S. J alas/UHH

M. Kirchen/UHH

The figures were reproduced by permission of authors or journals.

Acknowledgement

We would like to thank all authors and everyone who helped in the creation of this annual report. ●

Imprint

Publishing and contact

Deutsches Elektronen-Synchrotron DESY
A Research Centre of the Helmholtz Association

Hamburg location:

Notkestr. 85, 22607 Hamburg, Germany
Tel.: +49 40 8998-0, Fax: +49 40 8998-3282
desyinfo@desy.de

Zeuthen location:

Platanenallee 6, 15738 Zeuthen, Germany
Tel.: +49 33762 7-70, Fax: +49 33762 7-7413
desyinfo.zeuthen@desy.de

www.desy.de

ISBN 978-3-945931-10-3

doi: 10.3204/PUBDB-2017-01405

Editing

Klaus Balewski
Ilka Flegel, Kapellendorf

Layout

Sabine Kuhls-Dawideit

Production

Britta Liebaug

Printing

EHS Druck GmbH, Schenefeld

Editorial deadline

1 March 2017

Editorial note

The authors of the individual scientific contributions published in this report are fully responsible for the contents.

Reproduction including extracts is permitted subject to crediting the source.
This report is neither for sale nor may be resold.



Deutsches Elektronen-Synchrotron A Research Centre of the Helmholtz Association

The Helmholtz Association is a community of 18 scientific-technical and biological-medical research centres. These centres have been commissioned with pursuing long-term research goals on behalf of the state and society. The Association strives to gain insights and knowledge so that it can help to preserve and improve the foundations of human life. It does this by

identifying and working on the grand challenges faced by society, science and industry. Helmholtz Centres perform top-class research in strategic programmes in six core fields: Energy, Earth and Environment, Health, Key Technologies, Structure of Matter, Aeronautics, Space and Transport.

www.helmholtz.de